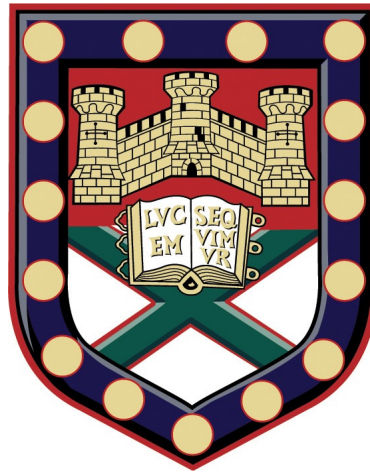


**University of Exeter**



**The role of Raman Spectroscopy in the detection  
of dysplasia in Barrett's oesophagus**

**Miss Emma Upchurch**

**Masters by Research in Physics Thesis**

**Supervisors: Prof Barr, Prof Stone,  
Prof Shepherd, Dr Kendall.**

**September 2017**



# The role of Raman Spectroscopy in the detection of dysplasia in Barrett's oesophagus

Submitted by Miss Emma Upchurch to the University of Exeter

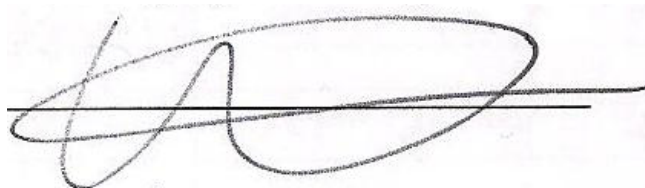
As a thesis for the degree of Masters by Research in Physics

September 2017

This thesis is available for Library use on the understanding that it is copyright material and that no quotation from the thesis may be published without proper acknowledgement.

I certify that all material in this thesis which is not my own work has been identified and that no material has previously been submitted and approved for the award of a degree by this or any other University.

Signature:

A handwritten signature in black ink, consisting of a large, stylized 'E' followed by a horizontal line and a large, rounded flourish.

## Abstract

### Introduction

The incidence of oesophageal adenocarcinoma is increasing. Although improvements have been seen, the overall 5 year survival rate remains poor, at 15.1%. As with other cancers, the survival rate is highest when the disease is confined to the oesophagus.

Barrett's oesophagus is an acquired condition, characterised by the replacement of the normal distal squamous epithelial lining of the oesophagus with columnar epithelium. Oesophageal adenocarcinoma develops, in most instances, along a pathway of increasing dysplasia in the sections of Barrett's oesophagus. If dysplasia can be diagnosed accurately, then this would permit treatment prior to the development of adenocarcinoma.

### Methods

Samples of Barrett's oesophagus with varying degrees of dysplasia and adenocarcinoma were measured with Raman point and mapping spectroscopy. Analysis was performed using Matlab®.

### Results

Samples of squamous epithelia, Barrett's oesophagus without dysplasia, with low-grade dysplasia, with high-grade dysplasia and oesophageal adenocarcinoma were measured and analysed. 2078 point spectra measurements and 117 map regions were analysed.

Raman point spectra measurements and Raman mapping differentiated samples without dysplasia from those with dysplasia, and differentiated samples of low-grade dysplasia from those of high-grade dysplasia and adenocarcinoma. The specificity and sensitivity were, however, low.

### Conclusion

This research has illustrated the ability of Raman spectroscopy to discern samples of Barrett's oesophagus with low-grade dysplasia from those with higher grades of dysplasia. This capability could be utilised clinically with in-vivo measurements to identify the areas requiring detailed surveillance and biopsies.

The majority of patients with Barrett's oesophagus and low-grade dysplasia will never progress to adenocarcinoma. There is currently no means, either via histopathology or via a biomarker, to identify the minority who will develop high-grade dysplasia or adenocarcinoma. Raman spectroscopy may have the ability to do this and I believe this is the path that this technology should pursue.

## Acknowledgements

I would firstly like to thank everyone at the Biophotonics Research Unit at Gloucestershire Hospital where I was based, not only for providing the funding and, hence, my salary, but mainly for the help and support they provided during the year of research and the subsequent months of “writing up”.

Martin Isabelle deserves special credit for providing essential support and solutions, particularly where the Ethics Approval and Sample acquisition seemed to be determined to stop all efforts to gain any results. He also had to endure sharing an office with me and the resultant moaning that came with this arrangement. Without his help and support, I would not and could not have completed this work.

In addition, Gavin Lloyd provided must needed advice and expertise on the analysis that would have taken hours for me to sift through. His input was invaluable. I would also like to thank the other members of the Biophotonics team (Jonathan, Leanne, Robert and Allison) for their help and friendship, as well as Research and Development team for their input and advice, particularly regarding the complicated world of the Ethics approval.

A small portion of my work was completed at the University of Exeter and this would not have been possible without the organisation and support of Ellen Green at the Biophysics lab.

My supervisors have provided support throughout the process, however, I reserve the greatest thanks for Professor Hugh Barr who has been a constant source of support and encouragement. He not only helped instigate, carry out and complete the project, but has always been a source of entertainment and ceaseless inspiration and made the process enjoyable and worthwhile.

My final thanks extend to my family and friends who have endured hours of grumbling, although we usually managed this over a glass (or two) of wine!!

## Contents

Declaration	3
Abstract	4
Acknowledgements	6
List of Contents	8 - 12
List of Figures	13 - 15
List of Tables	16
List of Abbreviations	17 - 18
List of Appendices	19
Bibliography	164 - 179

## List of Contents

### Section A: Literature Review

Chapter 1:	Barrett's Oesophagus	20
1.1:	Definition	20
1.2:	Epidemiology of Oesophageal Adenocarcinoma	21
1.3:	Epidemiology of Barrett's oesophagus	22
1.4:	Risk factors for Barrett's oesophagus	24
1.5:	Dysplasia in Barrett's oesophagus	24
1.6:	Natural History of Barrett's oesophagus	25
1.7:	Risk factors for malignant progression	27
1.8:	Diagnosis of Barrett's oesophagus and Dysplasia	28
1.8.1:	Endoscopic Assessment	29
1.8.2:	Histopathology	30
1.8.3:	Additional Tools	32
1.9:	Active Surveillance and Screening Techniques	33
1.10:	Management of Barrett's oesophagus	34
1.10.1:	Barrett's oesophagus without dysplasia	34
1.10.2:	Indeterminate for dysplasia	36
1.10.3:	Low-grade dysplasia	36
1.10.4:	HGD and Early Adenocarcinoma	38
1.10.5:	Strategies for Chemoprevention	42
1.11:	Future Developments	43
1.11.1:	Risk stratification Biomarkers	43
1.11.2:	Advanced imaging and diagnostic tools	44
1.11.2.1:	High Resolution Endoscopy	44
1.11.2.2:	Chromoendoscopy	45
1.11.2.3:	Narrow Band Imaging	45
1.11.2.4:	Autofluorescence	46
1.11.2.5:	Confocal Fluorescence Microendoscopy	46
1.11.2.6:	Optical Coherence Tomography	46



1.11.2.7:	Spectroscopy	47
Chapter 2:	Vibrational Spectroscopy	48
2.1:	Fundamental Principles	48
2.1.1:	Electromagnetic Radiation	48
2.1.2:	Biospectroscopy	49
2.2:	Raman Spectroscopy	49
2.2.1:	Underlying Principles	49
2.2.2:	Challenges and Advantages to Raman Spectroscopy of Biological Samples	51
2.2.3:	Clinical Applications of Raman Spectroscopy in the Oesophagus	53
2.3:	Fourier-Transform Infrared Spectroscopy	54
2.3.1:	Underlying Principles	54
2.3.2:	Challenges and Advantages to FTIR Spectroscopy of Biological Samples	57
2.2.3:	Clinical Applications of FTIR Spectroscopy in the Oesophagus	57
2.4:	Autofluorescence	58
2.4.1:	Underlying Principles	58
2.4.2:	Challenges and Advantages to Autofluorescence of Biological Samples	59
2.4.3:	Clinical Applications of Autofluorescence in the Oesophagus	59
2.5:	Point Spectra versus Imaging Mapping	61
2.6:	Chemometrics	61
2.6.1:	Principle Component Analysis	62
2.6.2:	Linear Discriminant Analysis	62
2.6.3:	Training Models and Leave One Sample Out Cross Validation	62

## Section B: Aims and Methods

Chapter 3:	Aims and Objectives	64
3.1:	Introduction and Aims	64
3.2:	Objectives	65
Chapter 4:	Methodology	66
4.1:	Ethical Approval	66
4.2:	Sample Collection	66
4.2.1:	Identifying Samples	66
4.2.2:	Processing of Samples	67
4.2.3:	Confirmation of Histology	68
4.3:	Sample Measurement	68
4.3.1:	Pre-measurement Preparation	68
4.3.2:	Raman Point Spectra Measurements of Oesophageal Tissue	69
4.3.3:	Raman Mapping of Oesophageal Tissue	71
4.3.4:	Autofluorescent Imaging of Oesophageal Tissue	72
4.4:	Data Pre-processing and Analysis	73

## Section C: Summary of Measurements, Results and Analysis

Chapter 5:	Summary of Measurements	74
5.1:	Raman Point Spectra of Oesophageal Tissue	74
5.2:	Raman Mapping of Oesophageal Tissue	76
5.3:	Autofluorescence of Oesophageal Tissue	78
5.4:	Data Analysis	78
Chapter 6:	Results and Analysis	79
6.1:	Classification Models	79

6.1.1:	Determining the presence of dysplasia: Barrett's oesophagus without dysplasia versus Barrett's oesophagus with dysplasia	79
6.1.1.1:	Raman Point Spectra	79
6.1.1.2:	Raman Mapping	81
6.1.1.3:	Comparison: Point Spectra to Mapping	85
6.1.2:	Determining the grade of dysplasia: Barrett's oesophagus with LGD versus Barrett's oesophagus with HGD and Adenocarcinoma	86
6.1.2.1:	Raman Point Spectra	86
6.1.2.2:	Raman Mapping	88
6.1.2.3:	Comparison: Point Spectra to Mapping	90
6.1.2.4:	Can point spectra be used to form a robust classification model	90
6.1.3:	Where does Low-Grade Dysplasia fit?	92
6.2:	Paraffin	93
6.2.1:	The Impact of Paraffin	93
6.2.2:	Comparison to Stainless Steel Slides	95
6.3:	Biochemical Peaks	96
6.3.1:	Is there a purpose to biochemical peak assignment?	96
6.3.2:	Peak Differences	98
6.3.3:	Low-Grade Dysplasia	100
6.4:	Autofluorescence	101

#### Section D: Summative Discussion and Conclusions

Chapter 7:	Summative Discussion and Conclusions	103
7.1:	The dilemma of Low-Grade Dysplasia	103
7.2:	Building a model from an imperfect Gold Standard	104
7.2.1:	The 'Not so Gold' Gold Standard	104

7.2.2:	Molecular Biomarkers to Improve the Gold Standard	106
7.2.3:	The benefit of Hindsight	108
7.3:	Where do we go from here?	109
7.3.1:	Automated Histology: Reducing the burden on the Histopathology Department	109
7.3.2:	Real time, in-vivo Raman Spectroscopy	111
7.3.3:	Enhanced Risk Stratification	112
7.4:	Final Thoughts	113

## List of Figures

### Chapter 1:

1.1:	H&E Stained Histopathological Section of Barrett's Oesophagus	20
1.2:	Oesophageal adenocarcinoma rate from 1970 to 2013	21
1.3:	Oesophageal adenocarcinoma rate according to patient age	22
1.4:	Endoscopic appearance of Barrett's oesophagus	29
1.5:	Histopathological Section of Barrett's Oesophagus with LGD	30
1.6:	Histopathological Section of Barrett's Oesophagus with HGD	31
1.7:	Oesophageal Biopsy sample showing Adenocarcinoma	32
1.8:	Management Algorithm for the Management of Barrett's oesophagus without dysplasia, from the BSG Guidelines	35
1.9:	Management Algorithm for the Management of Barrett's oesophagus with dysplasia, from the BSG Guidelines	37
1.10:	Layers of the Oesophageal Mucosa	39
1.11:	Management Algorithm for the Management of Barrett's oesophagus with HGD or adenocarcinoma, from the BSG Guidelines	40
1.12:	EMR of a visible lesion in the Oesophagus	41
1.13:	Chromoendoscopy using indigo carmine staining of Barrett's Oesophagus with HGD	45
1.14:	Cross-sectional OCT images and corresponding histology showing buried glands (red arrowheads) from a patient <i>in vivo</i>	47

### Chapter 2:

2.1:	Electromagnetic Radiation Spectrum	48
2.2:	Stokes and Anti-Stokes Shift Pattern	50
2.3:	Example of a Raman Spectrum	51
2.4:	Schematic Representation of a Raman Spectrometer	51
2.5:	Schematic Diagram of some of the vibrations that molecular bonds undergo when excited	55
2.6:	Infrared Spectrum of Ethanol ( $\text{CH}_3\text{CH}_2\text{OH}$ )	56
2.7:	Schematic Representation of FTIR Spectroscopy	56
2.8:	Schematic Representation of Autofluorescence	58

2.9:	Autofluorescent image of the intestine of a mouse	59
------	---	----

#### Chapter 4:

4.1:	Raman Spectral Measurement of Paraffin Wax	68
4.2:	Renishaw System 1000 at the Biophotonics Research Unit	70
4.3:	Renishaw RA800 Series at the Biophotonics Research Unit	71
4.4:	Confocal Fluorescence Microscopy System at the University of Exeter	72

#### Chapter 5:

5.1:	H&E Stained Sample indicating the areas to be used for measurements	74
5.2:	White light image of tissue sample produced and area selected for mapping	76
5.3:	ANOVA for comparison of LGD with HGD and Adenocarcinoma	78

#### Chapter 6:

6.1:	Scatterplot of Raman Point Spectra Measurements classified by Histological Type	80
6.2:	ROC Curve for Dysplasia versus Non-Dysplasia: Point Spectra	81
6.3:	ROC Curve for Dysplasia versus Non-Dysplasia on CaF <sub>2</sub> Slides	82
6.4:	ROC Curve for Dysplasia versus Non-Dysplasia on Stainless Steel Slides	84
6.5:	ROC Curve for LGD versus HGD: Point Spectra	87
6.6:	ROC Curve for LGD versus HGD on CaF <sub>2</sub> Slides	88
6.7:	ROC Curve for LGD versus HGD on Stainless Steel Slides	89
6.8:	Raman Spectrum of Pure Paraffin highlighting the predominant peaks produced	94
6.9:	Average spectra of each map of Normal Squamous and Oesophageal Adenocarcinoma tissue	94

6.10: Mean Spectra of Normal Squamous and Oesophageal Adenocarcinoma Tissue	95
6.11: Mean Spectra by pathology	98
6.12: Magnification of peak at $1440\text{cm}^{-1}$ , which corresponds to paraffin	99
6.13: Magnified view of spectral peaks at $934\text{cm}^{-1}$ , $1036\text{cm}^{-1}$ , $1048\text{cm}^{-1}$	100

## List of Tables

### Chapter 1:

1.1:	Molecular events involved in the neoplastic transformation of Barrett's mucosa	28
1.2:	Morphological Features associated with LGD and HGD	31
1.3:	Tumour Classification of Oesophageal Adenocarcinoma, from the TNM Classification	39

### Chapter 5:

5.1:	Number of Samples and Regions per pathology	74
5.2:	Summary of Measured and Eliminated Point Spectra	75
5.3:	Summary of Samples and Regions measured using Raman Mapping	77
5.4:	Summary of Raman Map Measurements	77
5.5:	Averages of Raman Map Measurements	77

### Chapter 6:

6.1:	Analysis Results: Raman Point Spectra (No Dysplasia versus Dysplasia)	80
6.2:	Analysis Results: Raman Mapping (No Dysplasia versus Dysplasia) on CaF <sub>2</sub>	82
6.3:	Analysis Results: Raman Mapping (No Dysplasia versus Dysplasia) on Stainless Steel Slides	84
6.4:	Comparison Results: Point Spectra Training Set versus Map Spectra Training Set: No Dysplasia versus Dysplasia	85
6.5:	Analysis Results: Raman Mapping (Low Grade Dysplasia versus High Grade Dysplasia): Point Spectra	87
6.6:	Analysis Results: Raman Mapping (LGD versus HGD) on CaF <sub>2</sub> Slides	88
6.7:	Analysis Results: Raman Mapping (LGD versus HGD) on Stainless Steel Slides	89
6.8:	Comparison Results: Point Spectra Training Set versus Map Spectra Training Set: LGD versus HGD and adenocarcinoma	90



## List of Abbreviations

AC	Adenocarcinoma
ACG	American College of Gastroenterologists
AFI	Autofluorescent Imaging
AGA	American Gastroenterology Association
ANOVA	Analysis of Variance
AspECT	Aspirin and Esomeprazole Chemoprevention Trial
AUC	Area Under the Curve
BE / BO	Barrett's Oesophagus
BEST2	Barrett's oEsophagus Screening Trial 2
BOSS	Barrett's Oesophagus Surveillance versus Endoscopy at Need Study
BSG	British Society of Gastroenterology
CARS	Coherent Anti-stokes Raman Spectroscopy
CCD	Charge-coupled Detector
CFM	Confocal Fluorescence Microscopy
CLE	Confocal Laser Endomicroscopy
DNA	Deoxyribonucleic Acid
EMR	Endomucosal Resection
ESME	Extended Multiplicative Scatter Corrective
ESS	Elastic Scattering Spectroscopy
FTIR	Fourier-Transform Infra-Red
GI	Gastrointestinal
GOR	Gastro-oesophageal Reflux
GORD	Gastro-oesophageal Reflux Disease
H&E	Haematoxylin and Eosin
H <sub>2</sub> RA	Histamine Receptor Antagonists

HGD	High-Grade Dysplasia
HRE	High Resolution Endoscopy
IM	Intestinal Metaplasia
LDA	Linear Discriminant Analysis
LGD	Low-Grade Dysplasia
LOSOCV	Leave One Sample Out Cross Validation Study
LSS	Light Scattering Spectroscopy
NBI	Narrow Band Imaging
NICE	National Institute for Health and Clinical Excellence
NIR	Near Infra-Red
NSAIDs	Non-Steroidal Anti Inflammatory Drugs
NSq	Normal Squamous
OCT	Optical Coherence Tomography
OGD	Oesophagogastroduodenoscopy
PCA	Principal Components Analysis
PPI	Proton Pump Inhibitor
ROC	Receiver Operating Characteristic Curve
RNA	Ribonucleic Acid
SERS	Surface Enhanced Raman Spectroscopy
SMART	Stratified Medicine through Advanced Raman Technologies
SORS	Spatially offset Raman Spectroscopy
SURF	Surveillance versus Radiofrequency Ablation for patients with Barrett's Oesophagus and Low Grade Dysplasia
TNM	Tumour, Nodes, Metastases
WLE	White Light Endoscopy

## List of Appendices

- Appendix I:           Deparaffinisation Protocol
- Appendix II:          Details of Sample Measurements
- Appendix III:         Autofluorescent Results
- Appendix IV:         Biochemical Peak Assignment
- Appendix V:          Poster Presentations

### Towards an understanding of the biochemical changes of dysplasia.

Upchurch E, Old OJ, Lloyd GR, Isabelle M, Shepherd N, Stone N, Kendall C and Barr H. SPEC: International Spectroscopy Conference: Montreal, Canada, June 2016.

### Developments in Infrared Spectroscopy of colorectal pathology.

Upchurch E, Old OJ, Griggs R, Woods J, Lloyd GR, Isabelle M, Shepherd N, Cook T, Nallala J, Barr H, Stone N and Kendall C.  
Faraday Discussions: Advances in Vibrational Spectroscopy. Cambridge, England. March 2016.

- Appendix VI:         Publications

### Detection of Dysplasia in Barrett's oesophagus: Are there impending optical and spectroscopic solutions?

Upchurch E, Old OJ, Lloyd GR, Isabelle M, Kendall C, Shetty G, Pavlou A, Shepherd N and Barr H. *Gastroenterology, Hepatology and Endoscopy*. 2016. 1(3): 61-67.

### Principles and Techniques of Vibrational Spectroscopy and Autofluorescence.

Upchurch E, Old OJ, Lloyd GR, Pavlou A, Kendall C, Barr H and Isabelle M. *Recent Advances in Biotechnology*. 2016. Publisher: Avid Science.

## Section A: Literature Review

### Chapter 1: Barrett's Oesophagus

#### 1.1: Definition

Barrett's oesophagus, originally described in 1950 by the thoracic surgeon, Norman 'Pasty' Barrett (Barrett, 1950), is an acquired condition, characterised by replacement of the normal distal squamous epithelial lining of the oesophagus with columnar epithelium which is clearly visible above the gastro-oesophageal junction (Fitzgerald *et al* 2013). The importance of this change is the risk of its subsequent degeneration to adenocarcinoma.

Intestinal metaplasia may be present and, if so, is usually incomplete, comprising of the presence of mucus or goblet cells. Complete intestinal metaplasia can occur and is characterised by the additional presence of absorptive cells (Rothery *et al* 1986, Gottfried *et al* 1989). Intestinal metaplasia is thought to be an adaptive response to the increased cell loss that results from chronic inflammation. Inflammation is believed to induce tumour suppressor genes in the submucosal oesophageal gland ducts leading to clonal expansion of tissue that has an increased ability to survive in the acid-rich environments (Leedham *et al* 2008).

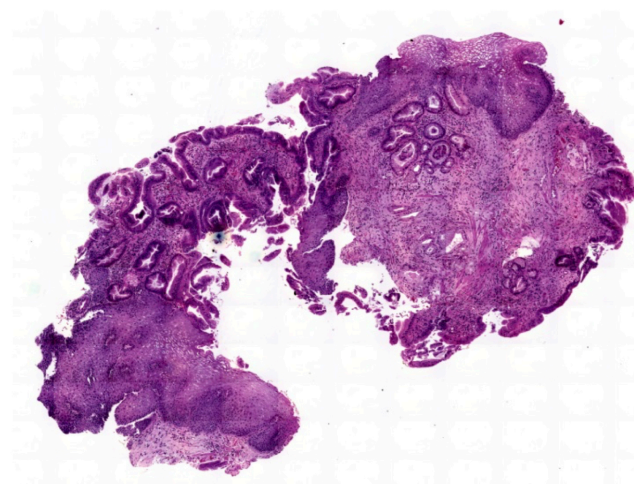


Figure 1.1: Haematoxylin and Eosin Stained Histopathological Section of Barrett's Oesophagus

Substantial controversy exists in the definition of and diagnostic criteria for Barrett's oesophagus. The UK (Fitzgerald *et al* 2013) and Japanese (Takubo *et al* 2009) definitions do not require the presence of intestinal metaplasia, whereas, in the USA, the AGA clearly states that intestinal metaplasia is required for diagnosis as it is the only type of columnar epithelium that unmistakably predisposes to malignancy (Spechler *et al* 2011). As well as studies which dispute this statement (DeMeester *et al* 2002, Chaves *et al* 2007, Kelty *et al* 2007, Liu *et al* 2009, Riddell and Odze 2009, Takabo *et al* 2009), difficulties also arise as the incidence of intestinal metaplasia may be underestimated due to sampling errors (Harrison *et al* 2007, Gatenby *et al* 2008), thereby, wrongly assigning patients as non-Barrett's and eliminating them from ongoing surveillance.

## 1.2: Epidemiology of Oesophageal Adenocarcinoma

The incidence of oesophageal adenocarcinoma has, since the 1970's, increased at an alarming rate. There are now 43% more cases than in the 1970's (Figure 1.2), encompassing 2% of all cancer cases (Cancer Research Stats, 2013). The highest incidence occurs in the older age range with 57% of cases diagnosed in those aged 70 and over (Figure 1.3) (Cancer Research Stats 2013).

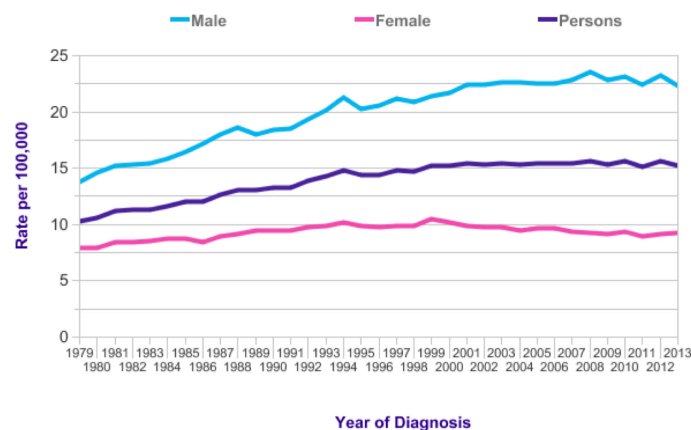


Figure 1.2: Oesophageal adenocarcinoma rate from 1970 to 2013 (Cancer Research UK, 2013)

The overall 5 year survival for oesophageal adenocarcinoma is 15.1% (Cancer Research Stats 2013), which although demonstrates a significant increase from the survival rates of the 1970's (4%), still means that this is the 5<sup>th</sup> leading cause of cancer related death in men. Survival rates are higher if disease is confined to the oesophagus at the time of diagnosis, making curative treatment in the form of surgical resection or chemoradiotherapy a possibility. Unfortunately, the majority of patients present at a time when the disease has spread beyond the confines of the oesophagus.

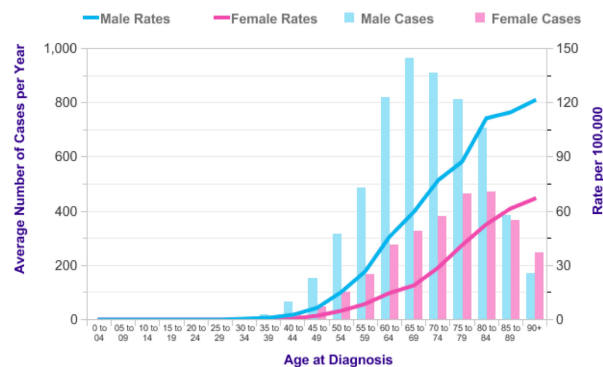


Figure 1.3: Oesophageal adenocarcinoma rate according to patient age (Cancer Research UK, 2013)

The striking increase in the incidence of oesophageal adenocarcinoma is thought to have been preceded by a similar, inconspicuous increase in the incidence of Barrett's oesophagus.

### 1.3: Epidemiology of Barrett's Oesophagus

The prevalence of Barrett's oesophagus in the population remains largely uncertain. Initial estimates were based on patients undergoing endoscopy for symptomatic diagnosis and these patients may represent a cohort of patients who differ from the general population, although the presence and extent of Barrett's oesophagus does not appear to correlate with the presence and severity of reflux symptoms. Three population studies have, nevertheless, looked at the prevalence in the general population with estimates of 1.3 % (Zagair *et al* 2008), 1.6% (Ronkainen *et al* 2005) and 1.9% (Zou *et al* 2011).

Methodological dilemmas in the identification of patients with Barrett's oesophagus has rendered the documentation of changes in incidence and prevalence problematic as increases may be related, in some part, to increased use of endoscopy and heightened awareness of and recognition of Barrett's oesophagus. Information from the Northern Ireland Barrett's Oesophagus Registry from 1993 to 2005 indicates an increase of 93% in the incidence (Coleman *et al* 2011), even when the total number of endoscopies performed is taken into account.

There are two main theories to explain the momentous increase in the incidence of Barrett's oesophagus. There has been an equally significant decrease in the incidence of *Helicobacter pylori* bacterial infection during the same time period. *H. pylori* infection causes gastric atrophy, resulting in a decrease in the production of gastric acid. It is the constant reflux of this acid into the oesophagus that results in the metaplasia of the lining epithelium and, thus, with less acid it is presumed that there will be less metaplasia. This theory of decreasing *H. pylori* incidence as the cause of increasing Barrett's oesophagus would not, however, explain the differing incident rates and age lag that exists between men and women.

The alternative hypothesis is that the increase in obesity, specifically that of abdominal obesity, has fuelled the increasing incidence. Abdominal obesity leads to an increase in intra-abdominal pressure. This increase in pressure causes reflux of acidic contents into the lower oesophagus, leading to metaplasia of the epithelial lining. It is also postulated that obesity causes a systemic pro-tumourigenic inflammatory state (Ryan *et al* 2008) and this leads to an increased incidence of Barrett's oesophagus in the face of ongoing acid reflux.

Barrett's oesophagus is more common in males with an overall male:female ratio of 2:1. There is an age shift in prevalence with men developing Barrett's oesophagus approximately 17-20 years before females (van Blankenstein *et al* 2005). This is consistent with the delay in age at which females develop oesophageal adenocarcinoma and may be accounted for by the protective mechanism of oestrogen which women have prior to the development of the menopause. In both sexes, nevertheless, the prevalence of Barrett's

oesophagus increases with age with a 7% increase added for each year of life (van Blankenstein *et al* 2005).

Marked ethnic differences in the epidemiology of Barrett's oesophagus exist with higher rates in white Caucasians (Devesa *et al* 1998; Brown *et al* 2008) and lower rates in black Americans and Asians (Ford *et al* 2005). The prevalence in the Hispanic community remains contradictory with some studies reporting similar (Bersantes *et al* 1998), and some lower, rates than in Caucasians (Abrams *et al* 2008; Corley *et al* 2009).

#### 1.4: Risk Factors for Barrett's oesophagus

The main established risk factors for Barrett's oesophagus are male gender, age greater than 50 years and a history of reflux symptoms (Eloubeidi *et al* 2001, Avidan *et al* 2002, Smith *et al* 2005, Cook *et al* 2005, Edelstein *et al* 2009). More recently, obesity in the form of an increased abdominal circumference (high waist:hip ratio) has been shown to lead to an increased risk of Barrett's oesophagus (Corley *et al* 2007, Edelstein *et al* 2009). Although traditionally believed to be solely an acquired condition, there is some evidence of familial clustering (Chak *et al* 2002). In these family groups, two loci (6p21 and 16q24) have been identified as being associated with this condition (Su *et al* 2012).

#### 1.5: Dysplasia in Barrett's oesophagus

Oesophageal adenocarcinoma develops, in most instances, along an established pathway of worsening dysplasia in a segment of Barrett's oesophagus and this is regarded as the best marker for malignant transformation.

Dysplasia is a morphological term, defined by Riddell *et al* (1983) as an unequivocal neoplastic epithelium strictly confined within the basement membrane of the gland from which it arises. It is a continuous spectrum, distinguished from regenerative non-neoplastic modifications, known as atypia, at one end, and from invasive cancer at the other extreme.



The diagnosis of dysplasia is based on architectural and cytological abnormalities (described in more detail in section 1.8.2). The degree of the abnormalities present determines the severity of the dysplasia. The majority of pathologists use a two-tiered system that distinguishes between low- and high-grade dysplasia.

A panel of International pathologists devised an alternative system, the Vienna Classification System, in 2000 (Schlemper *et al*) to minimise disagreement in classification. It is a five-tiered system, but as yet is still to be tested prospectively in a large series of patients.

#### 1.6: Natural History of Barrett's Oesophagus

Barrett's oesophagus is now recognised as the precursor to oesophageal adenocarcinoma, however, it is only a minority of patients, rather than the vast majority, who progress to adenocarcinoma. The metaplastic change to columnar epithelium is a response to the increased cell loss that is a result of chronic inflammation, typically as a result of gastro-oesophageal reflux. The annual conversion rate of Barrett's oesophagus to oesophageal adenocarcinoma, based on the seven published systematic reviews, varies from 0.3% to 0.6% (Shaheen *et al* 2000, Chang *et al* 2007, Thomas *et al* 2007, Yousef *et al* 2008, Wani *et al* 2009, Sikkema *et al* 2010, Desai *et al* 2012) and increases to 0.9 -1.0% if high-grade dysplasia is included alongside adenocarcinoma.

Two population based studies from Northern Ireland (Hvid-Jenson *et al* 2011) and Denmark (Bhat *et al* 2011) have shown a lower incidence of progression of 0.22% and 0.26% per year respectively. The most recent meta-analysis calculated the risk of progression as 0.33% per year (Desai *et al* 2012). This seems like a very small number of patients, however, this leads to a standardised incidence ratio of 11.3 which equates to an excess of >1000% more deaths in this cohort when compared [to the](#) general population.

Despite evidence from surveillance cohorts indicating an increased risk of cancer in the population diagnosed with Barrett's oesophagus, it remains problematic and extremely difficult to predict the risk for an individual patient.

Currently the only tool available is the presence of and grade of dysplasia within the Barrett's segment.

High-grade dysplasia is the nearest precursor to adenocarcinoma as exemplified by its presence in surgical resection specimens surrounding adenocarcinoma (Fléjou 2005) indicating that the cancer developed from an area of high-grade dysplasia. Although published studies are dominated by small samples from tertiary referral centres, the evidence indicates that 25% of patients with high-grade dysplasia will develop adenocarcinoma after an average of 2.5 years (Schnell *et al* 2001).

The step from high-grade dysplasia to adenocarcinoma is a much sturdier step than that of low-grade to high-grade dysplasia. Recent studies have challenged the traditional view that low-grade dysplasia progresses towards high-grade dysplasia and has suggested that low-grade dysplasia has the ability to regress. The phenomenon of regression may, however, be the result of misdiagnosis of low-grade dysplasia at initial biopsy rather than true regression (Jagadesham and Kelty 2014).

Recent studies have shown a rate of progression from low-grade to high-grade dysplasia or to adenocarcinoma of 30% (Montgomery *et al* 2001) and 28% (Skacel *et al* 2000) respectively. The most recent evidence places the annual risk of progression at 9% (Duits *et al* 2015). Of most interest, nevertheless, is that when three pathologists agreed on the diagnosis of low-grade dysplasia, 80% of patients disease progressed, whereas, when there was no agreement, 0% of patients progressed (Skacel *et al* 2000), suggesting that more developed low-grade dysplasia which is more easily identified is more likely to continue to high-grade dysplasia.

The diagnosis of low-grade dysplasia may in fact be a watershed moment in the natural history of Barrett's oesophagus [and](#) distinguishes a cohort of patients who are more likely to progress to significant disease. It is, therefore, imperative to identify this cohort to enable appropriate surveillance, accurate diagnosis of progression and timely intervention.

## 1.7: Risk factors for malignant progression

The presence and grade of dysplasia is the only tool that we currently have at our disposal to classify the risk of progression to adenocarcinoma and to identify those who would benefit from treatment or continuing surveillance. Evidence has highlighted the existence of other factors which predispose to malignant progression.

The most striking discriminator is the length of the segment of Barrett's oesophagus. The annual adenocarcinoma transition rate for long segment Barrett's oesophagus (defined as a segment >3cm) is 0.22% per year (Pohl *et al* 2015) which is significantly higher than the rate for short segment (1-3cm) and ultra-short (<1cm) which is documented as 0.03 and 0.01% per year respectively (Pohl *et al* 2015). For patients with high-grade dysplasia in a long segment of Barrett's oesophagus, the rate of progression to adenocarcinoma may be as high as 25% per year (Kastelein *et al* 2015).

Multifocal, as opposed to localised areas, of dysplasia have a higher risk of progression (Weston *et al* 2000, Buttar *et al* 2001) as does the presence of visible nodules or ulcers (Thurberg *et al* 1999, Weston *et al* 2000). An ulcer that fails to heal following intensive proton-pump inhibitor therapy is a particularly suspicious feature (Pech *et al* 2008).

The presence of intestinal metaplasia signifies an epithelium with a greater biological instability. There is a significant volume of evidence which indicates that intestinal metaplasia has the greatest risk of adenocarcinoma progression from dysplasia when compared to columnar epithelium without the presence of intestinal metaplasia (Skinner *et al* 1983, Smith *et al* 1984, Bhat *et al* 2011) which explains the rationale behind the definition of Barrett's oesophagus used in the AGA guidelines.

Certain genetic traits may result in a cohort of patients with a greater risk of malignant progression. These are summarised in Table 1.1. Aberrant p53, p53 mutation or p53 loss has been shown to increase the risk of developing dysplasia (Chatelain and Flejou 2003) and p53 overexpression has been shown to be an excellent predictor of dysplastic progression (Weston *et al* 2001). The British Society of Gastroenterology (Fitzgerald *et al* 2013) suggest using p53

immuno-staining as an adjunct to histopathology to aid diagnosis in uncertain cases.

<u>Molecular Event</u>	<u>Change Evoked</u>
Increased Proliferation	Ki67 expression in HGD
Cell Cycle Regulation E.g.: Cyclins D1 and E	Increased expression in cancer
Growth Factors and Growth Factor Receptors	Increased expression in cancer
P53	Frequent mutations in HGD and cancer
Cell Adhesion E.g.: E Cadherin	Decreased expression in cancer
Telomerase	Increased expression parallel to dysplasia

Table 1.1: Molecular events involved in the neoplastic transformation of Barrett's mucosa (adapted from Flejou, 2005)

Additional molecules are being investigated to determine their ability to predict patients at greater risk of malignant progression. Hypermethylation of p16 is an early predictor of progression, particularly in low-grade dysplasia (Wang *et al* 2009). Survivin, an apoptotic inhibitor, is overexpressed in oesophageal cancer and, to a lesser extent, in dysplastic tissue (Vallböhmer *et al* 2005). At present there are no markers in routine clinical practise to aid the identification of at-risk individuals.

#### 1.8: Diagnosis of Barrett's oesophagus and dysplasia

The diagnosis of Barrett's oesophagus is made at endoscopy. There is no screening programme in the United Kingdom, however, guidelines exist to identify which patients should be referred for endoscopy based on the likelihood

of the presence of an underlying cancer (Nice Guidelines NG12, 2014). These include, but are not restricted to, patients with dysphagia (difficulty in swallowing), age greater than 55 years with weight loss, upper abdominal pain and new-onset or treatment resistant dyspepsia.

The diagnosis of Barrett's oesophagus and the presence of dysplasia is confirmed by histopathology following biopsy, although this is not always as uncomplicated as it would seem.

#### 1.8.1: Endoscopic Assessment

Barrett's oesophagus has a classical appearance at endoscopy. There is proximal displacement of the squamo-columnar junction with the salmon pink columnar epithelium of Barrett's being seen as tongues of epithelium emerging into the distal oesophagus (Figure 1.4).



Figure 1.4: Endoscopic appearance of Barrett's oesophagus (Courtesy of Digestive Health Associates: South West Endoscopy Centre ([www.digestivehealth.net](http://www.digestivehealth.net)))

The reporting of endoscopic findings is via the Prague classification which records the circumferential extent, the maximal length and any additional visible islands of columnar-lined oesophagus.

Dysplasia in Barrett's oesophagus is difficult to identify at endoscopy as it appears macroscopically identical to non-dysplastic Barrett's oesophagus. The current protocol is, thus, to take random biopsies from each quadrant of the oesophagus at 1-2cm intervals in areas of macroscopically visible Barrett's oesophagus, known as the Seattle protocol. This protocol, even if rigorously adhered to, samples less than 5% of the mucosa and may miss up to 57% of

cases of dysplasia (Vieth *et al* 2004, Singh *et al* 2007). 34% of early stage oesophageal cancers (both squamous and adenocarcinoma) failed to be recognised in preceding endoscopies (Chadwick *et al* 2014).

### 1.8.2: Histopathology

Barrett's oesophagus is confirmed by the presence of columnar lined epithelium, with or without the presence of goblet cells, signifying intestinal metaplasia. The important question is, nevertheless, whether there is any evidence of dysplasia.

The diagnosis of dysplasia is based on morphological changes that are seen at microscopy (Table 1.2). Low-grade dysplasia is characterised by crypts with no, or minimal, architectural abnormalities combined with mild to moderate nuclear atypia (Figure 1.5). High-grade dysplasia is characterised by further abnormalities, with architecturally distorted crypts combined with a higher degree of cytological atypia (Figure 1.6). This typically includes complete loss of cell polarity, increased nuclear stratification, large ovoid-shaped nuclei and apoptotic debris within the crypt lumen.

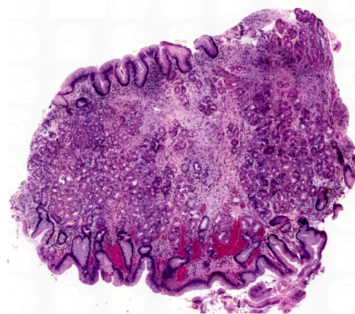


Figure 1.5: Barrett's Oesophagus with Low-Grade Dysplasia

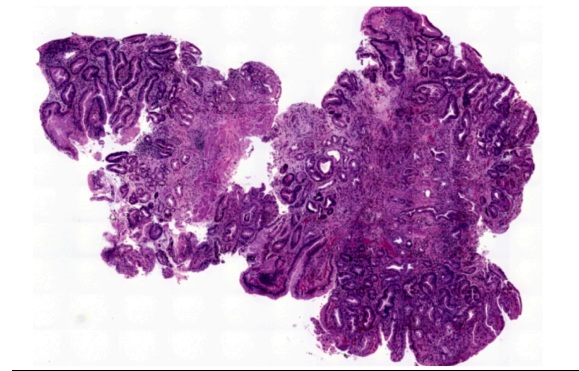


Figure 1.6: Barrett's Oesophagus with High-Grade Dysplasia

	<u>Low-Grade Dysplasia</u>	<u>High-Grade Dysplasia</u>
<u>Nuclei</u>	Enlarged, Crowded Hyperchromatic, Ovoid	Enlarged, usually Spheroidal Nuclear pleomorphism
<u>Mitotic Activity</u>	Substantial Atypical Mitoses + Stratification	Substantial Atypical Mitoses ++ Cellular Disorganisation
<u>Architectural Change</u>	Loss of basal-luminal differentiation axis Villosity may be present	Loss of basal-luminal differentiation axis Villosity often present Glandular budding and complex glandular structures are often present

Table 1.2: Morphological Features associated with Low and High-Grade dysplasia (Adapted from Fléjou and Svrcek 2007)

Neoplastic cells are typified by enlarged and hyperchromatic ovoid-shaped or elongated nuclei with membrane irregularity, nuclear pseudostratification and increased mitotic activity (Figure 1.7). The carcinoma is deemed intra-mucosal if there is no breach through the lamina propria. If there is penetration of this

layer, there is a risk of spread to the lymphatics and localised treatment may, therefore, be insufficient.

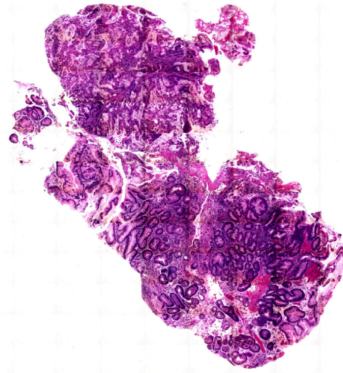


Figure 1.7: Oesophageal Biopsy sample showing Adenocarcinoma

At the other end of the spectrum, a degree of atypia that is more than that expected for regenerative changes, yet less than that expected for low-grade dysplasia can be seen. These samples are classified as indefinite for dysplasia and may simply be the result of inflammation which can make the interpretation of cellular changes challenging. Inadequate laboratory processing, such as poor staining, can add to this difficulty.

With the complex array of changes that occur along this spectrum, it is hardly surprising that a high degree of intra- and inter-observer variability exists (Kerkhof *et al* 2007, Lee *et al* 2010, Gaddam *et al* 2011). Given this and the implications of a diagnosis of dysplasia, it is recommended that all cases of suspected dysplasia, including indefinite for dysplasia (Fitzgerald *et al* 2013) are reviewed by a second GI pathologist.

### 1.8.3: Additional Tools

Parallel to the morphological changes seen, genetic alterations occur which affect gene expression and ultimately the regulation of the cell cycle. As discussed, certain genetic changes confer a greater risk of malignant progression and their identification, by immunohistochemistry, may, in the future, be used alongside histopathology to aid the diagnosis of dysplasia. It



may also find a role in risk stratification, determining which patients require intensive surveillance and/or early treatment.

Due to the complexity of the cell cycle and its control mechanism, a number of genetic alterations are likely to occur. The changes may well be unique to each individual and, thus, it may not be appropriate for these changes to be used at a population level.

### 1.9: Active Surveillance and Screening

The aim of endoscopic surveillance is to detect cancerous, or ideally precancerous, changes at a stage, prior to invasive cancer, where treatment is able to be curative. These changes would preferably be detected when treatment is not only curative, but also able to be less radical. There is, at this time, no evidence to demonstrate its efficacy in this aim, despite the widespread practise in Europe and North America.

The benefit for surveillance for non-dysplastic Barrett's oesophagus is, in particular, unclear, both in terms of detecting malignant progression and in cost effectiveness. The BOSS (Barrett's Oesophagus Surveillance versus endoscopy at need Study) trial, currently in its follow up phase, aims to address the question of the usefulness of endoscopic surveillance.

The published literature does suggest that cancers which are detected during surveillance are of an earlier stage and, hence, associated with improved survival (Streitz *et al* 1993, Peters *et al* 1994, Van Sindick *et al* 1998, Corley *et al* 2002, Cooper *et al* 2002, Fountoulakis *et al* 2004, Rubenstein *et al* 2008, Cooper *et al* 2009). The current surveillance recommendations are based on the presence or absence of dysplasia, the grade of dysplasia and the length of the Barrett's segment. At an individual level, the presence of significant comorbidities are taken into account to determine whether further endoscopies are in the best interest of the patient. Other factors that may influence the likelihood of malignant progression are not, however, factored into the surveillance strategy.

The incidence of oesophageal adenocarcinoma resulting from Barrett's oesophagus is too low to warrant broad population-based screening (Watson *et*

*al* 2005, Wang *et al* 2008). The cost effectiveness of endoscopic screening, even when restricted to patients with gastro-oesophageal reflux, is highly controversial with wide divergences in estimates of benefit (Inadomi *et al* 2003, Nietert *et al* 2003, Gerson *et al* 2004, Gupta *et al* 2011).

Non endoscopic devices could prove to be more cost effective. The Cytosponge, essentially a capsule attached to a string device which is swallowed and subsequently removed by pulling on the string, removing at the same time cells that line the oesophagus, has been shown to be more cost effective than endoscopy. Its diagnostic accuracy is currently being assessed in the Barrett's oEsophagus Screening Trial (BEST2) to determine its possible use as a screening modality.

#### 1.10: Management of Barrett's oesophagus

The management algorithm for Barrett's oesophagus, based on the evidence currently available and expert consensus, is dependent, primarily, on the presence and grade of dysplasia and, to a lesser extent, on the length of the segment of Barrett's oesophagus.

##### 1.10.1: Barrett's oesophagus without dysplasia

For patients in whom Barrett's oesophagus is confirmed by histopathology, but where there is no evidence of dysplasia, the management strategy is for ongoing surveillance via oesophago-gastro-duodenoscopy (OGD). The frequency of surveillance is dependent on the length of the Barrett's segment as a longer segment confers a higher risk of malignant progression (Figure 1.8).

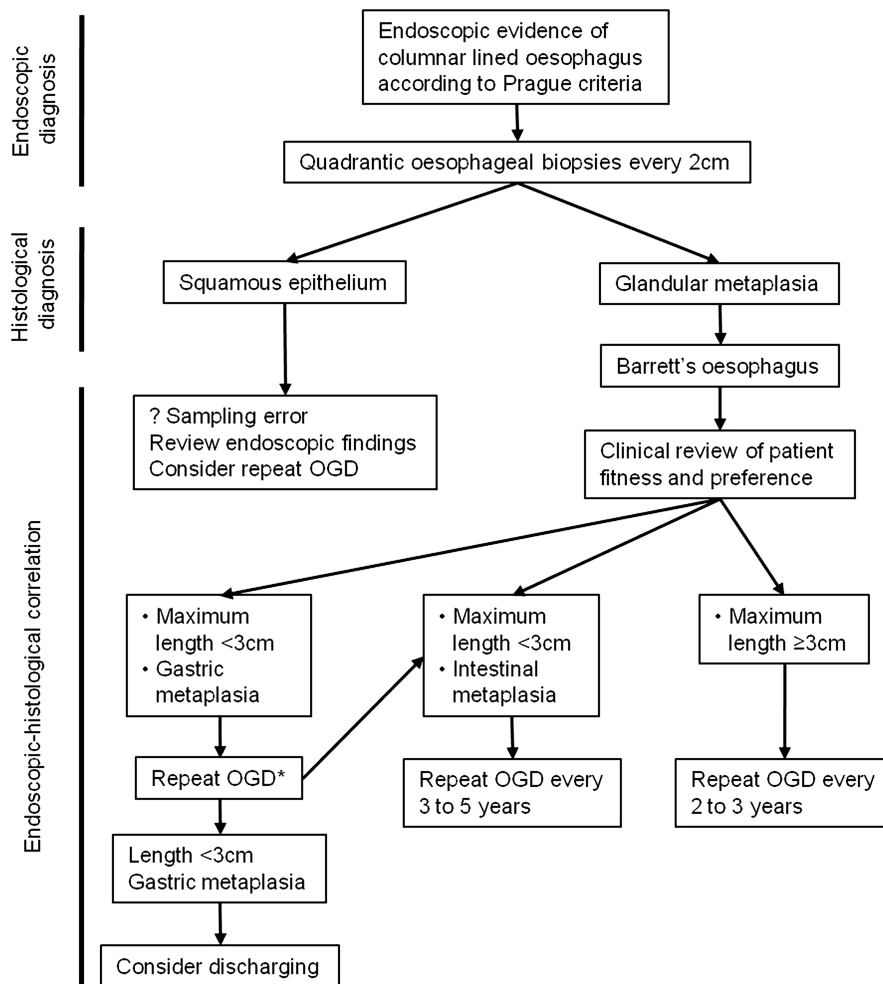


Figure 1.8: Management Algorithm for the Management of Barrett's oesophagus without dysplasia, from the British Society of Gastroenterology Guidelines (Fitzgerald *et al* 2013)

In patients with short segment or ultra short segment of Barrett's oesophagus and no evidence of intestinal metaplasia, the risk of malignant progression is felt to be so small that the patient can be discharged from surveillance. In a patient with additional risk factors, however, such as older age, obesity and ongoing reflux symptoms, a second endoscopy should be considered.

In patients with intestinal metaplasia, the current recommendation is for endoscopic surveillance. The frequency of this is dependent on the length of the segment of Barrett's oesophagus and should also reflect the presence of additional risk factors, such as male gender and older age. In a small cohort of patients, with significant comorbidities, surveillance may be inappropriate and they can be discharged from the surveillance programme.

### 1.10.2: Indeterminate for dysplasia

There is scant evidence detailing the management for patients with this diagnosis. This is likely to be, to a large extent, due to the difficulty surrounding this diagnosis with high inter-observer variability, thus, making it difficult to make consensus decisions regarding this potentially diverse group. It should be viewed as an interim diagnosis, not as the final conclusion.

In some cases, the cellular atypia present is a result of inflammation and improving this by commencing or optimising anti-reflux medical therapy may result in regression of the cellular atypia. All patients should, thus, receive high dose acid suppression to ensure control of inflammation. A repeat endoscopy in 6 months is recommended to clarify whether dysplasia is present (Figure 1.9), and if so, the patient is then managed according to the grade of dysplasia on repeat endoscopy. There is no current consensus on how to manage patients with repeated indefinite dysplasia.

### 1.10.3: Low-Grade Dysplasia

The management strategy for patients with low-grade dysplasia is currently surrounded by uncertainty which reflects the underlying uncertainty of its' natural history. Low-grade dysplasia does confer a greater risk of malignant progression as discussed above, yet it is unclear whether this risk warrants intense surveillance or even therapeutic intervention and the associated threat of complications.

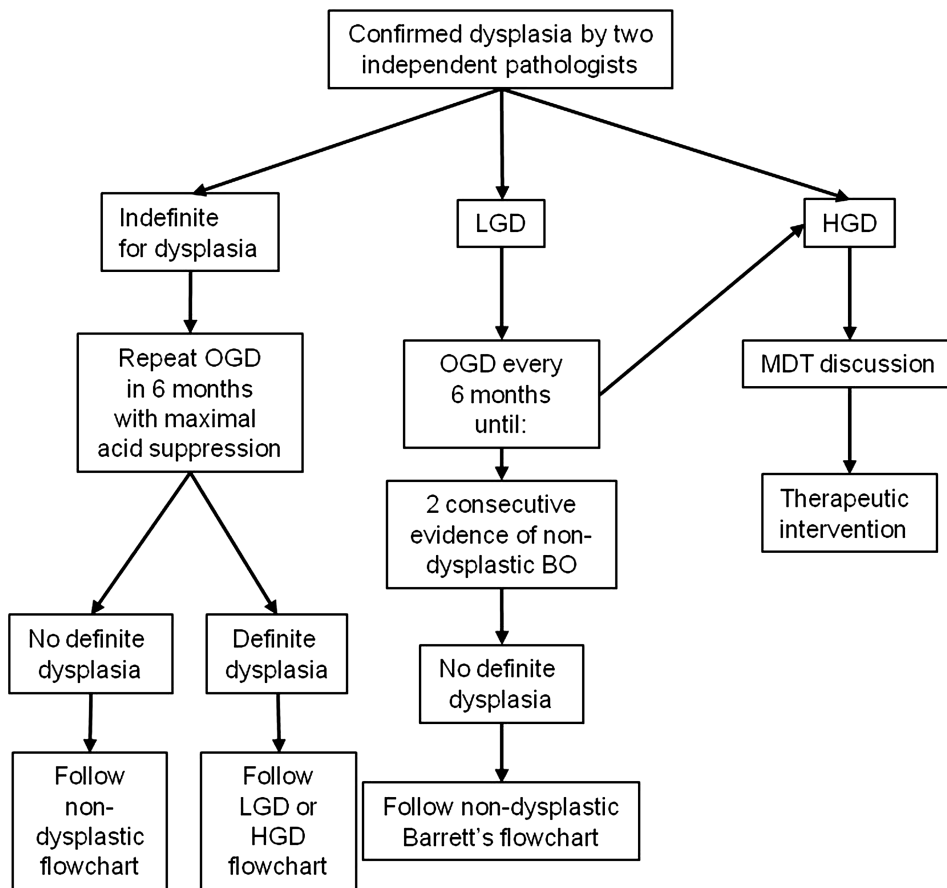


Figure 1.9: Management Algorithm for the Management of Barrett's oesophagus with dysplasia, from the British Society of Gastroenterology Guidelines (Fitzgerald *et al* 2013)

There is, at present, no data regarding the appropriate surveillance strategy for these patients. The overall consensus, based on expert opinion, appears to be that, following a first biopsy with low-grade dysplasia, patients should have a second endoscopy within a 6 – 12 month time interval (Figure 1.9).

A repeat endoscopy within a relatively short time period enables one to determine if the dysplasia is persistent or progressive, or even if there has been any regression. For a diagnosis that is plagued, at times, with significant levels of uncertainty due to the difficulty of diagnosis, a second set of biopsies may provide clarity and help to prevent the over-diagnosis of low-grade dysplasia. In a recent Dutch study (Duitz *et al* 2015), 73% of cases initially diagnosed as low-grade dysplasia were subsequently diagnosed as non-dysplastic or indefinite for dysplasia.

Recent evidence from the 'SURF' Study (SURveillance versus RadioFrequency ablation) (Phoa *et al* 2014), a multi-centre randomised clinical trial, found that

ablation in patients with low-grade dysplasia reduced the risk of progression to high-grade dysplasia or adenocarcinoma by 25%. Treatment related adverse events were recorded in 19.1%, predominantly that of mild oesophageal stricturing.

In patients with persistent low-grade dysplasia (i.e.: low-grade dysplasia on two consecutive endoscopies), or with other risk factors, such as long segment Barrett's or multifocal areas of low-grade dysplasia, the evidence would suggest that ablative therapy be recommended at this time. The British Society of Gastroenterology guidelines suggest endoscopic assessment plus biopsies in 6 month intervals until either regression or progression (Fitzgerald *et al* 2013), however, these recommendations were published before the results of the SURF Study.

If the development of low-grade dysplasia is in fact a defining moment in the natural history of Barrett's oesophagus, then ablative therapy at this early stage would appear to be a sensible approach. Further research is, however, needed to delineate the appropriate management for this diverse group.

#### 1.10.4: High-Grade Dysplasia and Early Adenocarcinoma

In patients in whom biopsies have shown high-grade dysplasia or early adenocarcinoma that is confined to the mucosa, endoscopic intervention is the preferred treatment modality. Early adenocarcinoma, designated as T1, indicates cancerous cells have spread into the lining of the oesophagus, up to but not including the muscularis propria. T1 cancers are divided into two groups: T1a where invasion is into the lamina propria, and T1b where invasion is into the submucosa (Table 1.3).

TX	Primary tumour cannot be assessed
T0	No evidence of primary tumour
T <sub>IS</sub>	Carcinoma in situ / High-Grade Dysplasia
T1	
T1a	Tumour invades lamina propria or muscularis mucosae
T1b	Tumour invades submucosa
T2	Tumour invades muscularis propria
T3	Tumour invades adventitia
T4	
T4a	Tumour invades adjacent structures: pleura, pericardium or diaphragm
T4b	Tumour invades other adjacent structures: aorta, vertebral body or trachea

Table 1.3: Tumour Classification of Oesophageal Adenocarcinoma, from the TNM Classification

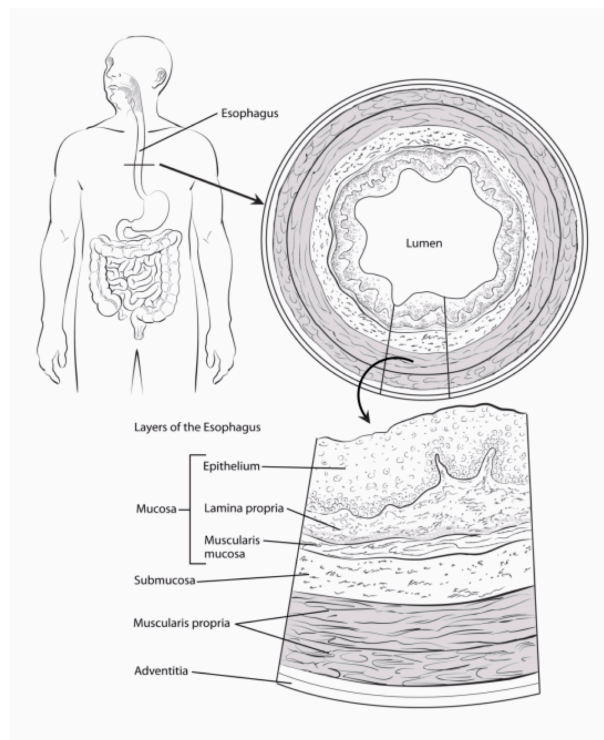


Figure 1.10: Layers of the Oesophageal Mucosa (Courtesy of [www.cancer.org](http://www.cancer.org))

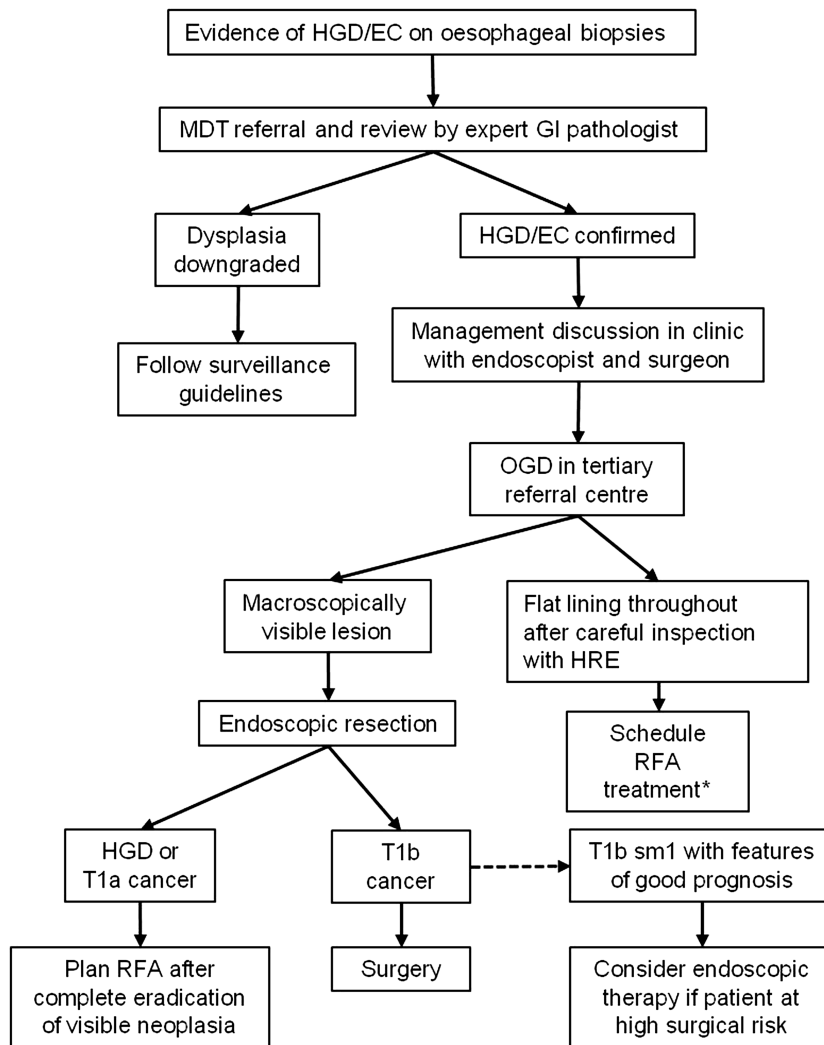


Figure 1.11: Management Algorithm for the Management of Barrett's oesophagus with high-grade dysplasia or adenocarcinoma, from the British Society of Gastroenterology Guidelines (Fitzgerald *et al* 2013)

High-grade dysplasia and T1a cancers are associated with a low rate of lymph node metastases with evidence indicating rates of 0% and 0-10% respectively (Buskens *et al* 2004, Liu *et al* 2005, Stein *et al* 2005, Westerterp *et al* 2005, Abraham *et al* 2007, Prasad *et al* 2009, Alvarez *et al* 2010, Barbour *et al* 2010, Sepesi *et al* 2010). T1b cancers, on the other hand, carry a risk of up to 46%. This is also reflected in the 5 year recurrence free and overall survival rates of 100% and 91% in patients with T1a cancer, compared to 60% and 58% in patients with T1b cancer. Patients with T1b cancer, therefore, are not suitable for endoscopic intervention, whereas, for those with high-grade dysplasia or T1a cancer, endoscopic intervention is the preferred approach Figure 1.11).



For patients with visible lesions of high-grade dysplasia or T1a cancer, endoscopic resection is the preferred modality as, not only does this remove the lesion, but it enables histopathological review to confirm the diagnosis and grade (Figure 1.12). If the grade is found to be greater than T1a with submucosal invasion, then patients should be considered for subsequent surgical intervention in the form of oesophagectomy.

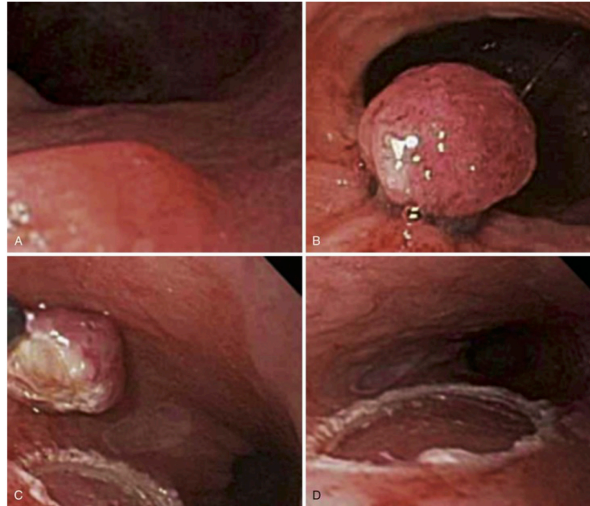


Figure 1.12: Endoscopic Mucosal Resection of a visible lesion in the Oesophagus (Courtesy of Gastrointestinal Tract Endoscopic and Tissue Processing Techniques and Normal Histology (Adler *et al* 2015))

Greater than 20% of patients who are treated by endoscopic resection for high-grade dysplasia or T1a cancer develop a metachronous lesion within 2 years and, thus, as well as resection of the visible lesion, the remaining Barrett's oesophagus requires treatment. This should occur even if there is no evidence of dysplasia in the remaining Barrett's oesophagus.

For flat areas of high-grade dysplasia, ablation is the recommended treatment. Radiofrequency has the best safety and side-effect profile with efficacy equal to that of other ablative techniques (Fitzgerald *et al* 2013), although there is a paucity of data comparing techniques.

Despite evidence that endoscopic resection and ablation results in long-lasting elimination of dysplasia, there remains a risk of both recurrence and of 'buried' dysplasia occurring in the crypts of the glands. Endoscopic follow up is,

therefore, recommended at 3 monthly intervals for the initial 12 months following treatment and then for at 12 monthly intervals.

For patients with T1b cancer, surgical resection is the treatment of choice, due to the significant risk of lymph node metastases. Oesophagectomy has a mortality rate of 2% when performed in specialised centres, yet has a significant short term morbidity of 6-37% (Sujendran *et al* 2005, Williams *et al* 2007). Surgical follow up studies report the recurrence of Barrett's oesophagus following curative surgery and although the risk of developing dysplasia or malignancy is unknown, the presence of goblet cells has been seen in 'neosquamous' epithelium in the oesophageal conduit. In view of this, patients who have undergone curative surgery also require endoscopic follow up. The current recommendation is for this to occur at 2, 5 and 10 years.

#### 1.10.5: Strategies for chemoprevention

Chemoprevention, defined as the use of pharmacological agents or other strategies to prevent the development of cancer has been sought to prevent the progression towards malignancy that occurs in Barrett's oesophagus. Different agents have been studied in this setting, including non-steroidal anti-inflammatories and statins, however, the majority of evidence has been for proton-pump inhibitors (PPIs).

Evidence from cohort studies with patients using PPIs for symptom control have shown a significantly reduced odds ratio for the development of dysplasia compared to those not taking PPIs (El-Serag *et al* 2004), although this could, in some way be explained by the severity of the reflux symptoms. There is insufficient evidence to recommend the use of PPIs solely as a chemopreventative agent to prevent the formation of Barrett's oesophagus or malignant progression, despite the scientific plausibility that would indicate a benefit. Their use for symptom control as required is advocated.

Anti-reflux surgery in the form of fundoplication is offered to a cohort of patients with gastro-oesophageal reflux. There is no evidence that this offers superior acid suppression for the prevention of neoplastic progression and, as such, should not be offered. It should, however, still be recommended to suitable patients for symptom control and they will continue to require endoscopic

surveillance based on the presence and grade of dysplasia in the Barrett's oesophagus.

Aspirin has been shown in other cancers, including those of the GI tract, to improve outcome. The Aspirin and Esomeprazole Trail (AspECT) (Jankowski *et al*) is currently in progress and should help to answer the question of their use in Barrett's oesophagus.

### 1.11: Future Developments

A considerable dilemma in managing Barrett's oesophagus relates to the difficulty that exists in accurately identifying patients who are at risk of malignant progression and selecting those requiring treatment and/or surveillance. Risk stratification biomarkers and optical techniques are being investigated for this role.

#### 1.11.1: Risk Stratification Biomarkers

Although risk factors for the likelihood of malignant progression are known, factors other than the presence and grade of dysplasia and, to a lesser extent, the length of the segment of Barrett's oesophagus, are not used to stratify patients based on the likelihood of malignant progression. If additional markers could be identified, this would enable surveillance and treatment to be selectively targeted.

As discussed briefly in section 1.7, hypermethylation of p16 may be an early predictor of progression. This information could be used alongside histology information to identify patients who are at greatest risk of progression. The changes in p16 and p53 are, however, non-specific with mutations occurring in a multitude of cancers. This non-specificity may make risk stratification difficult.

An alternative would be to utilise immunophotodiagnostic technology, for example, by using monoclonal antibodies that are specific for tumour-related antigens. Cell surface lectins are carbohydrate binding structures that are displayed on the surface of cells to serve as cell-cell binding sites. In the progression from non-dysplastic Barrett's oesophagus to adenocarcinoma, changes in the binding patterns of lectins have been identified (Bird-Lieberman

*et al* 2012). The specific changes can be located at endoscopy using monoclonal antibodies, thus, guiding, the identification of areas that should be biopsied.

#### 1.11.2: Advanced Imaging Tools

One of the major difficulties in the management of Barrett's oesophagus is the identification of and accurate diagnosis of dysplasia. Endoscopy enables the visualisation of Barrett's oesophagus, however, the presence of dysplasia is not macroscopically distinguishable and the diagnosis often relies on sampling by random quadrant biopsies. These biopsies, due to sampling error, may miss areas of dysplasia, thus, underestimating the risk of malignant progression for that individual.

A number of optical techniques have been developed and investigated to ascertain their role in solving this significant problem.

##### 1.11.2.1: High Resolution Endoscopy

Traditional endoscopy generates an image of 300,000 pixels. High resolution endoscopes, in contrast, generate images of >1,000,000 pixels. This substantial increase in resolution enables improved detection of areas of Barrett's mucosa (Kara *et al* 2005, Kara *et al* 2005a) and greater detection of visible lesions and nodules. Areas of nodularity or visible abnormalities are more likely to harbour high-grade dysplasia or early adenocarcinoma.

High resolution endoscopy is by no means perfect, however, with only 79% of dysplasia detected (Kara *et al* 2005) and with a substantial inter-observer variability (Kara *et al* 2005, Curvers *et al* 2008). The performance of and experience of the endoscopist has a significant impact, regardless of the instrument used, with the mean inspection time per cm of oesophagus having, perhaps, the greatest influence on the detection of both Barrett's mucosa and additional abnormalities (Gupta *et al* 2011). Techniques, which ultimately rely on the operator, will need to take this into account when assessing their reliability.

### 1.11.2.2: Chromoendoscopy

Chromoendoscopy describes the use of exogenous dyes to aid the detection of abnormalities. The dyes are sprayed onto the mucosal surface at the time of endoscopy via a specially designed catheter.

Lugol's solution, one of the dyes used, interacts with glycogen present in the normal squamous epithelium resulting in a brown/black discoloration. It does not, however, have the same effect on columnar epithelium which distinguishes Barrett's oesophagus, thus, enabling effective differentiation between the two.

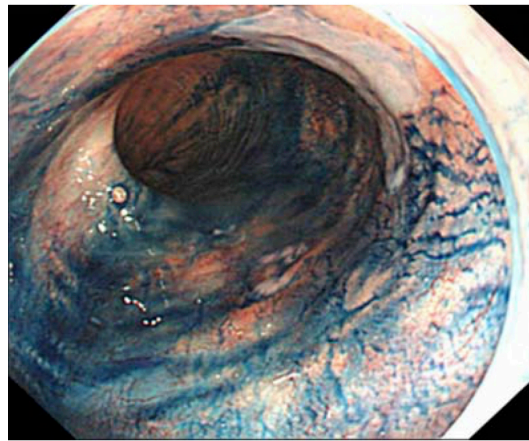


Figure 1.13: Chromoendoscopy using indigo carmine staining of Barrett's Oesophagus with High-Grade Dysplasia (Courtesy of gastrohep.com)

Methylene blue and indigo carmine are alternative stains that can highlight areas of intestinal metaplasia. They do not, however, aid the identification of areas of dysplasia within the intestinal metaplasia. Acetic acid enhances the surface topography allowing heightened feature enhancement. In some studies, it has been shown to be superior in the identification of dysplastic regions when compared to white light endoscopy (Longcroft-Wheaton *et al* 2011).

### 1.11.2.3: Narrow Band Imaging

Narrow band imaging uses electronically activated filters to limit the wavelength spectrum of blue and green light and to remove the spectrum of red light. This preserves the wavelengths which are absorbed by haemoglobin, resulting in attenuated delineation of the mucosal architecture based on the underlying vascular pattern. This pattern is altered in disease.

Studies using narrow band imaging revealed a high sensitivity for distinguishing gastric mucosa from intestinal metaplasia (Curvers *et al* 2009) and, using high magnification, for identifying high-grade dysplasia (Curvers *et al* 2009). Narrow band imaging is the most commonly used advanced imaging technique, excluding high resolution endoscopy, although only 14% of endoscopists referring patients to a tertiary centre had used this modality (Bennett *et al* 2015).

#### 1.11.2.4: Autofluorescence

All tissues produce autofluorescence when illuminated by ultraviolet (<400nm) or short visible (400 – 550nm) light. Naturally occurring molecules in the tissue, termed fluorophores, become excited, emitting a longer wavelength of fluorescent light. The number, concentration and distribution of these fluorophores in different tissue states produce distinct autofluorescent patterns (Kara *et al* 2004).

#### 1.11.2.5: Confocal Fluorescence Microendoscopy

This imaging technique is an extension of autofluorescence and, by imaging endogenous and exogenous fluorophores within the cells of the tissue sections, a histological image of the tissue can be produced (Kara *et al* 2007). High-grade dysplasia was able to be differentiated from non-dysplastic Barrett's in ex vivo samples using this method due to the alterations in the mucosal autofluorescent picture that occurs with dysplasia (Kara *et al* 2006).

#### 1.11.2.6: Optical Coherence Tomography

Optical coherence tomography is an imaging system that is, in some ways, akin to ultrasonography. It utilises electromagnetic waves to produce images based on the detection of reflected light as opposed to the detection of reflected sound (Filip *et al* 2011). The resolution of the system allows identification of villi, glands and capillaries (DaCosta *et al* 2003).

In vivo studies have shown that this modality can distinguish between squamous epithelium, columnar epithelium of Barrett's oesophagus and adenocarcinoma (Li *et al* 2000, Poneris *et al* 2001, Zuccaro *et al* 2001, Evans *et al* 2005, Evans *et al* 2006), yet the ability to differentiate between grades of

dysplasia was lower with a specificity of 75% for distinguishing high-grade dysplasia from adenocarcinoma (Evans *et al* 2006).

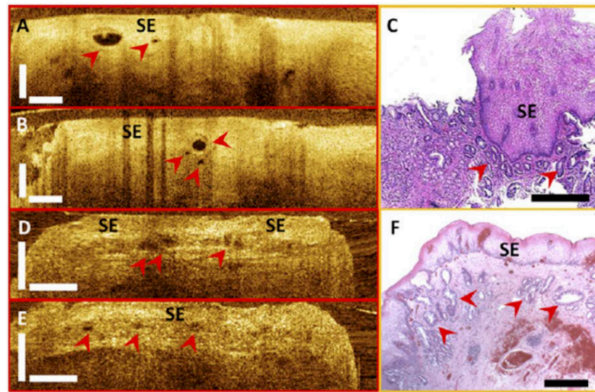


Figure 1.14: Cross-sectional optical coherence tomography images and corresponding histology showing buried glands (red arrowheads) from a patient *in vivo* (Courtesy of Tsai *et al* 2014)

A supplementary benefit of this modality is its ability to provide cross-sectional imaging which allows assessment of the depth of invasion as well as the presence of buried glands in a previously treated oesophagus (Figure 1.14). Developments in these fields are occurring with incorporation into capsule endoscopy for screening to detect Barrett's oesophagus.

#### 1.11.2.7: Spectroscopy

Spectroscopy utilises information that is obtained from the detection of changes in energy level in the molecules and bonds of a tissue that occur when the sample is excited by light.

Light scattering spectroscopy, also referred to as elastic scattering spectroscopy, uses the reflectance of scattered white light to provide microstructural information regarding the tissue. For example, nuclear enlargement and crowding can be detected and this information can be used to differentiate dysplasia with sensitivities and specificities of >90% (Wallace *et al* 2000).

The two other main forms of spectroscopy, Raman and Infra-red, will be discussed in greater detail in the next chapter.

## Section A: Literature Review

### Chapter 2: Vibrational Spectroscopy

#### 2.1: Fundamental Principles

##### 2.1.1: Electromagnetic Radiation

Electromagnetic radiation is a form of energy that exists all around us, taking many forms, including radio waves, gamma rays and visible light. It consists of electromagnetic waves which are synchronised oscillations of electric and magnetic fields which are created when an atomic particle is accelerated by an electric field.

The behaviour of electromagnetic radiation depends on its frequency and wavelength. Higher frequencies, such as gamma rays, have shorter wavelengths, whereas, lower frequencies at the other end of the spectrum, such as radiowaves, have longer wavelengths (Figure 2.1).

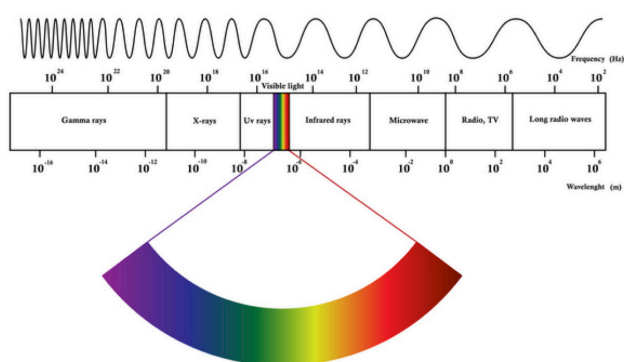


Figure 2.1: Electromagnetic Radiation Spectrum (Courtesy of LiveScience  
([www.livescience.com/38169-electromagnetism.html](http://www.livescience.com/38169-electromagnetism.html)))

Visible light is electromagnetic radiation that occurs in the wavelength range of 400-700nm, sandwiched between ultra-violet and infrared rays. In this region, the electromagnetic radiation consists of photons that are capable of causing



excitation that can lead to changes in molecular bonding or chemistry. At the lower end of this spectrum, in the infrared region, there is no visible light as the photons do not have enough individual energy to cause a lasting change in the conformation of the visible molecule.

### 2.1.2: Biospectroscopy

When light interacts with a material, the result is a number of different processes, including reflectance, transmission, scattering, absorption and vibration. These processes occur when the incident radiation induces changes in the energy level of the tissue. The change in energy state of the tissue is detected and has the ability to provide detailed biochemical information regarding the molecular composition and structure of the tissue.

Vibrational spectroscopy, namely infra-red (IR) and Raman spectroscopy, interrogate tissues in a non-destructive manner, producing spectra based on the interaction of light with the tissue. The spectrum is, in essence, an intrinsic molecular fingerprint, providing information regarding DNA, carbohydrate, protein and lipid content.

## 2.2: Raman Spectroscopy

### 2.2.1: Underlying Principles

Molecules consist of atoms which are held together by chemical bonds, each of which has a characteristic vibrational energy. When illuminated by electromagnetic radiation, the bonds vibrate as the molecule enters a virtual energy state. A photon, from the light source itself, is absorbed by the material, exciting an electron into a higher, albeit unstable, virtual energy level. As the electron decays back to a lower energy level, it emits this energy as a scattered photon. If the scattered radiation has the same wavelength as the electromagnetic radiation, this is termed elastic, or Rayleigh, scattering (Figure 2.2).

When the incident photon interacts with the electric dipole of the molecule, the excited electron decays back to a different energy level from that of its starting position due to interactions between the incident electromagnetic waves and

the vibrational energy levels of the molecules in the sample. This occurs in approximately  $1/10^6$ - $10^8$  photons and is termed inelastic scattering. The difference in energy level between the incident (non-scattered) photons and the scattered photons corresponds to the energy of the molecular vibration and is termed the Raman shift or scatter.

Two forms of Raman scattering exist. If the final energy level is higher than the original state, the inelastically scattered photon will be shifted to a lower frequency. This shift is known as a Stokes shift. If, however, the final vibrational state is less energetic, the photon will be shifted to a higher frequency, known as an anti-Stokes shift (Figure 2.3).

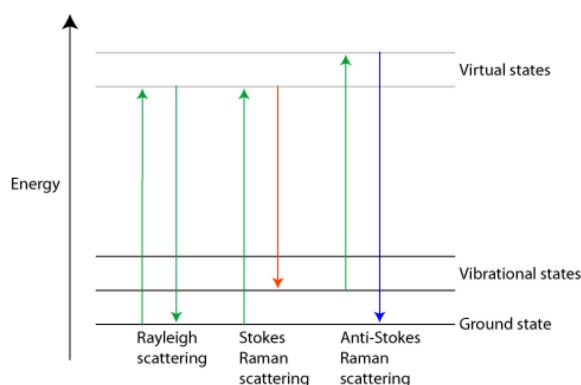


Figure 2.2: Stokes and Anti-Stokes Shift Pattern (Courtesy of SolTPoMS, University of Cambridge ([www.doitpoms.ac.uk/tlplib/raman/printall.php](http://www.doitpoms.ac.uk/tlplib/raman/printall.php)))

By detecting the scattered photons and their energy level, a unique spectrum is created. The Raman shift, measured in wavenumbers, is plotted on the x-axis against the intensity of the scattered light on the y-axis, as exemplified in figure 2.3. The unique spectrum of Raman peaks based on the bonds present provides an abundance of information regarding the chemical bonds associated with DNA, RNA, proteins, lipids, carbohydrates and other biomolecules. The intensity of the scatter is directly proportional to the concentration of molecules within the specimen and, hence, quantitative information can also be attained.

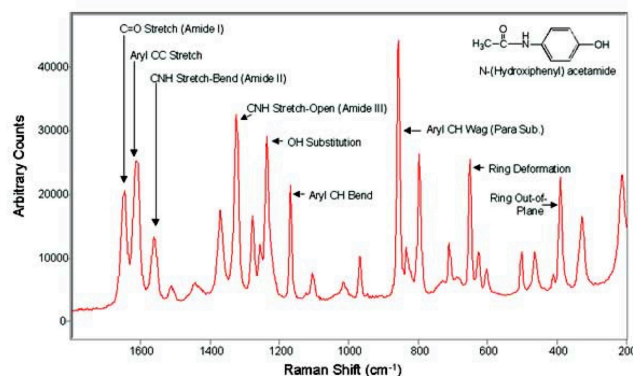


Figure 2.3: Example of a Raman Spectrum (Courtesy of Eckenrode *et al* 2001)

### 2.2.2: Challenges and Advantages to Raman Spectroscopy of Biological Samples

The main difficulty faced with Raman spectroscopy is its inherently weak signal. Raman spectroscopy detects inelastically scattered photons, however, only a fraction,  $1/10^6$ - $10^9$ , of photons undergo this form of scattering (Kendall *et al* 2009). The weak signal is further compounded by ambient light. This needs to be removed to avoid distracting and confusing spectral contributions. Raman spectrometers must, therefore, aim to exclude all confounding signals.

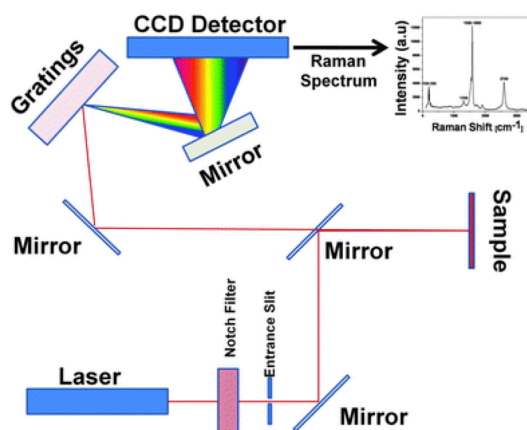


Figure 2.4: Schematic Representation of a Raman Spectrometer (Courtesy of Biswas *et al* 2010)

In a Raman spectrometer, the monochromatic light from the laser is focused onto the sample. Scattered light is reflected and filtered through a series of steps to eliminate any light that is elastically scattered, thereby, enhancing the signal (Figure 2.4). Diffraction grating splits the beam, based on its wavenumber, prior to its reflection onto the charge-coupled detector (CCD). The CCD registers the number of photons at each region and translates this into a specific spectral map of the sample.

A number of advanced Raman-based technologies which are able to produce a stronger signal have been developed and are currently being investigated in the research domain. Coherent anti-Stokes Raman spectroscopy (CARS), for example, employs multiple photons, whereas, surface enhanced Raman spectroscopy (SERS) uses specially prepared metal surfaces or nanoparticles to enhance the signal. Other examples of advanced techniques that utilise and adjust the energy from the incoming laser source are resonance Raman and resonance hyper Raman spectroscopy.

A further disadvantage of Raman is that it is only able to penetrate a few hundred microns into a tissue sample (Matousek and Stone, 2009). This is particularly relevant when considering the use of this technology in-vivo. Spatially offset Raman spectroscopy (SORS) uses the principle that photons migrate and measure spectra from surface areas at distances from the excitation point. A scaled subtraction of the spectra from spatially offset points enables the production of pure spectra from the individual layers of the sample (Matousek 2009), enabling the determination of the depth of dysplastic changes.

The Raman signals from the –OH bonds present in water molecules are very weak, resulting in an insignificant contribution of water molecules to the resultant spectra (Kong *et al* 2015). This is extremely advantageous as it allows the examination of fresh tissue without prior preparation. This, therefore, allows this technology to be utilised for real time in vivo sampling and analysis. This is in contrast to FTIR Spectroscopy where the influence of water remains a significant dilemma.

Spectroscopic analysis, including both Raman and FTIR, is a tremendously attractive diagnostic tool. It is able to provide information on the biochemical

constituents of tissue and, thus, could detect biochemical and molecular changes that predate morphological alterations, allowing identification of at risk individuals, and enabling early, less invasive treatment. It may assist with the significant subjectivity and, therefore, inter and intra observer variability that can exist when analysing and assigning pathological classification based on morphological changes alone.

Automated classification systems could be developed for use in the laboratory in conjunction with histopathology to enable earlier and less subjective detection of cancerous and precancerous changes. This system would, in addition, free up valuable histopathologist time to analyse certain pathological samples rather than the reams of biopsies from endoscopic surveillance. This would be an economically attractive option.

The development of fibre-optic probes, in addition, has paved the way for in vivo measurements with the added benefits of real time diagnosis, thus, helping to identify potentially abnormal areas at the time of imaging and highlighting areas of the oesophagus requiring further examination.

### 2.2.3: Clinical Applications of Raman Spectroscopy in the Oesophagus

Raman spectroscopy has long been shown to be able to discriminate between different pathological states in the oesophagus. In an analysis of snap-frozen biopsy samples, this technology accurately discriminated between 8 pathology groups, including different subtypes of Barrett's oesophagus such as the presence of intestinal metaplasia (Kendall *et al* 2000).

The biochemical changes underlying the spectral differences seen in the different pathological states have been determined (Shetty *et al* 2006). Higher levels of DNA, actin and oleic acid, for example, are present in dysplastic glandular tissue and cancerous tissue, likely signifying the abnormal DNA content and hyperchromatic state of neoplastic cells (Bergholt *et al* 2011). In contrast, higher levels of glycogen are seen in normal squamous tissue representing the normal metabolism of glucose that occurs in non-neoplastic tissue (Bergholt *et al* 2011).

This technology has not yet made its move into routine clinical practise. One area where it could be utilised is that of real time diagnosis. From the turn of the century, a number of research groups have trialled in vivo Raman probes. Work in 2011 demonstrated that the identification of cancer in the oesophagus could occur with a sensitivity of 91% and a specificity of 94% and, importantly, with an acquisition time of 0.4-0.5 seconds (Bergholt *et al* 2011). Dysplastic change was, however, not differentiated in this study. Earlier studies had shown that with a variety of probes, predominantly in ex vivo samples, different grades of dysplasia were able to be determined with a range of sensitivities and acquisition times (Shim *et al* 2000, Wong *et al* 2005, Wong *et al* 2005a, Almond *et al* 2012, Almond *et al* 2014).

The technological development of Raman probes will help to advance the use of this technology and studies are currently being planned and in progress. The use of a real time probe may reduce the need for multiple biopsies and their associated small complication risk. A major limitation, nevertheless, is the ability of the Raman probe to interrogate only a small volume of mucosa at one time. This will undoubtedly prevent its use as a wide field scanning modality, however, it will still be an ideal adjunct to the clinical diagnostic arsenal for point measurements to aid diagnosis and to determine margins following endoscopic resection.

An alternative place for this technology is in the laboratory as an adjunct to histopathology in ex vivo samples. It has been shown that 2mm diameter sections can be mapped over a time period of 30-90 minutes which enables the accurate discrimination of pathology (Hutchings *et al* 2010). This tool could be utilised in samples where histopathology has not reached a consensus regarding the diagnosis and, thus, act as a third expert.

## 2.3: Fourier-Transform Infra-Red Spectroscopy

### 2.3.1: Underlying Principles

William Herschel initially discovered infrared radiation (IR) in 1800. Many decades later, in the 1970s, commercially driven IR spectrometers led to the

broad application of IR spectroscopy and its position as one of the most important analytical methods in science.

When infrared radiation is beamed onto a tissue sample, the chemical bonds present in the molecule vibrate. The vibrations consist of symmetrical stretching, asymmetrical stretching, scissoring, rocking, wagging and twisting (Figure 2.5). If the frequency of the vibration of the chemical bond equals that of the infrared radiation, the result is a temporary alteration in the dipole moment of the molecule.

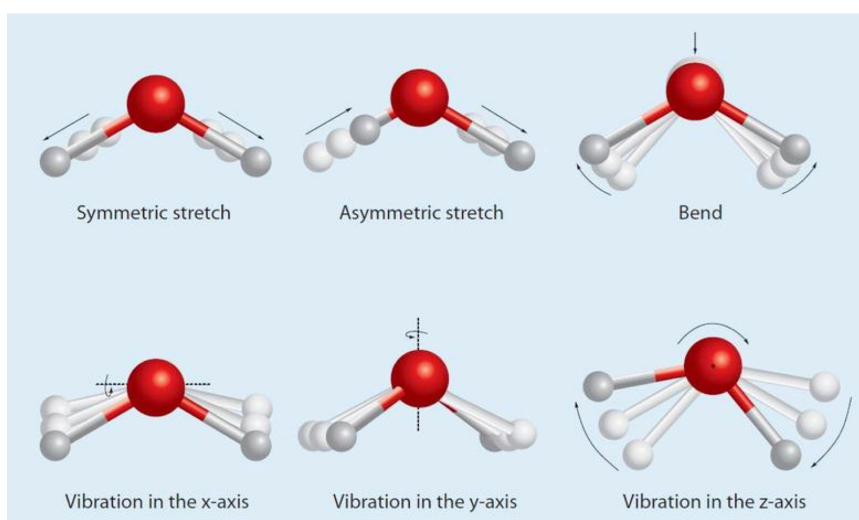


Figure 2.5: Schematic Diagram of some of the vibrations that molecular bonds undergo when excited ([skcchemistry.wikispaces.com](http://skcchemistry.wikispaces.com))

The change in the dipole moment results in the formation of light. By measuring this transmitted light, the energy absorbed at each wavelength is determined. An absorbance spectrum, as exemplified in figure 2.6, is produced.

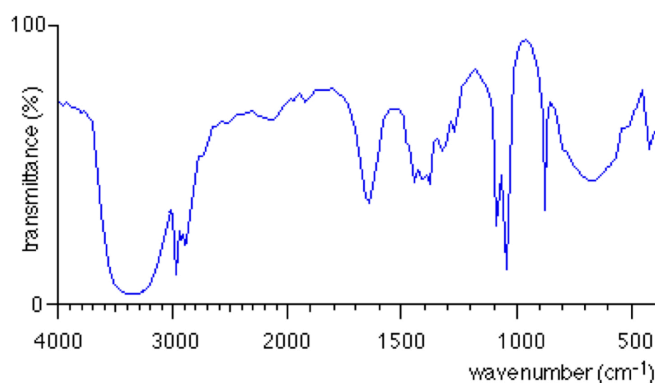


Figure 2.6: Infrared Spectrum of Ethanol ( $\text{CH}_3\text{CH}_2\text{OH}$ ) (chemguide.co.uk)

The first commercial Fourier Transform Infrared (FTIR) spectrometer was pioneered by Digilab in 1969. In this spectrometer, an interferometer is used to guide the infrared beam through the sample (Figure 2.7). A moving mirror allows information from multiple wavelength frequencies to be collected simultaneously and subsequently distributed. This results in a higher signal-to-noise ratio for a given scan time, known as Fellgett's advantage, leading to superior results when compared to a scanning (dispersive) spectrometer.

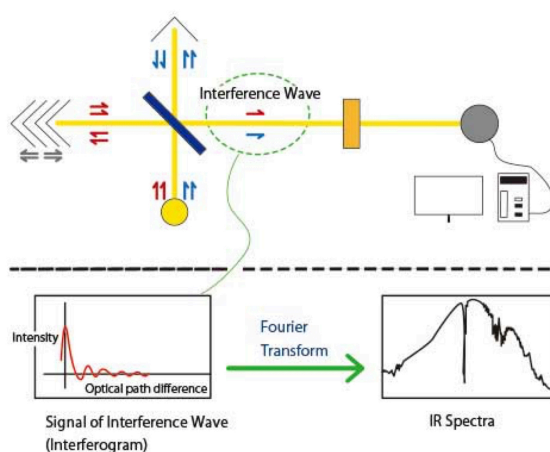


Figure 2.7: Schematic Representation of FTIR Spectroscopy (courtesy of Jasco, UK)



### 2.3.2: Challenges and Advantages to FTIR Spectroscopy of Biological Samples

The advantages of FTIR include the ability to gain information in a non-destructive manner from a small amount of tissue and to gain this information in a short amount of time.

Water is highly absorbent in the mid infrared range of  $400 - 4000 \text{ cm}^{-1}$ . This is the range at which most other vibrations occur and, thus, masks the vibrations from the tissue sample itself. As the majority of biological tissue has high water content, the ability of FTIR to gain meaningful data from in vivo measurements is limited.

There is, however, an intense drive to be able to produce real time, in vivo measurements. Fibre-optic evanescent wave spectroscopy (FEWS)-FTIR with endoscope compatible fibre-optic silver halide probes have been shown, in the research setting, to be feasible (Mackanos *et al* 2010), and allow in vivo measurements.

FTIR is ideal for use with paraffin-embedded tissue samples as, although paraffin is visible in the fingerprint region, this can be overcome with spectral subtraction and, hence, not affect interpretation of the tissue. These preparations are routinely used in histopathology for Haematoxylin and Eosin (H&E) staining and immunohistochemistry and, thus, the technique of FTIR could be used as an adjunct in the laboratory without additional sample preparation and the associated costs that would entail.

### 2.3.3: Clinical Applications of FTIR in the Oesophagus

The development of adenocarcinoma follows an established pathway, commencing prior to the establishment of any visible morphological changes. DNA, protein, glycoprotein and glycogen produce peaks in the wavelength range of  $950 - 1800 \text{ cm}^{-1}$  and differences in these peaks are seen in low-grade dysplasia. Studies have shown that these changes are able to identify and classify dysplasia in fresh oesophageal samples with a high sensitivity of 92% and a specificity of 80% (Wang *et al* 2007).

The ability of FTIR to distinguish pathologies in paraffin embedded samples has also been demonstrated. Glycoproteins from goblet cells, the characteristic feature of intestinal metaplasia, were identified based on their spectral changes (Quaroni and Casson 2009).

## 2.4: Autofluorescence

### 2.4.1: Underlying Principles

Some tissues produce fluorescence when they are illuminated. Fluorophores, the constituent biomolecules of the tissue, absorb a photon of high energy when illuminated. This results in the excitation of an electron into a vibrational state of higher energy. As the electron relaxes into its ground state, a photon of lower energy is released, causing the emission of light (Figure 2.8). Unlike in Raman spectroscopy, however, the resultant fluorescence is dependent on the frequency of incident light.

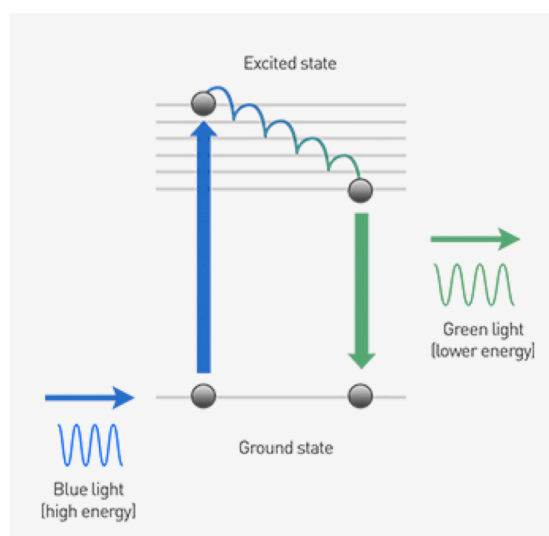


Figure 2.8: Schematic Representation of Autofluorescence

(Image courtesy of Thermo Fisher Scientific)

Most fluorophores are found in the submucosa, with collagen and elastin contributing highly green fluorescent signals. Epithelium and lamina propria in the mucosa provide a weaker contribution (Figure 2.9). Disease processes result in different autofluorescent patterns due to alterations in the type,

concentration and microdistribution of fluorophores that accompany the changes in the mucosa that are part of the disease process.

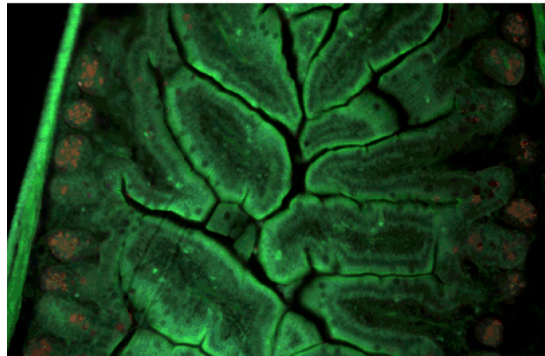


Figure 2.9: Autofluorescent image of the intestine of a mouse (en.wikipedia.org)

Confocal Fluorescence Microscopy (CFM) permits high resolution imaging of ex vivo tissue samples, yielding a wealth of information of the intrinsic cellular and extracellular autofluorescence as well as the microstructure of the tissue.

#### 2.4.2: Challenges and Advantages to Autofluorescence of Biological Samples

A significant advantage of autofluorescence is its ability to sample wide areas of the mucosal surface in a short space of time, meaning that the entire oesophagus can be sampled in a single endoscopy. This is in comparison to the spectroscopy techniques described above which can only sample a small area at one time.

The major disadvantage seen in all studies involving autofluorescence, not only those involving the oesophagus, is the non-specificity of these changes. Acute inflammation results in changes in the vascularity of the tissue. Changes in the vasculature also occur in dysplasia and it is impossible to detect the underlying cause of the changes using autofluorescence.

#### 2.4.3: Clinical Applications of Autofluorescence in the Oesophagus

Imaging of tissue autofluorescence is undertaken in real time, enabling interrogation of the entire mucosal lining. The first fluorescence endoscopic imaging system had varying results. Initial studies suggested that, in comparison to white light endoscopy alone, this system improved the detection

of early neoplasia (Haringsma *et al* 2001, Niepsuj *et al* 2003). Subsequent studies, however, found that the technique added no additional diagnostic value (Kara *et al* 2005).

The next generation system, which utilised green autofluorescence in addition to red, improved the sensitivity in the detection of severe neoplasms (Haringsma *et al* 2005). The newest development that has followed is a video-endoscopic system with the ability for white light and autofluorescent imaging. Normal squamous and non-dysplastic Barrett's oesophagus appear as a green discolouration, whereas, areas of high-grade dysplasia or oesophageal carcinoma have a blue to purple discolouration which improved the ability to detect these areas.

High-grade dysplasia was distinguishable by the increase in nuclear-to-cytoplasm ratio, causing a reduction in the amount of autofluorescent light, which is then detected by a change in the autofluorescent signal (Kara *et al* 2005). In addition, thickening of the mucosal layer occurs in early neoplastic lesions and leads to the attenuation of autofluorescence in this layer. Tissue haemoglobin absorbs light and as the vascularity and, hence, haemoglobin concentration changes, so too does the fluorescent signal.

The changes are, nevertheless, subtle and there was found to be an overall comparable red-green autofluorescent intensity ratio between Barrett's oesophagus with and without dysplasia suggesting that these changes alone are inadequate to detect areas of dysplasia. The obvious advantage of wide field viewing of autofluorescence would make it an ideal adjunct to a technology, such as Raman spectroscopy, that has higher sensitivity and specificity. Autofluorescence could identify the areas of mucosa of greatest interest which spectroscopy could then analyse to determine the presence of dysplasia. This combination, to date, has not been tested in research or clinical trials.

Additional work investigating autofluorescence in the colon has shown the presence of high numbers of autofluorescent lysosomal granules in dysplastic epithelial cells which could be diagnostic for dysplasia (DaCosta *et al* 2005). The lysosomal granules contain lipofuscin and may represent dysregulated 'waste disposal' in these cells, and/or are linked to high rates of cell apoptosis,

both of which are possible processes occurring in dysplastic change. If lipofuscin, or the lysosomes containing lipofuscin, or a similar molecule, is shown to be a reliable marker of dysplasia, and is shown to have a signature autofluorescent pattern, then this would enable the accurate detection of dysplasia. Currently, however, no such marker has been identified.

## 2.5: Point Spectra versus Imaging Mapping

Spectroscopy techniques can be utilised in two ways. Point measurements, where a single point of the sample, is measured; or mapping where a larger section of the sample is measured. The benefit of point spectra is the speed of acquisition of the measurement, however, as changes in tissue are not uniform, there is a risk that vital information is missed. For example, if the changes that depict dysplasia are not in the point sampled, then the diagnosis cannot be made. This can, however, be overcome by taking multiple point measurements for each sample.

Image mapping, on the other hand, generates a detailed chemical image of the sample. A complete spectrum is acquired at each and every pixel of the image, and then interrogated to generate false colour images based on the molecular composition and structure. The sacrifice for this volume of information is the time required to map the sample, often being multiple hours, and occasionally extending into days. This makes mapping impossible to perform in real time, in vivo measurements as it would be unfeasible to maintain tissue contact with a peristalsing GI tract for the length of time required, not to mention the effect on the patient.

## 2.6: Chemometrics

Analysis of biological samples is inherently complex due to the quantity of constituents within them. Chemometric analysis, when applied to the measured spectra, interprets the wealth of information obtained, to detect any qualitative or quantitative biochemical changes existing between samples. Statistical analysis can then be applied to identify and quantify the differences that may exist between samples.

Principal Component Analysis (PCA) and Linear Discriminant Analysis (LDA) are techniques that are frequently applied to the database of measured spectra. These techniques are able to extract biochemical information and to convert the information into a predicted diagnosis.

Pre-processing steps can also be included to improve the performance of pattern recognition. Extended Multiplicative Scatter Correlation (EMSC), for example, is used to reduce the influence of confounders, such as paraffin, on the resultant spectrum.

#### 2.6.1: Principle Component Analysis (PCA)

PCA is an orthogonal linear transformation technique which transforms correlated variables into linearly uncorrelated variables, called principle components. The first principle component comes to lie on the first coordinate and contains the largest degree of variance which exists in the data set. The second principle component, which occupies the second coordinate, accounts for the next highest amount of variability and so on. Analysis of variance (ANOVA) can be applied to the principle components to identify which have the greatest variance and, hence, which should be used to build the resultant classification models.

#### 2.6.2: Linear Discriminant Analysis (LDA)

LDA is a similar statistical method which expresses one dependent variable as a linear combination of other features or measurements. LDA takes into account information from the group that the data originated from and, hence, is known as a 'supervised' technique. This is in contrast to PCA which assumes no prior knowledge or information and is, thus, termed an 'unsupervised' method. By taking into account information from the group, LDA maximises the differences between groups, whilst minimising the differences that exist within the group.

#### 2.6.3: Training Models and Leave One Sample Out Cross Validation (LOSOCV)

The analysis techniques described above are used to produce a classification model. This model can then be tested to see how the results will generalise to an independent data set. If this test is done using the training dataset, a falsely

optimistic performance can be inferred as the data being tested is contained within the dataset.

The use of a separate dataset where the data being tested was not used to, or contained within the classification model is a preferable situation and prevents to possibility of overfitting. This, however, requires a larger dataset which is often not feasible or practical. Removal of the sample being tested from the dataset without the need for a separate database is a compromise which prevents overfitting without unduly affecting the number of samples required. This testing technique is known as leave one sample out cross validation (LOSOCV).

## Chapter 3: Aims and Objectives

### 3.1: Introduction and Aims

There are areas in the understanding of and management of Barrett's oesophagus that require further research in order to transform the care of patients and to reduce the incidence of oesophageal adenocarcinoma. The British Society of Gastroenterology (BSG) guidelines express, in their recommendations, 11 areas that require investment and development. The use of advanced imaging modalities to improve the detection of dysplasia and the cost effectiveness of this endeavour as well as more studies on the natural history of Barrett's oesophagus, especially in the context of LGD are just 2 of the themes.

Oesophageal adenocarcinoma is preceded by the development of dysplasia in a segment of Barrett's oesophagus. With the current endoscopic diagnosis and surveillance, it is difficult to visualise areas of dysplasia and, once biopsied, to ascertain definitively the presence and grade of dysplasia. Years of research have looked at a variety of imaging modalities that could aid the identification of dysplasia.

The vibrational spectroscopy techniques of Raman and FTIR, as well as tissue autofluorescence, offer a number of potential advantages as tools for clinical diagnosis. As well as a less subjective identification of dysplasia and the capacity for real-time diagnosis, these technologies may also be able to identify changes that occur prior to any morphological changes. There may be changes that occur that help to differentiate, for example degrees of low-grade dysplasia, that have previously been classified together and may enable risk stratification for these patients.

This research aims to further the understanding of these advanced imaging modalities, predominantly their ability to predict and understand biochemical changes that exist between the different pathological states.



### 3.2: Objectives

The objectives for this thesis are:

- 1) To develop classification models based on Raman point-based and Raman map-based measurements;
  - a. that classify Barrett's oesophagus without dysplasia from Barrett's oesophagus with dysplasia.
  - b. that classify Barrett's oesophagus with low-grade dysplasia from Barrett's oesophagus with high-grade dysplasia and adenocarcinoma.
- 2) To compare the results obtained from point and map-based measurements to determine if the classification model developed from the point-based measurements is able to predict the pathology classification of data from the map-based data.
- 3) To analyse potential biochemical peak assignments from the point-based measurements to ascertain the biochemical changes that are seen in the different pathology states.
- 4) To see if we can determine where low-grade dysplasia fits on the spectrum of Barrett's oesophagus without dysplasia through to oesophageal adenocarcinoma and if there are any features that indicate the risk of progression for these patients.

## Section B

### Chapter 4: Methodology

#### 4.1: Ethical Approval

Ethical approval for the project was granted by the Gloucestershire Local Ethics Committee as a non-substantial amendment of the SMART project. The SMART (Stratified Medicine through advanced Raman Technologies) project was granted ethical approval in 2015. Archived tissue samples, identified from hospital pathology databases, were used. No fresh tissue samples were collected for the study and, therefore, patient consent for tissue use was not required, nor obtained.

#### 4.2: Sample Collection

##### 4.2.1: Identifying Samples

Samples were identified from a hospital database which had been created by the pathology lab manager. The database recorded all oesophageal biopsy and oesophagectomy samples from June 2013 to December 2015. The samples had been coded as Barrett's oesophagus (+/- dysplasia) or oesophageal adenocarcinoma based on the pathology review completed at the time of sample acquisition for clinical purposes. Each sample was recorded with a unique code and, thus, pseudo-anonymised with the researcher not seeing any patient identification details.

For some samples, a second pathologist opinion had been sought as part of the clinical diagnostic process. This was according to the protocol in practise at the time of sample acquisition. BSG guidelines from 2013 (Fitzgerald *et al*) state that all cases of suspected dysplasia are reviewed by a second GI pathologist, with review in a cancer centre if intervention is being considered.

Specimens of Barrett's oesophagus without dysplasia, Barrett's oesophagus with low-grade dysplasia, Barrett's oesophagus with high-grade dysplasia and adenocarcinoma were selected based on their original histopathology report. 10 specimens from each group were selected. An additional 10 samples from normal squamous lined oesophageal biopsies were selected as the control group.

Once the cases had been identified, the samples were located from the pathology laboratory based at Cheltenham General Hospital. The archived samples had been routinely processed at the time of their acquisition and kept in paraffin embedded tissue blocks in ideal conditions according to the local departmental protocols.

50 samples in total were chosen for analysis (10 from each group of; normal squamous, Barrett's oesophagus without dysplasia, Barrett's oesophagus with low-grade dysplasia, Barrett's oesophagus with high-grade dysplasia and adenocarcinoma). The samples had been acquired during the time period of November 2014 to February 2016.

#### 4.2.2: Processing of Samples

Acquisition of samples took place in the histopathology laboratory at Cheltenham General Hospital in July and August 2016. Once the paraffin-embedded tissue blocks had been located and sourced from the storage department, contiguous sections of 7  $\mu\text{m}$  thickness were prepared on calcium fluoride slides. Contiguous samples are used so that each section closely resembles the other sections, thus, ensuring correlation between histology and spectroscopic measurements.

Calcium fluoride slides were selected as calcium fluoride produces only 1 significant Raman peak which is not only distinct, but occurs at a wavelength ( $323\text{ cm}^{-1}$ ) outside that of the wavelength range in which tissue produce spectra ( $400 - 1800\text{ cm}^{-1}$ ) and, thus, can be eliminated from data analysis. In addition, calcium fluoride produces a low background intensity.

The calcium fluoride slides, once prepared, were placed in plastic coin cases to prevent scratching and other forms of physical damage and to reduce the likelihood of dust and other micro-particles affecting the sample. Each coin case was labelled with the unique code assigned from the histology database. The coin cases were stored in the Biophotonics Research Unit at Gloucestershire Royal Hospital.

#### 4.2.3: Confirmation of Histology

The samples used for analysis were selected based on their histological diagnosis, given at the time of sample acquisition. This diagnosis was produced from an experienced histopathologist employed at Gloucestershire Hospitals NHS Foundation Trust. In some instances, two opinions had been sought to confirm the diagnosis.

The areas of the section that were felt to strongly represent the overall pathology were identified according to the microscopic features (for example, appearance of glandular tissue) by a post-doctoral research fellow in the Biophotonics lab. This was to ensure that spectral measurements would be taken from the appropriate area, and from the same area for the differing technologies. This was important as sections may show a heterogeneous mix of pathologies.

#### 4.3: Sample Measurement

##### 4.3.1: Pre-measurement Preparation

For each sample, the H&E section was scanned, in high resolution, onto computer software (Microsoft PowerPoint 2016). This allowed the regions that best reflect the overall diagnosis to be highlighted and labelled. On average, four regions were selected for each sample. Selection of regions also ensured that the same area was used for measurement on each modality.

Archived tissue blocks are embedded in paraffin wax as this provides support for the tissue and ensures durability for long term storage without deterioration of the tissue sample. Paraffin wax, nevertheless, produces a significant Raman signal (Figure 4.1) with distinctive peaks (at  $888\text{cm}^{-1}$ ,  $1061\text{cm}^{-1}$ ,  $1131\text{cm}^{-1}$ ,  $1171\text{cm}^{-1}$ ,  $1294\text{cm}^{-1}$ ,  $1417\text{cm}^{-1}$ ,  $1440\text{cm}^{-1}$  and  $1462\text{cm}^{-1}$ ). These peaks are in the fingerprint region and would, therefore, render the interpretation of tissue spectra impossible. The sections were, therefore, deparaffinised according to local protocol (Appendix I) using Hexane ( $\text{C}_6\text{H}_{14}$ ) prior to commencing Raman measurements. The samples were deparaffinised in batches which were selected at random and contained a mixture of pathologies.

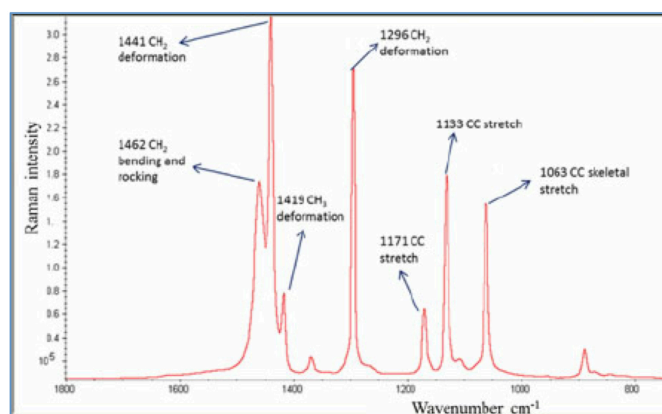


Figure 4.1: Raman Spectral Measurement of Paraffin Wax (Mian *et al* 2014)

For all samples, Raman point spectra were taken initially, followed by Raman mapping at a later date, although the time interval between the two modalities varied. The samples were stored in plastic coin cases between measurements to avoid contamination. In general, samples were not measured in group order to ensure that any variables such as temperature and humidity did not affect one pathology group to a greater extent. The exception to this was, however, the normal squamous epithelium samples which were obtained at a later date and, thus, measured as a cohort in the latter days of measurement.

Autofluorescence measurements are unaffected by paraffin and, thus, these measurements were taken from a contiguous slide which had not been deparaffinised on a different date. As these measurements were not the main focus of the research, only 10 samples were used.

#### 4.3.2: Raman Point Spectra Measurements of Oesophageal Tissue

Raman point spectra were measured using the Renishaw System 1000 at the Biophotonics Research Unit at Gloucestershire Royal Hospital (Figure 4.2) using 830 nm NIR excitation from a diode laser source. Calibration was carried out by the user on each occasion that measurements took place. Silicon is used to calibrate the Raman shift wavenumber value as it has a single sharp peak at  $520.4 \text{ cm}^{-1}$  which is then used as a reference point. Manual entry of the required wavenumber offset is entered as required.

A standard sample of green glass is measured to detect spectrometer detector sensitivity. Green glass has a smooth fluorescent spectral signal with four

Raman peaks across a broad wavenumber range. An energy transfer function correction can be applied to correct for variations in detector sensitivity. Cyclohexane is used in the calibration process to detect changes in laser wavelength. The distinctive peaks of cyclohexane which appear at 801, 1027, 1264 and 1441  $\text{cm}^{-1}$  enable the recognition of any wavenumber drift.

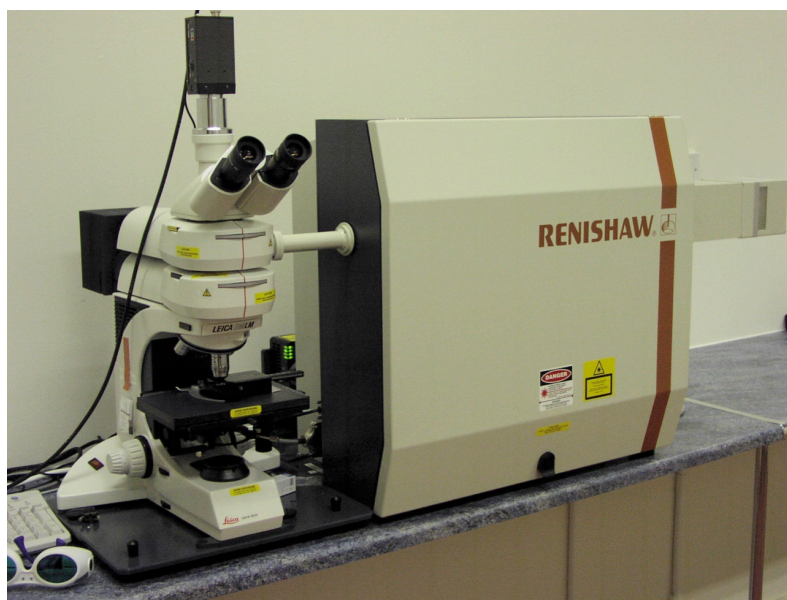


Figure 4.2: Renishaw System 1000 at the Biophotonics Research Unit

The deparaffinised samples on calcium fluoride slides were measured with an acquisition time of 30 seconds using a Leica x50 magnification. Signal to noise ratio is proportional to the square of the intensity of incident light multiplied by the acquisition time. An acquisition time of 30 seconds was, therefore, selected as this provides an appropriate sampling time without compromising on spectral information.

Each of the 50 samples had an average of 4 regions (range 1 – 4 regions) which had been preselected as described. An average of 15 point spectra were measured in succession from random points, selected manually, within each region. Once measured, the samples were stored in plastic coin cases to await Raman mapping.

### 4.3.3: Raman Mapping of Oesophageal Tissue

Raman maps were measured using the Renishaw RA800 Series bench top Raman system at the Biophotonics Research Unit in Gloucestershire Royal Hospital (Figure 4.3). This system uses an excitation wavelength of 785 nm, a long working distance (50x) Leica objective lens to focus the laser beam and a motorised xyz stage to move the sample under the linear laser beam.

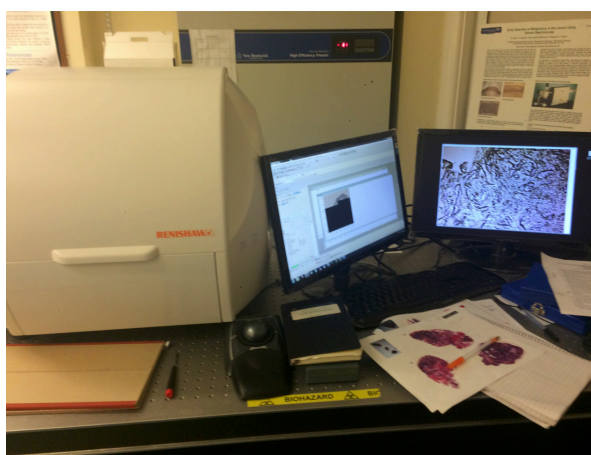


Figure 4.3: Renishaw RA800 Series at the Biophotonics Unit

Prior to any sample measurements, the instrument was calibrated. On this system, an automated process, known as Performance Qualification, optimised system alignment and made wavenumber adjustments based on known reference standards of green glass, silicon and polymer readings.

Raman streamline mapping is performed by moving the sample on the motorised stage under the laser beam. Streamline mapping generates high definition 2D chemical images of very large sample areas rapidly by illuminating with a line of laser light. This prevents laser induced sample damage and ensures that a high quality image is produced. The size and area of the section to be mapped was based on the regions selected on the high resolution H&E stain. This ensured that the same area that had been analysed with point spectra was captured for mapping. The size of the section was selected to ensure capturing within the selected area with an appropriate timeframe.

On average, two regions from each sample were mapped (range 1 – 4 regions) with a diverse range of size area depending on the size of the area of interest and the time. The larger maps were typically from samples of adenocarcinoma which had a single larger section of interest as compared to the other pathologies which had multiple smaller areas of interest.

#### 4.3.4: Autofluorescent Imaging of Oesophageal Tissue

Autofluorescence was measured using the Leica TCS SP5 Confocal System (Figure 4.4) at the University of Exeter. Ten specimens, two from each pathology set (Normal squamous epithelium, Barrett's oesophagus without dysplasia, Barrett's oesophagus with low-grade dysplasia, Barrett's oesophagus with high-grade dysplasia and Adenocarcinoma), were measured on the same day at three different wavelengths (476, 488 and 496nm).



Figure 4.4: Confocal Fluorescence Microscopy System at the University of Exeter

Paraffin embedded specimens mounted on calcium fluoride slides were used. These samples were not the same as those used for the Raman measurements, but were adjacent cuts from the same specimen block. Paraffin does not produce an autofluorescent signal at these wavelengths and, thus, deparaffinisation was not undertaken prior to sample measurement.



The same area that was used to measure both Raman point spectra and Raman maps was selected for autofluorescent measurement. Measurements from each wavelength were taken sequentially.

#### 4.4: Data pre-processing and Analysis

In-house software programs written in Matlab® R2016a (Mathworks, USA) were developed for the pre-processing and data analysis of Raman point spectra and Raman mapping data. Data was analysed by PCA (principle component analysis), LDA (linear discriminant analysis) and LOSOCV (leave one sample out cross validation).

## Section C: Summary of Measurements, Results and Analysis

### Chapter 5: Summary of Measurements

#### 5.1: Raman Point Spectra of Oesophageal Tissue

10 samples of each pathology type (Normal squamous, Barrett's oesophagus without dysplasia, Barrett's oesophagus with low-grade dysplasia, Barrett's oesophagus with high-grade dysplasia and oesophageal adenocarcinoma) were selected. 1 sample, initially classified as Barrett's oesophagus with high-grade dysplasia, was reclassified based on histopathological review to low-grade dysplasia.

Pathology	Number of Samples	Number of Regions
Normal Squamous	10	32
Barrett's oesophagus without dysplasia	10	33
Barrett's oesophagus with low-grade dysplasia	11	37
Barrett's oesophagus with high-grade dysplasia	9	30
Oesophageal adenocarcinoma	10	29

Table 5.1: Number of Samples and Regions per pathology

1 to 4 regions from each sample were used for point spectra measurements, resulting in a range of 29 to 37 regions depending on pathology (Table 5.1). The regions had selected based on the quality of that area for defining the pathology of the sample as a whole. They were identified and highlighted on scanned H&E sections as described in the methods section. The scanned images were used to identify the correct area at the time of measurement (as depicted in Figure 5.1).

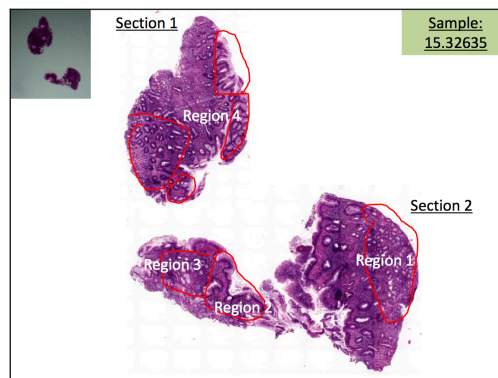


Figure 5.1: H&E Stained Sample indicating the areas to be used for measurements

From each region, approximately 15 point spectra were measured. Following measurements, each spectrum was analysed and compared to the mean of the sample. Spectra which contained cosmic rays or which were significantly abnormal compared to the other spectra from that sample were eliminated prior to analysis. The number of spectra measured and the number eliminated is shown in Table 5.2.

Overall 16% of the measured spectra were eliminated from the final analysis. Of note, the highest percentage of eliminated spectra was from the normal squamous specimens. These samples were measured separately over a period of 2 days in September at the end of the study period due to delayed procurement of these samples. Samples from the other 4 groups were measured in a random order over the course of 12 days in August. It may be that the conditions on the days on which the normal squamous samples were measured were subtly different resulting in a higher proportion of abnormal spectra.

<u>Pathology</u>	<u>Number of Point Spectra Measured</u>	<u>Number of Point Spectra eliminated</u>	<u>Number of Point Spectra for Analysis</u>
Normal Squamous	467	107 (23%)	360
Barrett's oesophagus without dysplasia	470	61 (13%)	409
Barrett's oesophagus with LGD	588	86 (15%)	502
Barrett's oesophagus with HGD	490	87 (18%)	403
Oesophageal adenocarcinoma	465	61 (13%)	404
Total	2480	402 (16%)	2078

Table 5.2: Summary of Measured and Eliminated Point Spectra

In total 2480 spectra were measured on 14 days in a 2 month period. After elimination, 2078 point spectra remained for analysis. Appendix II details all samples measured.

## 5.2: Raman Mapping of Oesophageal Tissue

The same samples that were used for point spectra measurements were then used for Raman Map Measurements. Between measurements, the samples were stored at room temperature out of the light in protective plastic coin cases, nevertheless, three slides were damaged and were unable to be used for mapping measurements. The time between measurements on the two systems ranged from 6 hours to 37 days, although the vast majority were completed within 7 days. 8 samples had a delay of greater than 7 days from point measurement to mapping due to availability of the Raman mapping machine which was also being utilised for other research projects as well as availability of the researcher. During this research project, clinical on-calls were continued. These occurred in a 3 week block every 9 weeks and meant that measurements had to be suspended during this time.

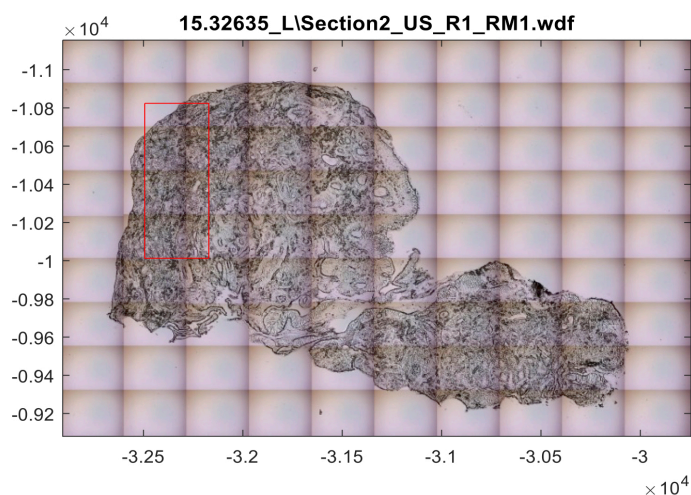


Figure 5.2: White light image of tissue sample produced and area selected for mapping

The number of regions selected for each sample was based on the size of the region and, thus, fewer areas were utilised for mapping when compared to the point spectra measurements. The complete sample was scanned, as indicated in Figure 5.2, and the region selected by comparison with the H&E stain. The number of specimens and regions are shown in Table 5.3.

<u>Pathology</u>	<u>Number of Samples</u>	<u>Number of Regions Mapped</u>
Normal Squamous	9	18
Barrett's oesophagus without dysplasia	10	27
Barrett's oesophagus with LGD	10	27
Barrett's oesophagus with HGD	9	24
Oesophageal adenocarcinoma	9	21
Total	47	117

Table 5.3: Summary of Samples and Regions measured using Raman Mapping

In total 117 regions were mapped. The number of points measured in each map was dependent on the size of the region selected and ranged from 238 to 108350 points. The total number of points measured in each pathology is shown in Table 5.4 and the average number in Table 5.5. Measurements were undertaken on 20 days in a 2 month period.

<u>Pathology</u>	<u>Number of Points Mapped</u>	<u>Time Taken (mins)</u>
Normal Squamous	68712	867
Barrett's oesophagus without dysplasia	91251	1172
Barrett's oesophagus with LGD	112898	1445
Barrett's oesophagus with HGD	218442	1504
Oesophageal adenocarcinoma	179001	2179
Total	670304	7167

Table 5.4: Summary of Raman Map Measurements

<u>Pathology</u>	<u>Average Number of Points Mapped / Region</u>	<u>Average Time (mins) / Region</u>
Normal Squamous	3817	48
Barrett's oesophagus without dysplasia	3380	43
Barrett's oesophagus with LGD	4181	54
Barrett's oesophagus with HGD	9102	63
Oesophageal adenocarcinoma	8524	104
Total	5729	61

Table 5.5: Averages of Raman Map Measurements

### 5.3: Autofluorescence of Oesophageal Tissue

Ten samples, two from each pathology group, were selected for autofluorescent measurements. The one region that most accurately depicted the underlying pathology was measured. The area was measured with three wavelengths, 476, 488 and 496nm, sequentially. All ten samples were measured on a single day.

### 5.4: Data Analysis

Principle component analysis was used to identify variance between the measured spectra. Analysis of variance, with a 0.95 confidence threshold for inclusion, was subsequently utilised for each comparison to identify which components provided the variance between the data sets, as exemplified in figure 5.3.

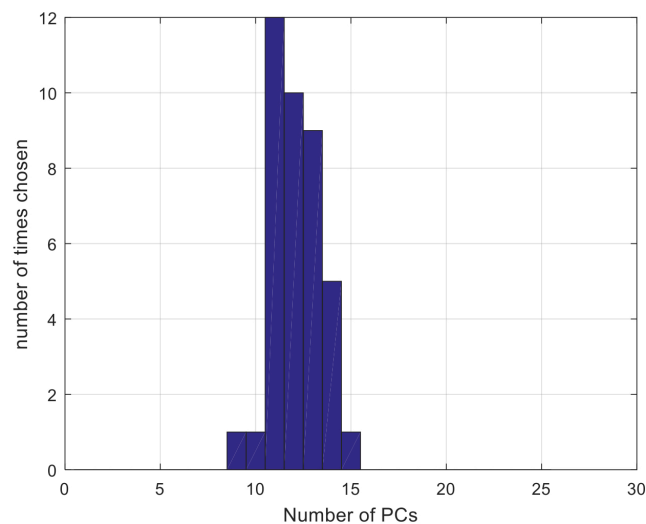


Figure 5.3: ANOVA for comparison of LGD versus HGD and Adenocarcinoma

Linear Discriminant Analysis was performed using the principal components identified from the training dataset (i.e.: all measured spectra). The classification model was then tested on the test dataset using LOSOCV (i.e.: all data excluding the sample currently being tested). This enabled the sensitivity and specificity of the dataset to be calculated and assessed.

## Section C: Summary of Measurements, Results and Analysis

## Chapter 6: Results and Analysis

### 6.1: Classification Models

#### 6.1.1: Determining the presence of dysplasia: Barrett's oesophagus without dysplasia versus Barrett's oesophagus with dysplasia

One of the aims of this project was the development of classification models for diagnosing dysplasia in Barrett's oesophagus. The diagnosis of dysplasia is clinically important as the management differs for patients without dysplasia as they have an extremely low risk of malignant progression. For patients whose biopsies indicate the presence of dysplasia, the management ranges from repeat endoscopy (for low-grade dysplasia) to either endoscopic resection or even oesophagectomy (for high-grade dysplasia and adenocarcinoma).

Raman spectroscopy needs to be able to differentiate, with high specificity and sensitivity, between the presence and absence of dysplasia for it to be a viable modality. Previous studies have shown that Raman spectroscopy is able to achieve this in the GI tract (Kendall *et al* 2003). Ideally it will also be able to determine the grade of dysplasia and be able to classify samples that are indeterminate for dysplasia as with dysplastic or inflammatory. This study has used both point spectra and map data to determine if Raman spectroscopy can identify dysplasia and if low-grade dysplasia can be differentiated from high-grade dysplasia and adenocarcinoma.

To determine if Raman spectroscopy is able to effectively distinguish samples with dysplasia from those without, the samples were split into two groups: Barrett's without dysplasia as one group, and Barrett's with dysplasia as the other group. The Barrett's with dysplasia group was formed from Barrett's oesophagus with low-grade dysplasia, Barrett's oesophagus with high-grade dysplasia and oesophageal adenocarcinoma.

##### 6.1.1.1: Raman Point Spectra

When all the samples obtained using point spectra measurements were analysed, the most striking difference appears in the samples of oesophageal

adenocarcinoma (Figure 6.1). The other histology types are more closely aligned to each other.

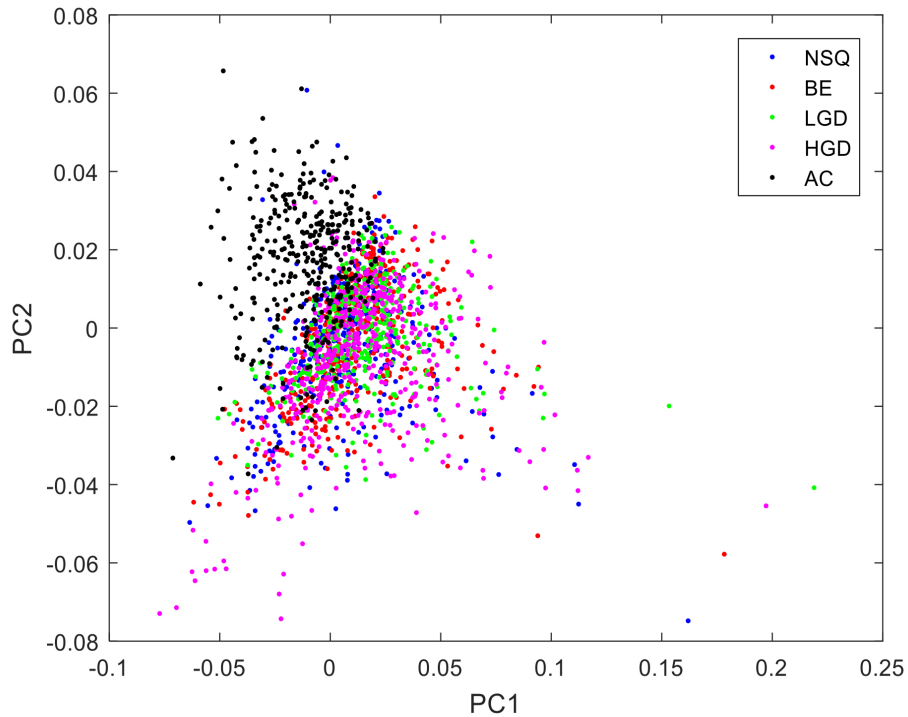


Figure 6.1: Scatterplot of Raman Point Spectra Measurements

When the samples were analysed based on their segregation into a group without dysplasia and a group with dysplasia (as described above), using principals component analysis (Training Set), the results indicate that the two groups are able to be differentiated with a sensitivity of 0.69 and a specificity of 0.68 (Table 6.1).

Barrett's Oesophagus without Dysplasia versus Barrett's oesophagus with Dysplasia: Point Spectra			
	Sensitivity	Specificity	AUC
Training Set	<b>0.69</b>	<b>0.68</b>	<b>0.76</b>
Test Set	<b>0.46</b>	<b>0.59</b>	<b>0.53</b>

Table 6.1: Analysis Results: Raman Point Spectra (No Dysplasia versus Dysplasia)

When plotted on a Receiver Operating Characteristic (ROC) curve, the Area under the Curve (AUC), which indicates how well the diagnostic groups can be differentiated, is 0.76. An AUC of 1 is a perfect classification model, whereas, 0.5 indicates that that the differentiation is no better than chance alone. This



indicates that the ability to differentiate samples with dysplasia from those without is possible, although the accuracy is limited.

The results for the test set, performed using LOSOCV, are unsurprisingly poorer with an AUC of 0.53 (Figure 6.2) which is only marginally better than chance. In particular, the sensitivity was low at 0.46, meaning that a significant number of samples with dysplasia were incorrectly classified as not having dysplasia using this classification model.

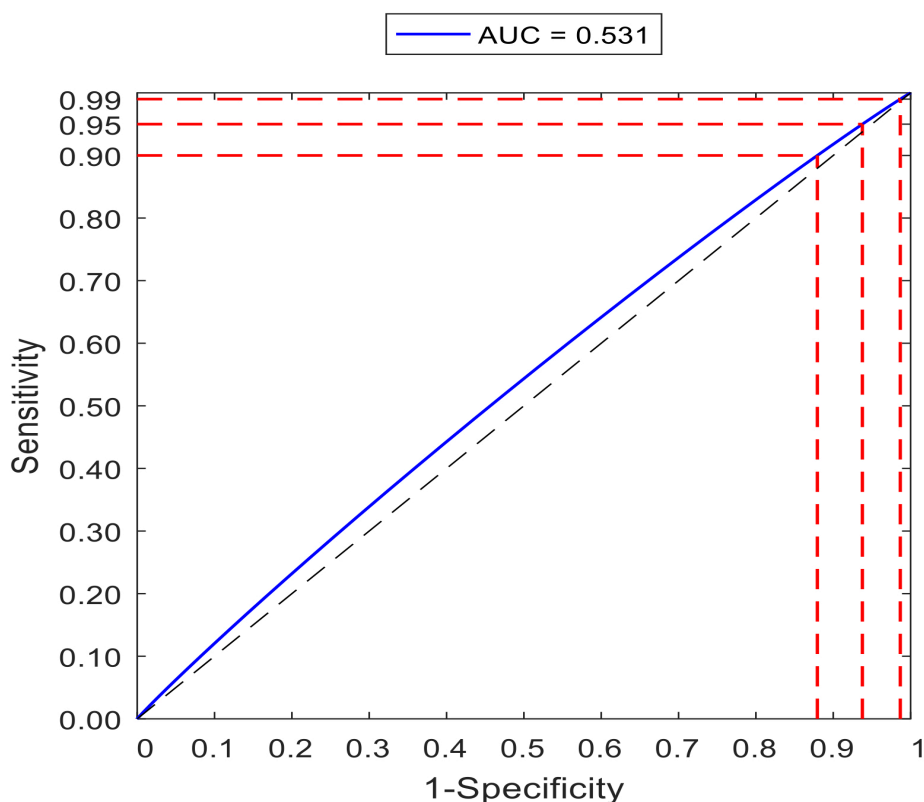


Figure 6.2: ROC Curve for Dysplasia versus Non-Dysplasia: LOSOCV: Point Spectra

#### 6.1.1.2: Raman Mapping

Using Raman mapping data, it was also possible to differentiate between samples with and without dysplasia. The training set results predict an AUC of 0.84 (as exemplified in Figure 6.3) which indicates that Raman mapping is significantly better than chance alone for differentiating the two pathologies.

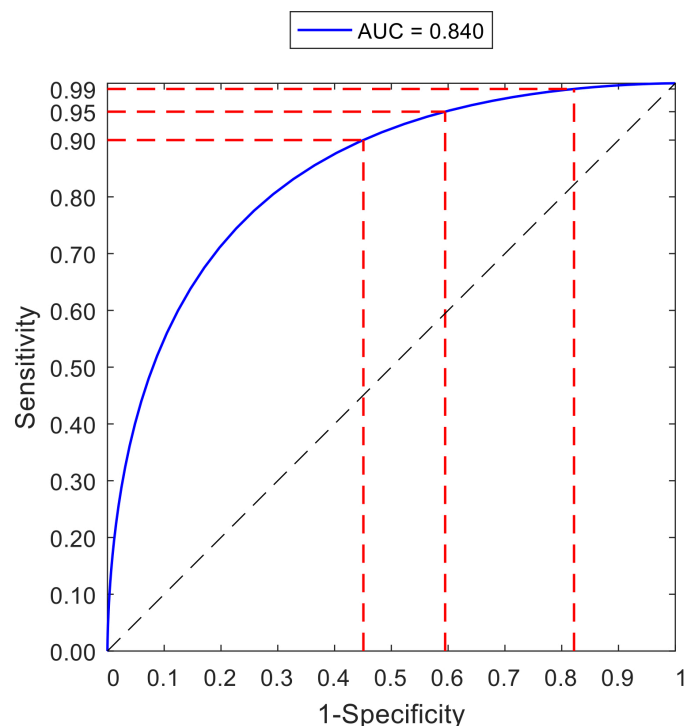


Figure 6.3: ROC Curve for Dysplasia versus Non-Dysplasia on CaF<sub>2</sub> Slides: PCA.

The test set, however, demonstrated poor results (see Table 6.2), with a sensitivity of only 0.26 and a specificity of 0.84. These results are poorer than expected based on previous research results and indicate an inadequate ability to correctly identify dysplasia when present. The training set, which does not remove a sample to test the results, also has a poor sensitivity of 0.52.

Barrett's Oesophagus without Dysplasia versus Barrett's oesophagus with Dysplasia: Raman Mapping (Calcium Fluoride Slides)			
	Sensitivity	Specificity	AUC
Training Set	<b>0.52</b>	<b>0.93</b>	<b>0.84</b>
Test Set	<b>0.26</b>	<b>0.84</b>	<b>0.35</b>

Table 6.2: Analysis Results: Raman Mapping (No Dysplasia versus Dysplasia) on CaF<sub>2</sub>

The reasons for this are likely to include the small sample numbers, particularly in the Barrett's oesophagus without dysplasia group. In addition, the group with dysplasia included a range of grades of dysplasia from low-grade to adenocarcinoma which may have affected the sensitivity. The pathway from low-grade dysplasia to adenocarcinoma encompasses a variety of morphological and biochemical changes. Not only are these changes variable

along the pathway, they are also variable in, for example, two patients who both have low-grade dysplasia. This means that in a group that contains samples from both ends of the spectrum (low-grade dysplasia to adenocarcinoma), there will be significant differences between the samples. These differences may be greater than the difference between Barrett's oesophagus without dysplasia and low-grade dysplasia, resulting in the poor results seen when comparing these two cohorts of samples.

All data from the Raman maps was included in the analysis. Although the area that best represents the underlying pathology was selected for mapping, there undoubtedly were areas surrounding that was normal oesophageal tissue. This means that in, for example, a sample of low grade dysplasia, there will be areas that contain none of the features of low grade dysplasia and are normal oesophageal tissue. These areas will lower the sensitivity and specificity of the analysis as identical areas will be present in samples of adenocarcinoma. All spectra that was obtained was included in the analysis as this will reflect the likely situation in clinical practise to minimise the necessary pre-preparation of samples and, hence time and money required for this technology.

Lastly, the samples were affected by residual paraffin which remained despite following the standard and thorough protocol for de-paraffinisation. Different tissue pathologies have been shown to hold onto residual paraffin to a varying degree (Nallala *et al* 2015), which is a likely result of the different biochemical make-up of the tissues. This would have resulted in differences between the groups and within the group containing the wide range of degrees of dysplasia. The residual paraffin is further discussed in Section 6.2.

In addition to de-paraffinisation, chemical bleaching of pathology during oven and clearing agent chemical treatment may affect the underlying sample and may do this to a different degree dependent on the biochemical make-up of the underlying tissue. Whether this occurs and the degree to which it does is unknown.

The same comparison between Barrett's oesophagus without dysplasia and Barrett's oesophagus with dysplasia was undertaken using Raman mapping data from samples on stainless steel slides. These samples, which were obtained from the same archived tissue blocks as the samples on calcium

fluoride slides, were prepared and measured during a similar time frame for the SMART project (Stratified Medicine through Advanced Raman Technologies Project) in collaboration with Gloucestershire Royal Hospital, Renishaw, University College London and the University of Exeter.

Barrett's Oesophagus without Dysplasia versus Barrett's oesophagus with Dysplasia: Raman Mapping (Stainless Steel Slides)			
	Sensitivity	Specificity	AUC
Training Set	<b>0.65</b>	<b>0.91</b>	<b>0.85</b>
Test Set	<b>0.33</b>	<b>0.80</b>	<b>0.47</b>

Table 6.3: Analysis Results: Raman Mapping (No Dysplasia versus Dysplasia) on Stainless Steel Slides

The results obtained from the stainless steel slides (see Table 6.3) show results that are similar to the calcium fluoride slides for the training set with an AUC of 0.85 (see Figure 6.4). The test set results were marginally better with a sensitivity of 0.33 and a specificity of 0.80. Even when the effects of residual paraffin are excluded, the low number of samples used in the analysis and, perhaps most importantly, the grouping of all grades of dysplasia into one group has resulted in poorer than expected outcomes.

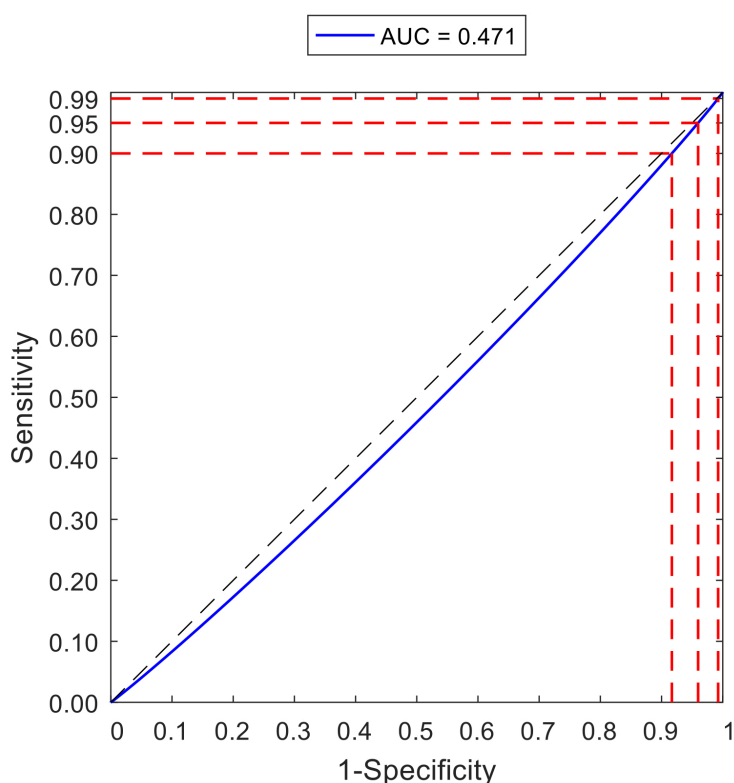


Figure 6.4: ROC Curve for Dysplasia versus Non-Dysplasia on Stainless Steel Slides: LOSOCV

The range of differences that are seen as cells progress through dysplasia results in subtle differences in the Raman maps, particularly as a large area that may contain different and varying features is mapped. The area of the sample that was selected to be mapped represented the grade of dysplasia, however, there would have been surrounding areas which would not have been representative of the underlying pathology. In addition, there are a range of features which represent each grade of dysplasia. The amassing of all grades of dysplasia in one group would have resulted in a broad range of changes which is likely to have affected the cross validation results as there would have been significant differences between, for example, the area adjacent to low-grade dysplasia and the central of an area of adenocarcinoma.

### 6.1.1.3: Comparison: Point Spectra to Mapping

The point spectra measurements are from a single point of the sample that is mapped over a period of 30 seconds, whereas, Raman mapping samples a greater area over a significantly longer period. It is hypothesised that the results obtained from the point spectra measurements will be inferior as less information is contained within each spectra. In addition, it is possible that the small area measured will miss vital and, perhaps, diagnostic information.

When comparing the classification models for point spectra and Raman mapping (on calcium fluoride slides) for Barrett’s oesophagus without dysplasia and Barrett’s oesophagus with dysplasia and adenocarcinoma, the overall results in terms of the AUC were similar; 0.76 versus 0.84. The sensitivity and specificity results were, however, quite different (see Table 6.4).

Barrett’s Oesophagus without Dysplasia versus Barrett’s Oesophagus with Dysplasia and Adenocarcinoma			
	Sensitivity	Specificity	AUC
Point Spectra	<b>0.69</b>	<b>0.68</b>	<b>0.76</b>
Map Spectra	<b>0.52</b>	<b>0.93</b>	<b>0.84</b>

Table 6.4: Comparison Results: Point Spectra Training Set versus Map Spectra Training Set: No Dysplasia versus Dysplasia

The specificity, also known as the true negative rate, measures the proportion of negative results that are correctly identified as negative. As mapping encompasses a larger area, it is likely that if any areas of dysplasia were present, they would be identified and this is reflected in the specificity of 0.93 which is significantly better than 0.68 obtained with point spectra measurements.

The sensitivity, on the other hand, measures the proportion of positive results that are correctly identified as positive. Point measurements may miss the area of interest and, thus, not include the area of dysplasia which would result in a falsely negative result. It was surprising, therefore, that the sensitivity was higher at 0.69 in the point spectra measurements when compared to 0.52 obtained with Raman map measurements. This may be due to changes in the area surrounding dysplasia which, if measured, are also diagnostic of the overall histology of the sample.

#### 6.1.2: Determining the grade of dysplasia: Low-Grade Dysplasia versus HGD/Adenocarcinoma

Low-grade dysplasia, especially if persistent, may represent an important transition on the road towards malignancy. The ability to accurately identify low-grade dysplasia is essential if it is indeed a transition point and has been difficult to do with histopathology alone due to the subtle morphological changes and, hence, high variability among assessors. One of the aims of this study was to determine if low-grade dysplasia could be distinguished from that of high-grade dysplasia and adenocarcinoma.

For this analysis, Barrett's with low-grade dysplasia was compared to Barrett's oesophagus with high-grade dysplasia and oesophageal adenocarcinoma.

##### 6.1.2.1: Raman Point Spectra

These results have shown that point spectra measurements are able to differentiate low-grade dysplasia from that of high-grade dysplasia and adenocarcinoma. The results are, however, far from ideal. When testing the

classification model, the sensitivity and specificity results (Table 6.5) were poorer than they would need to be to be clinically applicable.

Barrett's Oesophagus with Low-Grade Dysplasia versus High-Grade Dysplasia: Raman Point Spectra			
	Sensitivity	Specificity	AUC
Training Set	<b>0.84</b>	<b>0.70</b>	<b>0.86</b>
Test Set	<b>0.66</b>	<b>0.59</b>	<b>0.68</b>

Table 6.5: Analysis Results: Raman Mapping (Low-Grade Dysplasia versus High-Grade Dysplasia): Point Spectra

The ROC curve (see Figure 6.5) shows an AUC of 0.68 on the test set. These results are better than those of no dysplasia versus dysplasia. This suggests that when the sample sets are closer to each other, rather than including a wide range of pathologies, the differences between groups are greater than the differences seen within groups and, thus, results in higher accuracy. Including multiple grades of dysplasia within a single subgroup increases the number of samples, however, as each sample of dysplasia differs slightly anyway, combining multiple grades introduces a significant range of variance within the group. Comparing each pathology individually to each other and creating a multi-point classification model may improve both the sensitivity and specificity and bring the accuracy to a level that is clinically applicable.

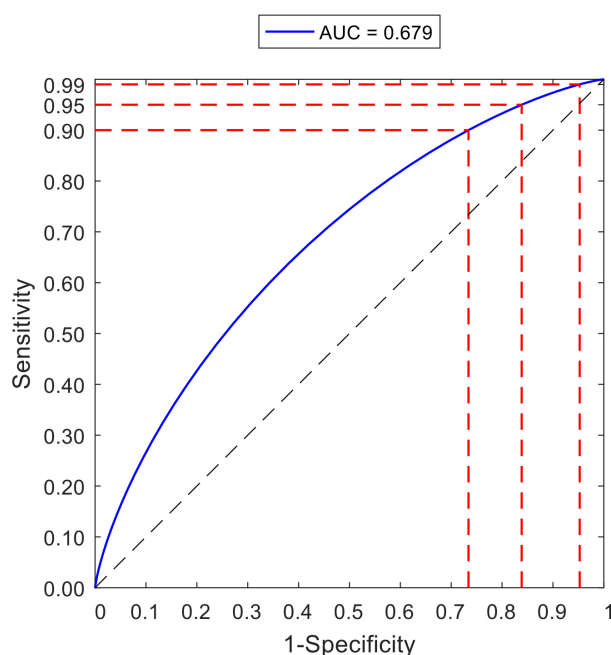


Figure 6.5: ROC Curve for LGD versus HGD: LOSOCV: Point Spectra

### 6.1.2.2: Raman Mapping

When using the results obtained from Raman mapping, the results were far from ideal (see Table 6.6). The training set had a sensitivity of 0.88 for high grade dysplasia, meaning that there was a high likelihood of the true positive results being identified. The specificity was, however, lower at 0.51, meaning that a proportion of low-grade dysplasia would be misidentified. Overall the AUC was calculated at 0.80 (see Figure 6.6). These poor results were exemplified in the test set which reported an extremely low specificity of 0.09.

Barrett's Oesophagus with Low-Grade Dysplasia versus High-Grade Dysplasia: Raman Mapping (Calcium Fluoride Slides)			
	Sensitivity	Specificity	AUC
Training Set	<b>0.88</b>	<b>0.51</b>	<b>0.80</b>
Test Set	<b>0.73</b>	<b>0.09</b>	<b>0.43</b>

Table 6.6: Analysis Results: Raman Mapping (Low-Grade Dysplasia versus High-Grade Dysplasia) on CaF<sub>2</sub> Slides

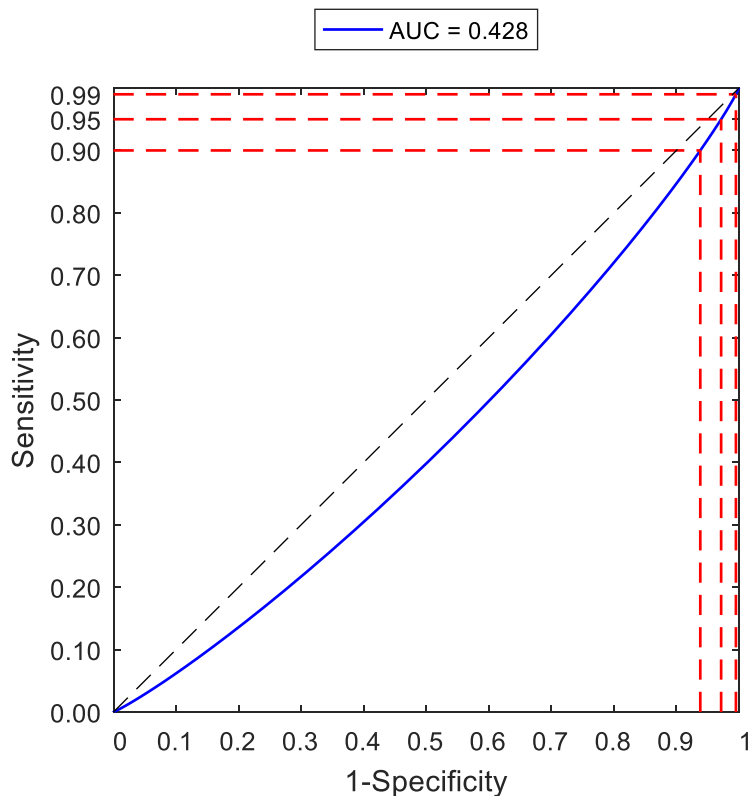


Figure 6.6: ROC Curve for Low-Grade Dysplasia versus High-Grade Dysplasia on CaF<sub>2</sub> Slides: LOSOCV



This extremely low specificity may be, in some part, due to the reduced amount of differences that exist between low-grade and high-grade dysplasia, thus, meaning that it is extremely difficult to differentiate between the two. Only very small numbers of samples were used and, as discussed, not all areas of the sample mapped represent low-grade dysplasia to the same degree. This is likely to have had a significant impact on the results obtained.

The same analysis was also completed on the samples measured on stainless steel slides. As with the earlier comparison, the results from these slides were better than those obtained from the calcium fluoride slides (see Table 6.7 and Figure 6.7), reflecting the influence that residual paraffin has on the results. The specificity, nevertheless, remained poor, especially on the cross validation analysis (test set).

Barrett's Oesophagus with Low-Grade Dysplasia versus High-Grade Dysplasia: Raman Mapping (Stainless Steel Slides)			
	Sensitivity	Specificity	AUC
Training Set	<b>0.94</b>	<b>0.72</b>	<b>0.92</b>
Test Set	<b>0.83</b>	<b>0.33</b>	<b>0.32</b>

Table 6.7: Analysis Results: Raman Mapping (Low-Grade Dysplasia versus High-Grade Dysplasia) on Stainless Steel Slides

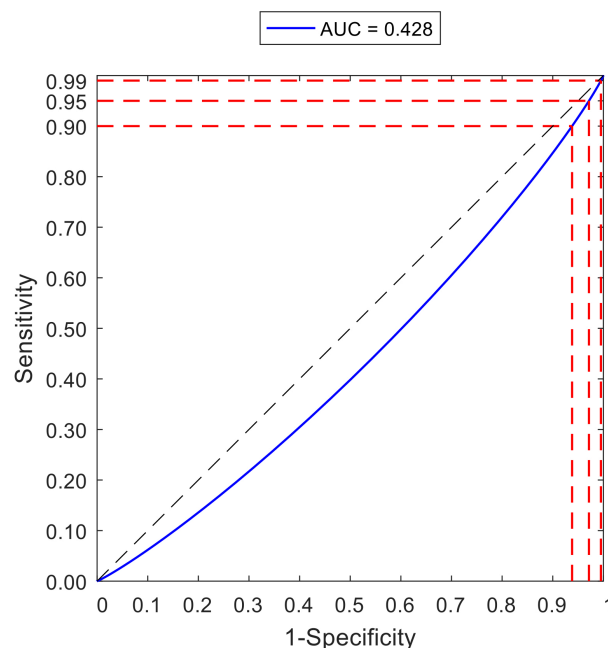


Figure 6.7: ROC Curve for Low-Grade Dysplasia versus High-Grade Dysplasia on Stainless Steel Slides: LOSOCV

### 6.1.2.3: Comparison: Point Spectra to Mapping

When differentiating Barrett's oesophagus with low-grade dysplasia from Barrett's oesophagus with high-grade dysplasia and adenocarcinoma, the results obtained from the point measurements and the map measurements were similar (see Table 6.8).

Barrett's Oesophagus with Low-Grade Dysplasia versus High-Grade Dysplasia and Adenocarcinoma			
	Sensitivity	Specificity	AUC
Point Spectra	<b>0.84</b>	<b>0.70</b>	<b>0.86</b>
Map Spectra	<b>0.88</b>	<b>0.81</b>	<b>0.80</b>

Table 6.8: Comparison Results: Point Spectra Training Set versus Map Spectra Training Set: LGD versus HGD and adenocarcinoma

The main difference was that the specificity was lower for the point spectra measurements, meaning that some samples would be classified as low-grade dysplasia when they were in fact high-grade and vice versa. This is important as the differentiation between the grades is clinically relevant and needed. The results may have been more similar in terms of sensitivity and specificity as each sample group contained a more narrowly specified collection of pathologies. This would have meant that the samples in each group were more closely aligned to each other, whereas, in the previous comparison the dysplastic group had a wide range of pathologies, some of which may have been closer to the other group than to other samples within the same group.

### 6.1.2.4 Can point spectra be used to form a robust classification model?

Point spectra measurements have the obvious advantage over mapping measurements of permitting rapid data acquisition. Multiple point spectra measurements can be acquired in a timeframe that is much shorter than that required for even a single map. As well as cost implications, the greatest benefit of rapid data acquisition is the ability for this to be performed in vivo as contact between the probe and mucosa can be maintained for the duration of the measurement. Even with multiple measurements, this could be completed within the realms of a standard diagnostic endoscopy.

Point spectra measurements with their rapid acquisition will, however, only be acceptable if the data obtained is good enough to differentiate the various pathologies. Although the data from both point and map measurements in this research were poor compared to previous published work, the sensitivity and specificity for diagnosing the pathologies varied between point and map data. To further aid the understanding of whether point spectra data alone is adequate for diagnosis, the map data was projected onto the training set formed from the point spectra.

Map data encompasses a larger tissue area and, thus, has a greater likelihood for including changes that are diagnostic and enable differentiation between pathologies in the spectra produced. Point spectra, in contrast, has a smaller area and may, thus, not include any or enough changes that are discernible in the resultant spectra. If this is the case, there is likely to be a higher risk of false negatives, or a lower sensitivity. It would be important to see if the areas surrounding the predominant area of interest also contain enough changes to enable differentiation by their spectra. This is likely to be especially pertinent in in vivo measurements where manoeuvring the endoscopic probe against the vertical wall of the oesophagus is extremely tricky and, thus, may result in the exact point of interest being slightly outside the measurement area. This knowledge will inform the size of point spectra required and the protocol for the number and spacing of measurements required.

If the point spectra data is ample for differentiation, then the diagnosis for each map sample should be attainable from this training set. The two Raman systems used for point spectra measurement and map measurements are, however, different in terms of wavelength, filters and optics. The models produced for each system, therefore, are different and are unable to compensate for the differences between the two systems. It was, therefore, impossible to project the map data onto the point spectra training set.

The differences in the systems and the need to compensate for these in the models produced exemplifies the importance of the data analysis. Without advances in this area, spectroscopy will be unable to be used routinely as it will

be impossible to create a classification model that can be used and comparable in different settings.

### 6.1.3: Where does Low-Grade Dysplasia fit?

The results obtained from this research show that Raman spectroscopy has the ability to differentiate Barrett's oesophagus with low-grade dysplasia from that of high-grade dysplasia and adenocarcinoma, although the results are far from flawless. Low-grade dysplasia provides some of the greatest difficulty in diagnosis by histopathological changes and is a huge challenge for all pathologists with increasing numbers of patients being diagnosed as indefinite for dysplasia and consensus on histopathological diagnosis being impossible. In addition, the exact meaning of a diagnosis of low-grade dysplasia for the patient is uncertain.

The samples of low-grade dysplasia were analysed to see if they more closely resembled those of Barrett's oesophagus without dysplasia or Barrett's oesophagus with high-grade dysplasia as this may clarify the position that low-grade dysplasia has on the spectrum towards malignancy. When analysing the samples with cluster analysis and rank tests, it shows that the samples of low-grade dysplasia are as similar to themselves as they are to everything else.

This result is not surprising given the small number of samples of low-grade dysplasia. It would be interesting to see if, with a higher number of samples, there is a closer resemblance to either Barrett's oesophagus without dysplasia or to Barrett's oesophagus with high-grade dysplasia. There may be different subgroups of low-grade dysplasia; one that does not progress towards malignancy, and one which does. It would be interesting to analyse the low-grade dysplasia samples in different groups, based on the certainty of the histopathologist report (i.e.: when all pathologists agree on the diagnosis compared to when there is disagreement between pathologists), and based on the subsequent progression of the samples (i.e.: are those samples that do progress to high-grade dysplasia distinguishable at an earlier stage when analysed by Raman Spectroscopy). This is further discussed in Section 7.1 and 7.2.3.

## 6.2: Paraffin

### 6.2.1: The impact of paraffin

For this project, archived tissue samples and, hence, formalin fixed paraffin embedded (FFPE) tissue samples were used. The formalin preserves the tissue for future analysis in a manner that enables easy storage and provides substantial support to the tissue to aid microtomy and tissue sectioning. Fixation in formalin, nevertheless, results in changes in the tissue. The process of fixation results in the breakage of hydrogen bonds within large intracellular molecules leading to a loss of protein conformation (Srinivasan *et al* 2002). Dehydration of intracellular proteins through the formation of cross-links between amine residues (Srinivasan *et al* 2002, Murk *et al* 2003, Gazi *et al* 2005) as well as the washing out of lipids also occurs (Masuda *et al* 1999). These changes have, however, been shown to produce spectral content that is closet to that seen in live cells and, by extension, formalin fixation is deemed to best preserve cellular integrity (Meade *et al* 2010).

As previously discussed, paraffin produces a distinctive Raman spectrum which overwhelms and obscures the spectrum of the tissue. De-paraffinisation of the samples took place prior to sample measurement, however, despite no visually apparent paraffin contamination, analysis of the samples revealed elements of retained paraffin.

A spectrum of pure paraffin wax has significant peaks at  $888\text{cm}^{-1}$ ,  $1061\text{cm}^{-1}$ ,  $1131\text{cm}^{-1}$ ,  $1171\text{cm}^{-1}$ ,  $1294\text{cm}^{-1}$ ,  $1417\text{cm}^{-1}$ ,  $1440\text{cm}^{-1}$  and  $1462\text{cm}^{-1}$  (see Figure 6.8) which are the result of stretching of the C-C bond and deformities of  $\text{CH}_2$  and  $\text{CH}_3$  (Faoláin *et al* 2005). Figure 6.9, which depicts the average spectra of the maps of both normal squamous and oesophageal adenocarcinoma tissue, also shows dominant peaks at  $1061\text{cm}^{-1}$ ,  $1131\text{cm}^{-1}$ ,  $1296\text{cm}^{-1}$ ,  $1440\text{cm}^{-1}$  and  $1462\text{cm}^{-1}$  which correlate to those of paraffin.

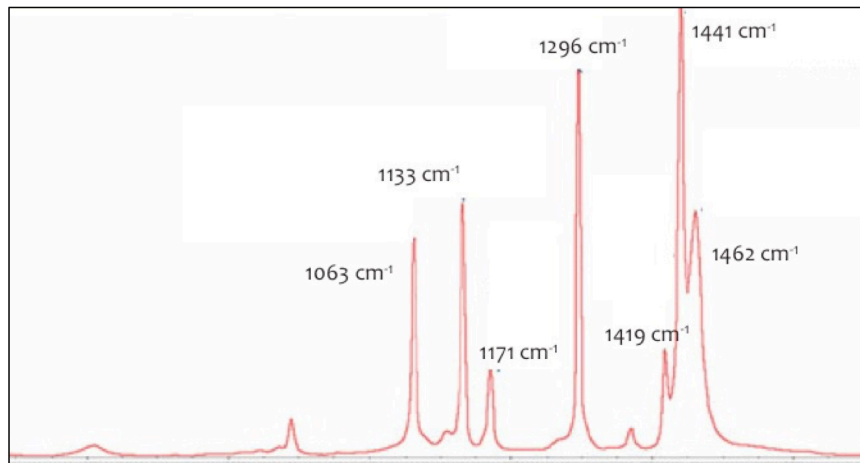


Figure 6.8: Raman Spectrum of Pure Paraffin highlighting the predominant peaks produced (adapted from Mian *et al* 2014)

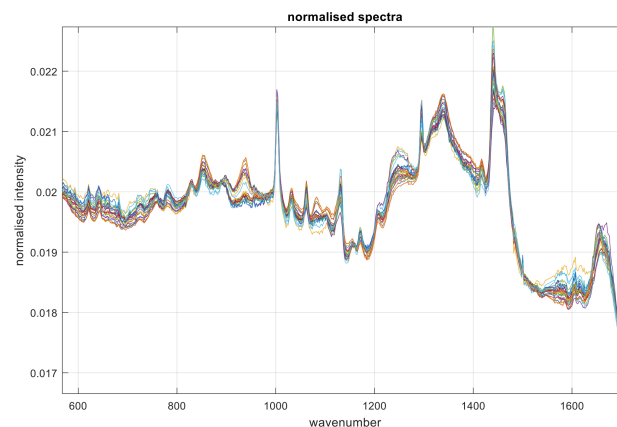


Figure 6.9: Average spectra of each map of Normal Squamous and Oesophageal Adenocarcinoma tissue

Raman spectroscopy is more sensitive to the incomplete removal of paraffin than infrared spectroscopy (Faoláin *et al* 2005), thus, the inability to remove paraffin completely raises important issues if this tool is to be clinically applicable and robust. Previous studies (Fullwood *et al* 2014, Nallala *et al* 2015) have compared a variety of agents used for de-paraffinisation. Long Hexane incubation (~18 hours) was shown to be the most effective agent, however, even with this chemical, some residual paraffin remained in the tissues.

The amount of paraffin remnants remaining in the tissue was not uniform, but varied depending on the underlying pathology with cancerous tissue retaining the most paraffin. Figure 6.10 highlights the difference between normal

squamous tissue and oesophageal adenocarcinoma tissue with differences in intensity at the paraffin peaks, indicating a different amount of paraffin, as well as differences due to the underlying histology. This difference in paraffin retention has been documented in previous studies (Nallala *et al* 2015), although the exact reasons are unclear.

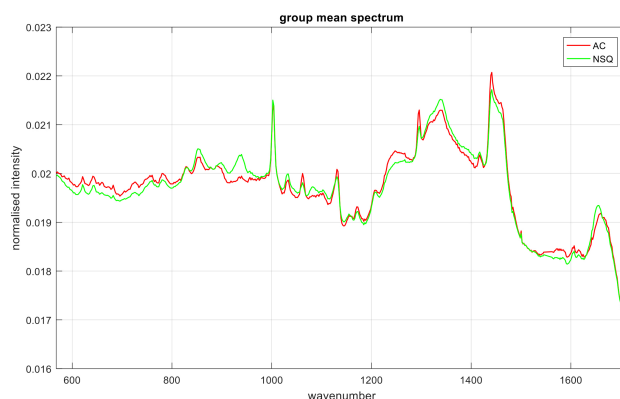


Figure 6.10: Mean Spectra of Normal Squamous and Oesophageal Adenocarcinoma Tissue

Calcium fluoride slides were selected as, despite their cost, they display a single predominant peak that is outside that of the tissue range and background peaks of lower intensity (Kerr *et al* 2015), however, their average surface roughness is high at 4.76nm (Fullwood *et al* 2015). This may affect the ability of deparaffinisation of samples on this slide, whereas, slides of a lower roughness, such as stainless steel, are better suited to the deparaffinisation process.

#### 6.2.2: Comparison to Stainless Steel Slides

As well as improved deparaffinisation, stainless steel has been shown to improve the Raman signal by reducing the background contribution of the slide by a factor of 6 (Lewis *et al* 2017). The results presented in this thesis, despite their downfalls, are improved when using samples mapped on stainless steel as compared to calcium fluoride slides.

The other advantages of stainless steel slides are reduced cost when compared to calcium fluoride slides. Not only is the original outlay higher for calcium

fluoride slides, but their fragility will, in all likelihood, result in higher costs relating to damages and may also result in a loss of samples.

An alternative approach to avoid the difficulties and implications that FFPE tissue brings is to use fresh or snap frozen samples. Fresh samples would enable reduced tissue processing and, hence, avoid the possibility that the paraffin and chemical de-paraffinisation process change the tissue constituents. For in-vivo use, this would be essential, however, it would necessitate immediate measurement which would, outside of research facilities, be impossible in most situations. Frozen tissue samples have their own difficulties with storage and thawing techniques, hence, it would seem improbable that this technology will be able to step away from FFPE tissue and, thus, choosing a suitable substrate slide is likely to be the preferential method to avoid the implications that residual paraffin brings.

### 6.3: Biochemical Peaks

#### 6.3.1: Is there a purpose to biochemical assignment?

The Raman spectrum that is produced when tissue is analysed is a direct function of the molecular composition of that tissue. Biological tissues have a multitude of biomolecules, each of which has its own distinctive Raman signature and, hence, each peak produced during analysis can be traced to the exact molecule or bond creating the peak. Significant overlap of the spectra, however, exists, creating broad signal envelopes (Pavićević *et al* 2012). This, combined with overlap that is produced from endogenous fluorescence, means that the assignment of a peak to a single molecule may be overly optimistic and ultimately misleading.

The spectrum reflects the underlying quantity and distribution of, predominantly, glycogen, DNA, lipids and proteins. Initial work that looked to elucidate the underlying causes of the resultant peaks in oesophageal tissue and the differences between benign and dysplastic tissue found increased DNA, oleic acid, collagen I and actin in areas of high-grade dysplasia, whereas, increased glycogen was seen in areas of normal squamous tissue (Shetty *et al* 2006).



Not only have subsequent studies (Bergholt *et al* 2011, Ishigaki *et al* 2016) corroborated these findings, but the biomolecular findings also reflect the changes that occur in neoplastic tissue. Neoplastic tissue shows increased DNA and histones which emulates the abnormal DNA content that occurs in malignancy. Furthermore, a well-established indicator of dysplasia and malignancy is an increase in the nuclear: cytoplasmic ratio which is reflected by a decrease in actin in the spectral peak. A major change that occurs in the process of malignancy is the change and variation in protein configuration. A higher concentration of  $\beta$ -pleated sheet conformation (Maziak *et al* 2007) and a lower concentration of extracellular collagen, possibly secondary to cleavage by matrix metalloproteinases, (Bergholt *et al* 2011) occurs in malignancy.

Despite replication of studies identifying the likely cause of each of the Raman peaks, a body of researchers (including Diem, Gerwert and Wood, 2016) refute the need for biochemical assignment and the uncertainty of the allocations. The complexity of the spectra produced from a tissue sample as well as the large number of overlapping bands mean that a significant element of the biochemical assignment is based on guesswork. Nevertheless, there is considerable similarity in peak assignment despite different methodology between studies which would indicate that the results are reproducible.

Differences in spectral pattern without knowledge of the underlying biochemical change that results in the spectral shift would enable discrimination between pathologies without any advancement in the understanding of the malignant progression. I would contend that it only by understanding the changes that occur, will the ability to manipulate and ideally prevent them be able to take place. Furthermore, by analysing the order in which the changes occur, the fundamental change that pushes patients onto the malignant pathway may be realised and become the gold standard for identifying patients at risk of progression. If, for example, this was an increase in a certain substance, a means of identifying this substance alone, could be utilised as a marker for risk stratification in patients. Simply comparing peaks in different pathologies to the current gold standard of histopathology will not move our understanding forward.

### 6.3.2: Peak Differences

As discussed in the classification models, the predominant difference in spectra occurs in the normal squamous tissue. The other tissue types (Barrett's oesophagus without dysplasia, Barrett's oesophagus with low-grade dysplasia, Barrett's oesophagus with high-grade dysplasia and adenocarcinoma) have more closely aligned spectral patterns as depicted in Figure 6.11.

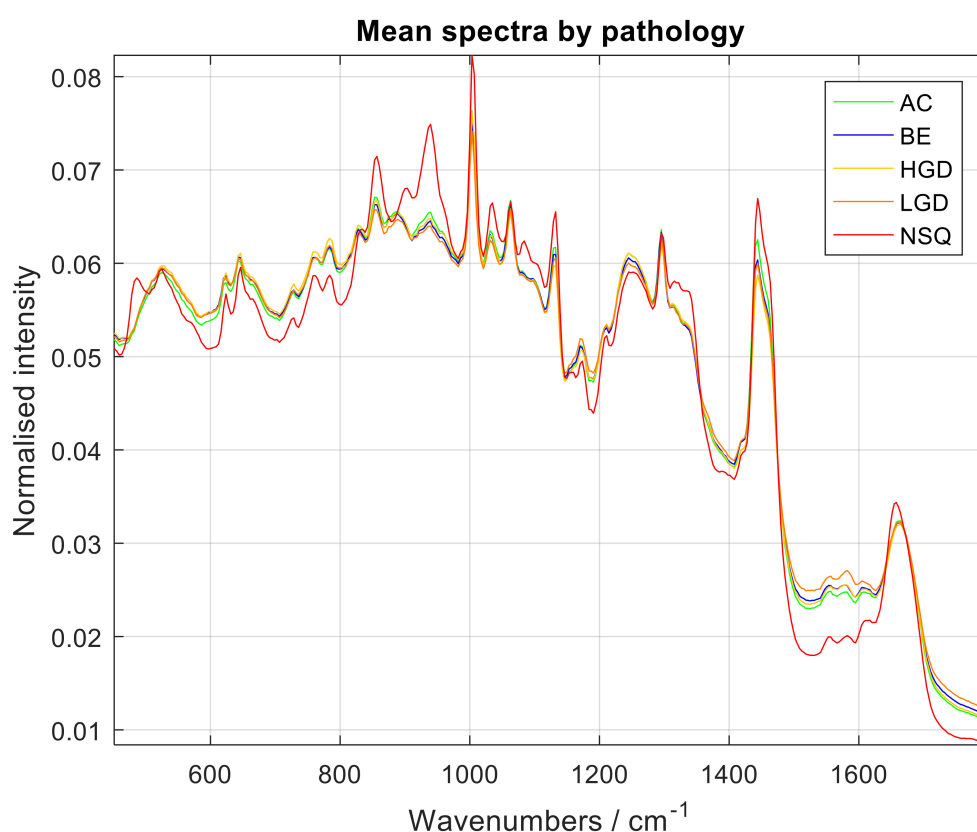


Figure 6.11: Mean Spectra by pathology

Normal squamous tissue samples show increased amplitude in peaks that have, in other studies, been shown to represent glycogen. These peaks include 852 cm<sup>-1</sup>, 934 cm<sup>-1</sup>, 1036 cm<sup>-1</sup>, 1048 cm<sup>-1</sup> and 1467 cm<sup>-1</sup> (Shetty *et al* 2006, Hutchings *et al* 2010). In addition, normal squamous tissue shows decreased amplitude in peaks that represent nucleic acids (1173 cm<sup>-1</sup>), DNA (720 cm<sup>-1</sup>, 748-755 cm<sup>-1</sup>, and 785 cm<sup>-1</sup>) and protein (820 cm<sup>-1</sup>), including amide III (1265

$\text{cm}^{-1}$ ) (Shetty *et al* 2006, Hutchings *et al* 2010, Almond *et al* 2014, Bergholt *et al* 2014, Chen *et al* 2014). A comprehensive review of biochemical assignments is included in Appendix II.

Differences in peaks were also observed at  $888 \text{ cm}^{-1}$ ,  $1131 \text{ cm}^{-1}$ ,  $1171 \text{ cm}^{-1}$ ,  $1294 \text{ cm}^{-1}$  and  $1440 \text{ cm}^{-1}$ . These peaks have been shown to be due to paraffin. Previous studies (Nallala *et al* 2015) have indicated that different tissue types retain paraffin variably following the same deparaffinisation regimen with adenocarcinoma preserving paraffin to a greater extent. My samples showed variation at these points, however, it was the normal squamous tissues that had the highest peaks. If the normal squamous peaks are eliminated, then the retention of paraffin is next highest in the adenocarcinoma tissue, as predicted by previous work (Figure 6.12). In my research, normal squamous tissue samples were obtained at a later date than the other samples and deparaffinised separately and, thus, may have a greater paraffin residue. This may account for some of the differences when comparing to the other tissue types.

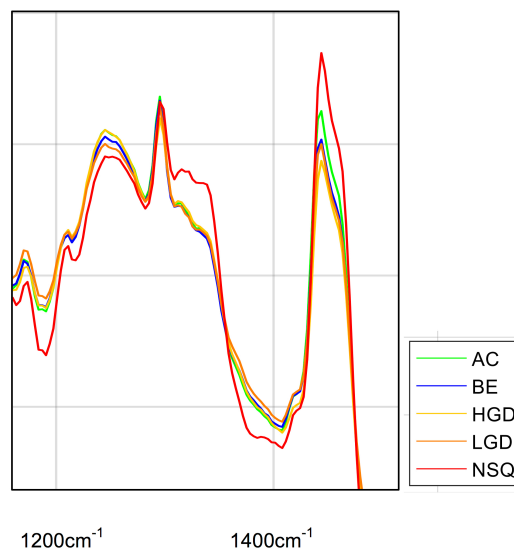


Figure 6.12: Magnification of peak at  $1440 \text{ cm}^{-1}$ , which corresponds to paraffin

Samples of Barrett's oesophagus without dysplasia, with low-grade and high-grade dysplasia and oesophageal adenocarcinoma show differences, albeit smaller. For example, as shown in Figure 6.13, adenocarcinoma represented by the green line, is closer to normal squamous than the other pathologies. There is not a graduated change with, for example, the amount of glycogen

decreasing in a continuum that matches the continuum of malignant progression. This may be because the greatest change is the transition to Barrett's oesophagus and the progression along the continuum to malignancy is not as gradual as suspected, but rather a series of significant steps that affect the spectra at certain points.

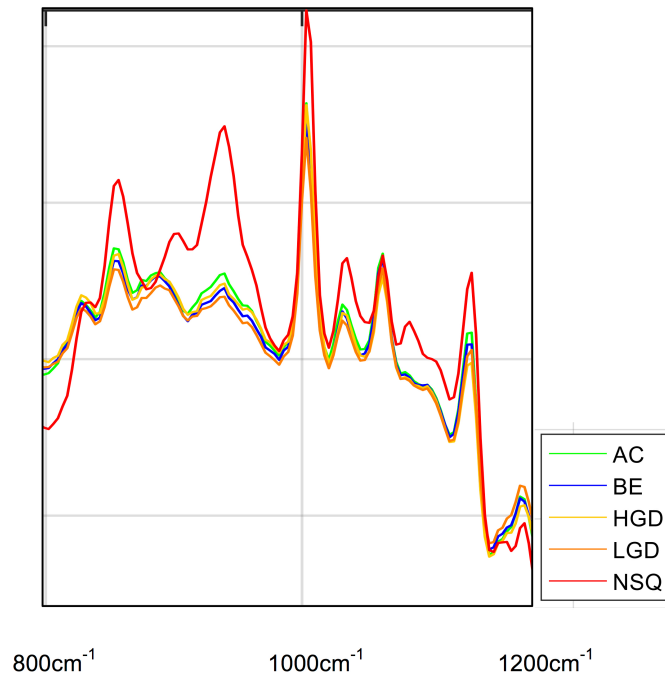


Figure 6.13: Magnified view of spectral peaks at  $934\text{cm}^{-1}$ ,  $1036\text{cm}^{-1}$ ,  $1048\text{cm}^{-1}$ .

### 6.3.3: Low-Grade Dysplasia

As discussed, the ability to distinguish dysplasia, particularly low-grade dysplasia from high-grade dysplasia, is paramount to helping both diagnostic abilities as well as the understanding of the progression of dysplasia. From analysing the peak differences, it is clear that there is not a change that occurs with the presence of dysplasia that is representative and diagnostic for the change, rather there are subtle differences in the concentrations of the tissue constituents. This is expected as the change of dysplasia is a series of morphological changes which alter the composition of the tissue and do not add or remove a single distinctive substrate.

This research only utilised ten samples of each grade of dysplasia. It would be noteworthy to see if there are changes that are different between the samples of dysplasia that progress to malignancy and those that do not. As discussed

earlier, the samples of low-grade dysplasia analysed did not show any alignment to either Barrett's oesophagus without dysplasia or to Barrett's oesophagus with high-grade dysplasia, however, it may be that there were not enough samples to identify this. The low number of samples resulted in a low number of biochemical changes being able to be captured in the measurements and subsequent analysis. It is not surprising, therefore, given the heterogeneity of changes of dysplasia that the classification model was unable to accurately differentiate the samples when it was built on a small selection of samples and, hence, a small selection of biochemical changes.

In the future it would be interesting to measure many more samples of low-grade dysplasia and see if certain samples of low-grade dysplasia were more aligned to high-grade dysplasia. This could identify those patients at risk of progression and highlight the changes in tissue constituents that mark this progression.

#### 6.4: Autofluorescence

Raman spectroscopy has, for a long time, been shown to distinguish between benign, dysplastic and cancerous tissue. The difference in spectra is a result of the biochemical changes. Modalities that utilise autofluorescence, such as confocal fluorescence microendoscopy, are also able to see changes at the cellular level. Research by DaCosta *et al* in 2005 found that dysplastic colonic cells had lower average green autofluorescence when compared to normal epithelial cells. The average red fluorescence was increased leading to a higher red to green ratio. A significant increase in the red fluorescence was in the apical regions of the cells due to a high presence of autofluorescent granules in this region.

Many cellular constituents exhibit fluorescent features including aromatic amino acids, reduced pyridine nucleotides and endogenous porphyrins (DaCosta *et al* 2005). The red autofluorescence seen in dysplastic cells was shown to be due to lysosomes, or their contents. Lysosomes are cellular organelles which contain hydrolytic enzymes and, thereby, acts as a 'waste disposal' system for the cell. For example, apoptosis of epithelial cells results in cell fragments which, due to oxidation and polymerisation, form lipofuscin within lysosomes.

Lipofuscin could be the focus of the fluorescence (DaCosta, personal communication). Regardless of whether it is lipofuscin or another molecule that is the cause of fluorescence, if such a molecule exists, this molecule could be responsible for the differences seen in the spectroscopic signature between disease states.

I undertook autofluorescence on a small selection of samples to ascertain if there are any visible differences. Unsurprisingly given the small sample, there were no accountable difference seen (See Appendix II for a selection of the results). Further work, focusing on the cellular constituents, may expose the changes indicated in previous research and provide focal areas for Raman mapping to identify the cellular constituents responsible for the change in autofluorescent signature.

A biomarker that is identifiable by fluorescence and/or spectroscopy and is diagnostic of dysplasia is highly sought after. If found, it could reduce the time required to obtain tissue samples and reduce the subsequent analysis time as identification of this marker would be enough to distinguish tissue that is dysplastic and tissue that is not. Perhaps more importantly, if a marker were to be discovered that typified the transition to dysplasia, then this could aid the understanding of why some patients with Barrett's oesophagus begin down the path to dysplasia and aid in identifying measures to prevent this.

## Section D: Summative Discussion and Conclusions

### Chapter 7: Summative Discussion and Conclusions

Dysplasia in Barrett's oesophagus is currently the only marker that we have at our disposal to ascertain the likelihood that an individual will progress along the path to malignancy. The diagnosis is, however, fraught with difficulty due to the subtle morphological changes which result in high variability amongst even specialist GI histopathologists. This is most apparent in the changes that characterise low-grade dysplasia with a Cohen kappa coefficient of only 0.27 (Kerkhof *et al* 2007). The changes that represent indefinite for dysplasia also provide a significant problem. This characterisation of dysplasia is important as patients are subjected to aggressive proton pump therapy and an earlier endoscopy. The consequence of a diagnosis of high grade dysplasia is even more important as the management is, in some instances, an oesophagectomy.

Improving the diagnosis of dysplasia will undoubtedly aid the management of individual patients. In addition, further understanding of the biochemical and structural changes that result in dysplasia and identification of the features of patients who have a higher risk of progression will aid in management stratification and identify those who will benefit from intensive surveillance or early treatment. Hopefully these strategies will result in a reduction in incidence of oesophageal adenocarcinoma and, hence, an improvement in survival.

#### 7.1: The Dilemma of Low-Grade Dysplasia

One of the controversies in the management of Barrett's oesophagus is the clinical significance and implication of a diagnosis of low-grade dysplasia. The most recent meta-analysis (Duits *et al* 2015) places the overall risk of progression of low-grade dysplasia to high-grade dysplasia at 9%. A shortfall of many of these studies is, however, the difficulty in the accurate assignment of low-grade dysplasia due to the, often subtle, features seen on histopathology review and, thus, the actual figure may be different.

Interestingly, the risk of progression to high-grade dysplasia was greatest, 80%, when three pathologists agreed on the diagnosis of low-grade dysplasia, and the risk lowest, 0%, when no pathologists agreed on the diagnosis (Skacel *et al* 2000). The reasons for this are uncertain. It may be that when a greater number of pathologists agree on the diagnosis of low-grade dysplasia, it is because the changes are more advanced and further along the continuum towards high-grade dysplasia and adenocarcinoma. It, thus, seems likely that the further along the continuum the tissue is, the less likely that it will stall or regress. Earlier in the pathway, when the changes are more subtle and, thus, more subjective, the tissue may well be unstable and be more likely to regress and lose the features of dysplasia.

An alternative explanation is that the cohort of patients who are more likely to progress have a single distinctive change that is a cornerstone in the risk of progression and may also be a very distinctive marker for pathologists. If there is a biomolecular change that signifies a watershed moment in the biology of low-grade dysplasia, and this is identifiable either by histology or by Raman spectroscopy, then this could separate the patients with low-grade dysplasia and aid in their risk stratification.

## 7.2: Building a Model from an imperfect Standard

### 7.2.1: The 'Not so Gold' Gold Standard

The presence of the morphological changes of dysplasia in Barrett's oesophagus is, at the present time, the best marker that we have to predict the development of adenocarcinoma. These changes, a result of the accumulation of genetic and epigenetic changes that cause disruption at the cellular level, however, are difficult to identify as they are a subtle continuum, as opposed to abrupt differences. There is also a marked overlap in the morphological changes of inflammation, regeneration and metaplasia with those of malignancy.

A multitude of studies (Reid *et al* 1988, Sagan *et al* 1994, Alikhan *et al* 1999, Baak *et al* 2002) have, for some time, demonstrated inter-observer variability in identifying the presence of dysplasia, as well as assigning the grade of



dysplasia. These findings were confirmed in a large, multicentre prospective study (Kerkhof *et al* 2007). This study used Cohen's kappa coefficient ( $\kappa$ ) which measures inter-observer variability whilst also taking into account the possibility that agreement occurs by chance (Cohen 1960). A score of  $\leq 0$  equates to no agreement with increasing agreement up to a score of 1. Even between expert GI Histopathologists, when differentiating Barrett's oesophagus without dysplasia versus low-grade dysplasia (including indefinite for dysplasia) versus high-grade dysplasia and adenocarcinoma, the kappa coefficient was 0.27 (Kerkhof *et al* 2007). This equates to a fair or minimal agreement, with 3 out of every 10 samples potentially being misdiagnosed.

The majority of studies assessing inter-observer variability found that the main source of disagreement was in the differentiation of Barrett's oesophagus without dysplasia and Barrett's oesophagus with low-grade dysplasia or indefinite for dysplasia. A more recent study, nevertheless, found that a considerable variability in the diagnosis of high-grade dysplasia. 40% of patients initially diagnosed as high-grade dysplasia were reclassified to low-grade dysplasia, and in some cases as no dysplasia or not even the presence of Barrett's oesophagus (Sangle *et al* 2015). The current recommendation for patients with high-grade dysplasia is for, after review by a specialist histopathologist, endoscopic resection (Fitzgerald *et al* 2013). If the results of this study are repeatable, it implies that 40% of patients may have undergone unnecessary intervention.

This difficulty in diagnosis has fuelled the desire to find an improved detection method for Barrett's oesophagus and, in particular, dysplasia. Multiple research groups have looked into using enhanced imaging modalities to identify these changes as discussed in previous chapters. When analysing their ability to differentiate changes and grades of dysplasia, they are compared to and analysed according to the current gold standard of histopathological review. This gold standard has, as discussed, been shown to be less than gold. This makes it extremely difficult to ascertain how good and how meaningful the results of research utilising different modalities are.

It may be, for example, that Raman spectroscopy is more sensitive than histopathology and, hence, actually appears to contradict the histopathology review when it is more accurate. How are we to assess which is the more

accurate assessment when the standard is far from flawless? Could we, for example, build a classification model from only the samples which have complete agreement from pathologists and use this to characterise the samples for which we are unsure?

### 7.2.2: Molecular Biomarkers to improve the Gold Standard

Alongside research looking at enhanced imaging techniques, an alternative branch of research has been looking into biomarkers. A biomarker is defined as a characteristic that is objectively measured and evaluated as an indicator of normal biological processes, pathogenic processes, or pharmacologic responses to a therapeutic intervention (Atkinson *et al* 2001).

p53, a tumour suppressor gene, is probably the most studied genetic marker in all cancer types. Multiple studies have shown that for patients with Barrett's oesophagus, aberrant p53 protein expression is associated with an increased risk of malignant progression (Kastelein *et al* 2013). Interestingly, the combination of established low-grade dysplasia with aberrant p53 expression results in a much higher progression than that of low-grade dysplasia alone (Kaye *et al* 2009, Kastelein *et al* 2013).

Flow cytometric analysis is able to detect changes in DNA content and chromosome number, known as aneuploidy. Evidence is accumulating that aneuploidy places the patient at a higher cumulative risk for malignant progression (Reid *et al* 2000). SOX2, a transcription factor, essential for maintaining self-renewal, has been shown to be overexpressed or upregulated in a number of cancers, including high Gleason grade prostate cancer and squamous cell lung cancer. In patients with Barrett's oesophagus, it has been shown that SOX2 expression is progressively lost as patient's progress along the path to malignancy (van Olphen *et al* 2015).

More recently, a panel of four genes, CDX2, p120 catenin, c-myc and Jagged1, was investigated to determine their ability, in combination, to aid histological assessment of Barrett's oesophagus. The four proteins, each from a different signalling pathway, showed the greatest change in expression between low-grade and high-grade dysplasia, yet could also aid in distinguishing Barrett's

without dysplasia from Barrett's with low-grade dysplasia (Karamchandani *et al* 2016).

These studies demonstrate that the morphological changes that are detected as dysplasia are preceded and caused by an array of genetic and epigenetic changes. Although these changes may occur to a different degree and in a different order in each individual, evidence has indicated that certain changes result in an increased risk of malignant progression, with the majority of changes occurring in the transition from low-grade to high-grade dysplasia.

It is apparent that a cohort of patients with Barrett's oesophagus will never progress along the path of malignant progression. Once low-grade dysplasia has occurred, a proportion of these patients will also not progress further along the pathway. The recommendation, however, for all these patients is surveillance endoscopy which is costly in terms of resources and finance and can be anxiety-inducing for the patient. It may be that the molecular changes are what differentiate and divide the two cohorts and, if identified, could aid management decisions. For example, patients with the beginnings of low-grade dysplasia without genetic changes may be in a state of flux and able to regress, whereas, once genetic changes have occurred, they may be unable to reverse the changes.

The molecular changes may impact on the histological features of dysplasia that are too subtle to be detectable by histopathological review. Raman spectroscopy has been shown to provide the greatest information regarding the molecular composition of the tissue. It may be, therefore, that there are differences that Raman spectroscopy can detect between, for example, patients with low-grade dysplasia who will not progress to malignancy and patients who will. Rather than comparing spectroscopic changes to the current gold standard of histopathology alone, it may be appropriate to compare to histopathological and molecular changes to see if this improves accuracy and detects a difference in the two cohorts of patients.

The British Society of Gastroenterology Guidelines suggest that the addition of a p53 immunostain to the histopathological assessment may improve the diagnosis of dysplasia (Fitzgerald *et al* 2013). It would be of interest to see if

patients with low-grade dysplasia and aberrant p53 expression have a different signature spectrum when compared to low-grade dysplasia and no aberrant p53 expression. If a difference could be detected, Raman spectroscopy could then be utilised as both a diagnostic and prognostic tool, and identify patients who would benefit from intense surveillance or early treatment and those who would not. If there were no barriers in terms of money and manpower, the next step in investigating Raman spectroscopy as a clinical diagnostic tool in Barrett's oesophagus would be to measure a large volume of samples which are stratified by histopathology as well as genetic changes and, if possible, stratified according to their progression in subsequent biopsy samples.

### 7.2.3: The benefit of hindsight

The ultimate aim of endoscopic surveillance and biopsy is to identify patients prior to their progression to invasive carcinoma. The majority of patients in the surveillance programme will never reach this point. Aside from the diagnosis of dysplasia, no identifiable feature has helped in the risk stratification of patients and it is only time that predicts which patients benefit from rigorous surveillance.

Histopathological diagnosis cannot detect, aside from dysplasia, which patients have a greater risk of progression. For example, there is not a specific feature that occurs in some patients with low-grade dysplasia and not in others, that distinguishes those with a greater risk of progression. Raman spectroscopy may be able to detect features via their unique spectrum that may not be distinguishable microscopically, hence, improve upon rather than match the current Gold standard.

One way of assessing this would be to identify patients in a retrospective study and separate the patients who progressed to high-grade dysplasia or adenocarcinoma from those that did not. By reviewing their original biopsies and performing Raman spectra of these biopsies, any differences, if present at an earlier stage, could be identified. If there are differences between the two groups, these could be representative of early biochemical changes that distinguish patients who will, or who are at a greater risk, of progression, thus, aiding management decisions.

### 7.3: Where do we go from here?

Raman spectroscopy and indeed other enhanced imaging modalities have been used in research settings for many years now. There has, as yet, not been a major breakthrough in the management of Barrett's oesophagus or a transition of any of these technologies into routine clinical practise. There are many potential reasons for this. One of them, however, is certainly not due to the need for advancements in the management of Barrett's oesophagus.

One of the primary reasons for the lack of transition to clinical practise is the difficulty in understanding where this technology would fit in the current clinical setting of the NHS. The two main areas where this technology could fit is in ex-vivo analysis and in-vivo diagnosis. For either of these roles there has, as yet, been no large scale, multi-centre research studies indicating an improvement in diagnosis and subsequent patient outcomes when this technology is utilised. For this to occur, there not only needs to be a large volume of centres utilising Raman spectroscopy that can enrol patients into the study, but there would also need to be a significant follow-up period extending into years. This is because the diagnosis of dysplasia is relevant in its likelihood to progress to high-grade dysplasia and adenocarcinoma, rather than simply the accuracy of the initial diagnosis.

Other issues in the integration of any new technology is overcoming the outlay costs which, in this case, would be high and overcoming scepticism among clinicians. The best way of removing scepticism is to show, with high quality research, how the new method can benefit patient care.

#### 7.3.1: Automated Histology: Reducing the burden on the Histopathology Department

Surveillance for patients with Barrett's oesophagus places considerable demands on endoscopy and histopathology departments in terms of resource allocation and, of course, cost. The benefits of enrolment onto a surveillance programme are actually unclear with a case control study indicating no substantial reduction in death from oesophageal cancer in those on the programme (Corley *et al* 2013). A prospective multi-centre trial, Barrett's Oesophagus Surveillance versus endoscopy at need Study (BOSS), is underway to answer the question as to the benefits of surveillance (Old *et al* 2015).

At the present time, the only method of risk stratification is dysplasia. If no additional markers or refinement of features that can segregate those at most risk can be found, then it is likely that surveillance with random biopsies as per the Seattle regimen and histopathological review will continue. In addition to the burden placed on endoscopy units, the preparation and review of the biopsies by the Histopathology department constitutes a substantial workload. It has been shown that 2mm diameter sections which were mapped over 30-90 minutes, provided sufficient information to enable the discrimination of pathology (Hutchings *et al* 2010).

An automated means of screening biopsy samples ascertained as part of the surveillance programme would significantly reduce the impact on Histopathologists. Given the number of biopsy samples taken from a routine surveillance endoscopy, which equates to at least 4 biopsies for every 1-2 cm of Barrett's oesophagus, a faster time frame than 30-90 minutes would be required. Point spectra would be markedly swifter, however, in this research, the specificity for identifying dysplasia was only 0.59. As discussed these results are poorer than expected, yet it may be that point spectra alone are inadequate and a higher volume of tissue with a reasonable time frame enables a high specificity which identifies the samples requiring further review by a histopathologist. This system would be ideal, at least until in vivo, real time probes could reduce the need for biopsies in some, but certainly not all, situations.

### 7.3.2: Real time, In-vivo Raman Spectroscopy

Several fibre-optic Raman probes have been developed specifically for compatibility with endoscopes (Shim *et al* 1999, Day *et al* 2009, Huang *et al* 2009). The first in vivo probe (Shim *et al* 2000), which sampled mucosal and submucosal samples, failed to achieve the high diagnostic discrimination required, however, subsequent studies have had better results, both in term of higher specificities and sensitivities of diagnosis, and in reduced spectral acquisition times.

An in vivo probe is a desired addition to the arsenal of clinical diagnosis. It would allow real time diagnosis of dysplasia and, thus, guide further management at the time of endoscopy. I would not envisage a time where high-grade dysplasia would be diagnosed and endoscopic resection completed in the same sitting although spectroscopy could be utilised to guide resection margins. I would imagine, however, that in vivo findings would guide the need for biopsies. For example, if no dysplasia is identified, biopsies would not be required. If dysplasia, of any grade, is detected then these areas would need to be biopsied, resulting in additional biopsies from areas of concern or uncertainty. For this to be clinically applicable, a high specificity would be required as the implications from missing any areas of dysplasia could be catastrophic, whereas, a biopsy of areas without dysplasia would be time-consuming but not a disaster.

The vast majority of research to date, even using Raman probes built specifically for use in a current endoscope, has been on ex vivo samples. This eliminates the technical difficulties of maintaining contact with an oesophageal mucosa with constant peristaltic waves. For this reason as well as the need for assessing multiple areas, acquisition time for each spectra must be rapid, whilst still maintaining a high specificity.

Recent work using in vivo probes (Bergholt *et al* 2011, Bergholt *et al* 2014) has demonstrated high specificity (>90%) in identifying oesophageal

adenocarcinoma and areas of dysplasia with short acquisition times of 0.5 seconds. These studies focused on abnormal areas of the oesophagus and, thus, the next step to determine the full value of this technology would be screening of an oesophagus with Barrett's oesophagus and no visible abnormalities to ascertain how many areas can be screened, how to ensure variable areas are assessed and what acquisition time provides an appropriate specificity.

Overall a strategy of only taking a biopsy of areas that show dysplasia on in vivo Raman spectroscopy would reduce the resources on the Histopathology department in the processing of samples, and reduce the risk, albeit small, of complications from the biopsy procedure itself. Of perhaps greatest importance, this strategy would ensure that more tissue is sampled from the areas of interest, improving the likelihood that, if present, dysplastic changes are identified. These areas would then be reviewed by a Histopathologist whose skills and expertise compliment and add to the knowledge that the Raman spectroscopy analysis provides.

### 7.3.3: Enhanced Risk Stratification

A considerable dilemma in the management of patients with Barrett's oesophagus is the inability to determine at an early stage which patients are at risk of progression to malignancy, thus, at present, all patients are enrolled onto a surveillance programme. Low-grade dysplasia appears to be an unstable, and possibly fluctuant, stage at which a cohort of patients set off on the path towards malignancy. Knowing this subset would enable treatment in the form of ablation at this very early stage, preventing progression and also refining the need for surveillance for the remaining patients with Barrett's oesophagus.

I would suspect that there are changes or markers that occur in low-grade dysplasia that can determine which patients are likely to progress. These markers could be related to cellular proliferation, apoptosis or migration, for example. Raman spectroscopy, with the potential to detect biomolecular changes in tissue, may be able to detect these changes. At present there have



been no studies in the oesophagus with potential biomarkers. In the colon, an in vivo pilot study using a peptide that binds with the human tyrosine kinase c-Met conjugated to a fluorescent cyanine dye enabled improved detection of colonic polyps, including polyps unidentifiable with white light endoscopy (Burggraaf et al 2015).

The rate-limiting step in the oesophagus, nevertheless, is the determination of which changes these may be. Improving the current gold standard with additional information from genetics or from longitudinal studies may identify which markers are significant. Not only will improved risk stratification have the potential to treat patients at a very early stage, hopefully improving outcome, but it would also rationalise resources and improve patient anxiety.

#### 7.4: Final Thoughts

The greatest means of improving the survival from oesophageal adenocarcinoma is the identification of at risk individuals and the prevention of the development of carcinoma. It has been well established that Barrett's oesophagus places an individual at greater risk, yet within this group it is difficult to ascertain those at greatest risk.

Spectroscopy has the ability to identify subtle changes in tissue that reflect the earliest changes that occur in the path to malignancy. This body of research again supports this, however, in order for this technology to become a useful adjunct in the fight against cancer, further work needs to incorporate this with other risk factors to determine if there are changes that identify which individuals are at risk. This will enable earlier treatment for those who will benefit as well as streamlining the surveillance workload which currently utilises a substantial amount of resources.

## Appendix I

### Deparaffinisation protocol

- Sections of FFPE tissue were cut and placed on calcium fluoride slides, stored in plastic coin cases and transferred from the Histopathology lab at Cheltenham General Hospital to the Biophotonics Research Unit at Gloucestershire Royal Hospital.
- The calcium fluoride slides were soaked in Xylene solution for at least 12 hours. Safety precautions of personal protection wear were undertaken and the work was carried out under a fume extraction system.
- After soaking in Xylene, each slide was rinsed alternatively with sterile water and methanol to rinse off the residual paraffin. This cycle was completed at least twice for each slide.
- The slides were left to air dry under the fume extraction hood. Once dry, the slides were stored in plastic coin containers and kept at room temperature in dark conditions until needed for measurements.

Appendix II

Details of Sample Measurements

<u>Sample Number</u>	<u>Histology</u>	<u>Point: Region 1</u>	<u>Point: Region 2</u>	<u>Point: Region 3</u>	<u>Point: Region 4</u>	<u>802 Map</u>	<u>Region 1</u>	<u>Region 2</u>	<u>Region 3</u>	<u>Region 4</u>
15.35188	BE	02/08/16 + 08/08/16	02/08/16	02/08/16	02/08/16	03/08/16	RM1 (Section 1: Region 1): 2478 points: 31.8 mins	RM3 (Section 2: Region 2): 3420 points: 48 mins	RM4 (Section 2: Region 3): 2640 points: 35.4 mins	RM2 (Section 1: Region 4): 238 points: 4.4 mins
15.33592	LGD	03/08/16	03/08/16	03/08/16	03/08/16	04/08/16	RM3 (Section 3: Region 1): 5483 points: 65 mins	RM2 (Section 1: Region 2): 7812 points: 100 mins	RM1 (Section 2: Region 3): 5950 points: 75 mins	X
15.34297	HGD	04/08/16	04/08/16	04/08/16	04/08/16	04/08/16	RM6 (Section 1: Region 1): 3477 points: 45 mins	RM5 (Section 5: Region 2): 1404 points: 18 mins	RM4 (Section 4+2: Region 3): 11025 points: 130 mins	X
15.20106	AC	18/08/16	18/08/16	18/08/16	18/08/16	25/08/16	RM1 (Section2: Region 1): 6402 points: 79 mins	RM3 (Section 6: Region 2): 1927 points: 26 mins	RM2 (Section 5: Region 3): 7004 points: 88 mins	X

15.32635	BE	04/08/16	04/08/16	04/08/16	04/08/16	08/08/16	RM1 (Section 2: Region 1): 2528 points: 31 mins	RM2 (Section 1: Region 2): 1505 points: 21 mins	X	RM3 (Section 1: Region 4): 1540 points: 19 mins
15.30884	LGD	08/08/16	08/08/16	08/08/16	08/08/16	08/08/16	RM1 (Section 3: Region 1): 1476 points: 20 mins	RM2 (Section 4: Region 2): 1485 points: 19 mins	RM3 (Section 1: Region 3): 8330 points: 101 mins	X
15.32885 _2	HGD	17/08/16	17/08/16	17/08/16	17/08/16	22/08/16	RM1 (Section 3: Region 1): 5504 points: 70 mins	RM2 (Section 4: Region 2): 2268 points: 31 mins	RM3 (Section 1: Region 3): 1740 points: 25 mins	X
15.17409 _1	AC	08/08/16	08/08/16	08/08/16	08/08/16	15/08/16	RM1 (Section 3: Region 1): 6083 points: 75 mins	RM3 (Section 1: Region 2): 9494 points: 116 mins	RM2 (Section 2: Region 3): 4473 points: 57 mins	X
15.29335	BE	08/08/16	08/08/16	08/08/16	08/08/16	11/08/16	RM4 (Section 4: Region 1): 11960 points: 142 mins	RM2 (Section 2: Region 2): 5859 points: 75 mins	X	RM3 (Section 1: Region 4): 3132 points: 40 mins
15.30026	LGD	09/08/16	09/08/16	09/08/16	09/08/16	16/08/16	RM1 (Section 1: Region 1): 9744 points: 117 mins	Section: High fusicin content	RM2 (Section 2: Region3): 1386 points: 20 mins	RM3 (Section 3: Region 4): 1640 points: 22 mins
15.32885 _3	HGD	09/08/16	09/08/16	09/08/16	X	09/08/16	RM1 (Section1: Region 1): 108350 points: 131 mins	RM3 (Section 3: Region 2): 1833 points: 25 mins	RM3 (Section 2: Region 3): 7797 points: 98 mins	X

15.17409 _2	AC	09/08/16	09/08/16	09/08/16	09/08/16	09/08/16	RM1 (Section 3: Region 1): 2250 points: 30 mins	RM 2 (Section 2: Region 2): 2538 points: 34 mins	X	RM3 (Section 2: Region 4): 675 points: 10 mins
15.25743 _1	BE	09/08/16	09/08/16	09/08/16	09/08/16	16/08/16	RM1 (Section 3: Region 1): 1400 points: 18 mins	RM2 (Section 3: Region 2): 2356 points: 30 mins	RM3 (Section 4: Region 3): 943 points: 13 mins	X
15.19302 _1	LGD	09/08/16	09/08/16	09/08/16	09/08/16	11/08/16	RM1 (Section 1: Region 1): 5561 points: 93 mins	X	RM2 (Section 1: Region 3): 1978 points: 27 mins	RM3 (Section 1: Region 4): 640 points: 9 mins
15.28130	HGD	18/08/16	18/08/16	18/08/16	18/08/16	26/08/16	X	X	RM1 (Section 1: Region 3): 12420 points: 147 mins	X
15.16592	AC	09/08/16	09/08/16	09/08/16	09/08/16	18/08/16	RM1 (Section 1: Region 1): 3312 points: 42 mins	RM3 (Section 2: Region 2): 7216 points: 89 mins	RM2 (Section 4: Region 3): 6000 points: 74 mins	X
15.25743 _2	BE	11/08/16	11/08/16	11/08/16	11/08/16	17/08/16	RM1 (Section 1: Region 1): 1608 points: 20 mins	X	RM2 (Section 2: Region 3): 812 points: 12 mins	RM3 (Section 2: Region 4): 1887 points: 25 mins

15.19302 _2	LGD	17/08/16	17/08/16	17/08/16	17/08/16	23/08/16	RM2 (Section 2: Region 1): 4466 points: 56 mins	RM1 (Section 1: Region 2): 4350 points: 53 mins	X	RM3 (Section 2: Region 4): 2480 points: 32 mins
15.26104	HGD	11/08/16	11/08/16	11/08/16	11/08/16	15/08/16	RM3 (Section 3: Region 1): 924 points: 13 mins	RM1 (Section 7: Region 2): 3552 points: 47 mins	RM2 (Section 2: Region 3): 2112 points: 30 mins	X
15.15313	AC	17/08/16	17/08/16	17/08/16	17/08/16	17/08/16	RM1 (Section 2: Region 1): 11421 points: 141 mins	RM2 (Section 1: Region 2): 5609 points: 70 mins	RM3 (Section 4: Region 3): 1716 points: 23 mins	X
15.25742 _1	LGD	19/08/16	19/08/16	19/08/16	X	22/08/16	RM3 (Section 1: Region 1): 4355 points: 55 mins	RM2 (Section 2: Region 2): 2294 points: 30 mins	RM1 (Section 2: Region 3): 1590 points: 23 mins	X
15.20664 _5G	AC	19/08/16	19/08/16	X	X	05/09/16	RM1 (Section 1: Region 1): 27816 points: 324 mins			
15.25742 _2	LGD	Not present	23/08/16	Section 3 (?HGD): 23/8/16		05/09/16	Not present	RM1 (Section 2: Region 2): 5546 points: 71 mins	RM2 (Section 4: Region 3): 12348 points: 150 mins	
15.30026 _3	LGD	22/08/16	22/08/16	22/08/16	22/08/16	26/08/16	RM1 (Section 1: Region 1): 2491 points: 33 mins	RM2 (Section 1: Region 2): 3626 points: 45 mins	RM3 (Section 2: Region 3): 900 points: 13 mins	X

15.17961	AC	23/08/16	23/08/16	23/08/16	X	26/08/16	RM1 (Section 1: Region 1): 18120 points: 217 mins	RM2 (Section 1: Region 2): 8148 points: 100 mins	X	X
15.19041	LGD (?HGD)	22/08/16	22/08/16	22/08/16	X	28/09/16	RM1 (Section 2: Region 1): 6161 points: 74 mins	RM2 (Section 1: Region 2): 2860 points: 37 mins	X	X
15.19299 _2	BE	19/08/16	19/08/16	19/08/16	X	23/08/16	RM1 (Section 1: Region 1): 2068 points: 27 mins	RM2 (Section 2: Region 2): 2664 points: 37 mins	RM3 (Section 3: Region 3): 3825 points: 48 mins	X
15.20664 _5C	AC	22/08/16	X	X	X	06/09/16	RM1 (Section 1: Region 1): 27248 points: 324 mins	X	X	X
15.25358	BE	22/08/16	22/08/16	22/08/16	X	25/08/16	RM1 (Section 2: Region 1): 5742 points: 71 mins	X	RM2 (Section 4: Region 3): 4554 points: 61 mins	X
15.21320	HGD	22/08/16	22/08/16	22/08/16	22/08/16	25/08/16	RM1 (Section 1: Region 1): 2325 points: 29 mins	RM2 (Section 8: Region 2): 3248 points: 42 mins	RM3 (Section 4: Region 3): 2628 points: 32 mins	X
15.00079	HGD	19/08/16	19/08/16	X	X	25/08/16	RM1 (Section 1: Region 1): 15827 points: 188 mins	RM2 (Section 1: Region 2): 18200 points: 212 mins	X	X

15.19299 _1	BE	22/08/16	22/08/16	22/08/16	X	26/08/16	RM1 (Section 3: Region 1): 3200 points: 42 mins	RM2 (Section 2: Region 2): 2886 points: 40 mins	RM3 (Section 4: Region 3): 1628 points: 22 mins	X
15.17268	AC	25/08/16	25/08/16	X	X	27/09/16	RM1 (Section 1: Region 1): 16074 points: 192 mins	RM2 (Section 1: Region 2): 5475 points: 68 mins	X	X
15.11932	LGD	25/08/16	25/08/16	25/08/16	X	06/09/16	RM1 (Section 1: Region 1): 2346 points: 33 mins)	RM2 (Section 1: Region 2): 5600 points: 72 mins	X	X
15.05026	BE	25/08/16	25/08/16	25/08/16	X	30/09/16	X	RM1 (Section 2: Region 2): 9047 points: 112 mins	RM2 (Section 2: Region 3): 6634 points: 85 mins	X
14.35789	HGD	25/08/16	25/08/16	25/08/16	X	06/09/16	RM1 (Section 1: Region 1): 3087 points: 40 mins	RM2 (Section 2: Region 2): 1995 points: 28 mins	RM3 (Section 2: Region 3): 3139 points: 40 mins	X
15.18519	AC	25/08/16	X	X	X	Slide broken	X	X	X	X
15.08465 _2	LGD	25/08/16	25/08/16	Slide broken	X	Slide broken	X	X	X	X
15.21473 _2	BE	25/08/16	X	X	X	26/09/16	RM1 (Section 1: Region 1): 4717 points: 62 mins	X	X	X



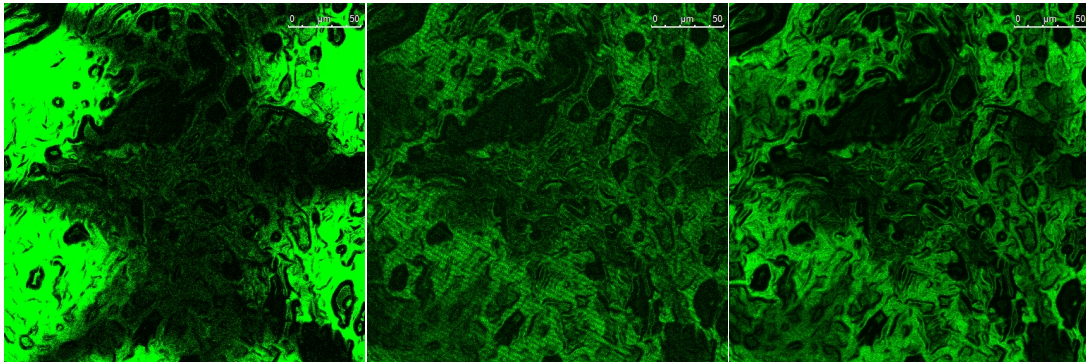
14.35738	HGD	25/08/16	25/08/16	25/08/16	X	06/09/16	RM1 (Section 1: Region 1): 1024 points: 15 mins	RM2 (Section 2: Region 2): 3268 points: 44 mins	RM3 (Section 3: Region 3): 1295 points: 18 mins	X
15.15382	NSq	26/09/16	26/09/16	X	X	28/09/16	RM1 (Section 1: Region 2): 2079 points: 26 mins	RM2 (Section 2: Region 2): 1150 points: 16 mins	X	X
16.24149	NSq	06/09/16	06/09/16	06/09/16	06/09/16	28/09/16	RM1 (Section 1: Region 1): 4346 points: 52 mins	RM2 (Section 1: Region 2): 1530 points: 22 mins	X	X
16.13136	NSq	06/09/16	06/09/16	06/09/16	06/09/16	29/09/16	RM1 (Section 1: Region 1): 1829 points: 26 mins	RM2 (Section 3: Region 2): 3822 points: 50 mins	RM3 (Section 4: Region 3): 2867 points: 38 mins	X
14.25714 _2	NSq	06/09/16	06/09/16	06/09/16	06/09/16	29/09/16	RM1 (Section 1: Region 1): 3102 points: 39 mins	RM2 (Section 2: Region 2): 2310 points: 30 mins	X	RM3 (Section 2: Region 4): 1323 points: 17 mins
16.24074	NSq	26/09/16	26/09/16	26/09/16	X	28/09/16	RM1 (Section 1: Region 1): 13568 points: 164 mins	X	X	X
16.2339	NSq	26/09/16	X	X	X	29/09/16	RM1 (Section 1: Region 1): 8844 points: 105 mins	X	X	X
16.23855	NSq	26/09/16	26/09/16	26/09/16	26/09/16	Slide	X	X	X	X

						broken				
15.8037	NSq	26/09/16	26/09/16	X	X	29/09/16	RM1 (Section 1: Region 1): 3256 points: 40 mins	X	X	X
16.23626	NSq	06/09/16	06/09/16	06/09/16	06/09/16	26/09/16	RM1 (Section1: Region 1): 4876 points: 65 mins	RM2 (Section 2: Region 2): 4000 points: 53 mins	RM3 (Section 3: Region 3): 2688 points: 32 mins	X
16.23342	NSq	06/09/16	06/09/16	06/09/16	06/09/16	29/09/16	X	X	RM1 (Section 2: Region 3): 3626 points: 48 mins	RM2 (Section 2: Region 4): 3496 points: 44 mins

Appendix III

Autofluorescent Results

Normal Squamous Tissue

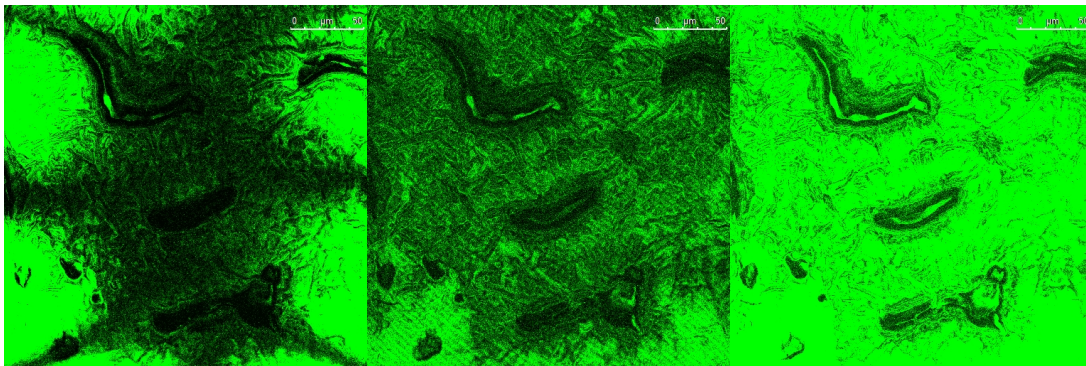


476nm

488nm

496nm

Barrett's oesophagus without Dysplasia

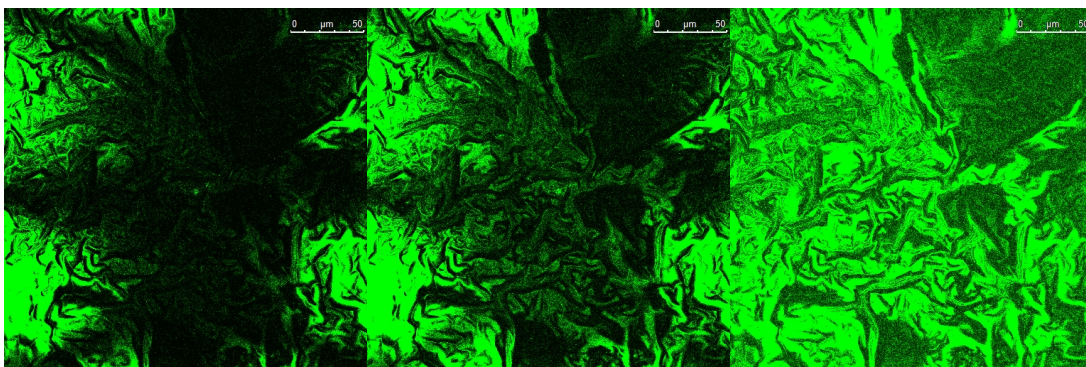


476nm

488nm

496nm

Barrett's oesophagus with Low Grade Dysplasia

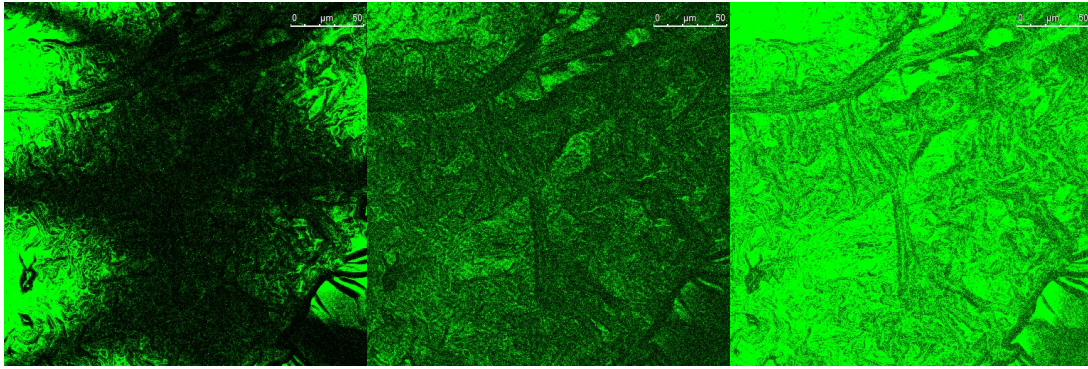


476nm

488nm

496nm

## Barrett's oesophagus with High Grade Dysplasia

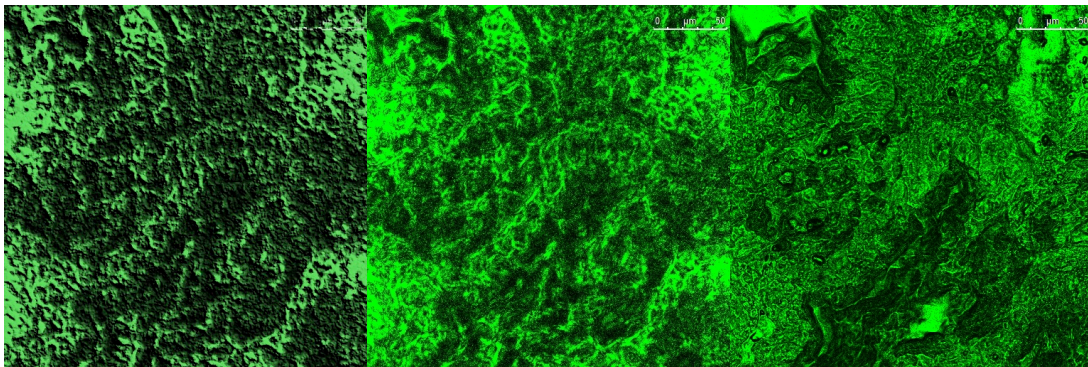


476nm

488nm

496nm

## Oesophageal Adenocarcinoma



476nm

488nm

496nm

Appendix IV

Biochemical Peak Assignment

	<u>Wavenumber (cm<sup>-1</sup>)</u>	<u>Reference</u>
Glycogen	470	Hutchings <i>et al</i> 2010
	484-90	Hutchings <i>et al</i> 2010, Almond <i>et al</i> 2013
	852-5	Shetty <i>et al</i> 2006, Hutchings <i>et al</i> 2010
	933-7	Shetty <i>et al</i> 2006, Almond <i>et al</i> 2013
	944	Hutchings <i>et al</i> 2010
	1036	Hutchings <i>et al</i> 2010
	1048	Shetty <i>et al</i> 2006
	1086-8	Hutchings <i>et al</i> 2010, Almond <i>et al</i> 2013
	1128	Almond <i>et al</i> 2013
	1135	Hutchings <i>et al</i> 2010
	1133-8	Shetty <i>et al</i> 2006, Hutchings <i>et al</i> 2010
	1467	Hutchings <i>et al</i> 2010
DNA	719-20	Shetty <i>et al</i> 2006
	748-55	Shetty <i>et al</i> 2006
	781-5	Shetty <i>et al</i> 2006, Hutchings <i>et al</i> 2010, Almond <i>et al</i> 2013
	885	Almond <i>et al</i> 2013
	1334-5	Almond <i>et al</i> 2013, Bergholt <i>et al</i> 2014
	1576-9	Hutchings <i>et al</i> 2010, Bergholt <i>et al</i> 2014
	1663	Shetty <i>et al</i> 2006
Nucleic Acids	1018-21	Almond <i>et al</i> 2013
	1173	REF 62
	1360	Almond <i>et al</i> 2013
	1511	Almond <i>et al</i> 2013
Protein	820	Shetty <i>et al</i> 2006
	852-5	Hutchings <i>et al</i> 2010
	884	Shetty <i>et al</i> 2006
	936-40	Hutchings <i>et al</i> 2010, Bergholt <i>et al</i> 2014
	1036	Hutchings <i>et al</i> 2010
	1223	Shetty <i>et al</i> 2006

	1261	Hutchings <i>et al</i> 2010
	1265 (Amide III)	Bergholt <i>et al</i> 2014
	1278	Shetty <i>et al</i> 2006
	1312	Hutchings <i>et al</i> 2010
	1453	Hutchings <i>et al</i> 2010
	1655-9 (Amide I)	Hutchings <i>et al</i> 2010, Bergholt <i>et al</i> 2014
	1663	Shetty <i>et al</i> 2006
Phenylalanine	1001-4	Hutchings <i>et al</i> 2010, Bergholt <i>et al</i> 2014
	1031	McManus <i>et al</i> 2012
Lipids	968	Dukor <i>et al</i> 2002
	1078	Bergholt <i>et al</i> 2014
	1302	Bergholt <i>et al</i> 2014
	1745	Bergholt <i>et al</i> 2014
Lactic Acid	750	Shetty <i>et al</i> 2006
	918	Shetty <i>et al</i> 2006
Glucose	842	Rehman <i>et al</i> 1995
Porphyrins	1618	Bergholt <i>et al</i> 2014

## Appendix V

### Posters

#### Towards an understanding of the biochemical changes of dysplasia.

Upchurch E, Old OJ, Lloyd GR, Isabelle M, Shepherd N, Stone N, Kendall C and Barr H.

SPEC: International Spectroscopy Conference: Montreal, Canada, June 2016.

#### Developments in Infrared Spectroscopy of colorectal pathology.

Upchurch E, Old OJ, Griggs R, Woods J, Lloyd GR, Isabelle M, Shepherd N, Cook T, Nallala J, Barr H, Stone N and Kendall C.

Faraday Discussions: Advances in Vibrational Spectroscopy. Cambridge, England. March 2016.

# Developments in infrared spectroscopy of colorectal pathology

Emma Upchurch<sup>\*1,2,4</sup>, Rebecca Griggs<sup>1,2,4</sup>, James J. Wood<sup>1, 2</sup>, Gavin R. Lloyd<sup>2</sup>, Martin Isabelle<sup>2</sup>, Neil A. Shepherd<sup>3</sup>, Tim A. Cook<sup>1</sup>, Jayakrupakar Nallala<sup>4</sup>, Nick Stone<sup>4</sup> and Catherine A. Kendall<sup>2</sup>  
*\*emma.upchurch.glos.nhs.uk*

## Introduction

Colorectal cancer is the second most common cause of cancer death in the UK and accounts for 13% of all new cancer cases each year. Most cancers arise from pre-existing adenomatous polyps. Histopathology provides the gold standard assessment of colonoscopic biopsies, however improved tools are sought.

Infrared spectroscopy (FTIR) can be used to map biochemical concentrations across a tissue section and discriminate between disease states. FTIR may therefore aid the diagnosing pathologist and lead to automated histopathological processing.

## FTIR Classification of Colorectal Pathology

### Sample collection & preparation:

- Colorectal tissue biopsies were snap frozen at colonoscopy.
- 10µm thick tissue sections microtomed onto CaF2 slides for FTIR.
- Contiguous H+E sections reviewed by specialist GI pathologist & identified as normal, hyperplastic, adenoma, cancer or ulcerative colitis.

### Infrared spectroscopy:

- Spectral maps of samples were measured using Perkin Elmer Spotlight 400 Spectrum One infrared imaging system (figure 1)
- Spectra were selected from areas of epithelium for analysis using 'in house' developed software. Mean spectra for each pathology group are shown in figure 2.
- Epithelial spectra were classified according to source pathology type using a mathematical model (Principal Components analysis with Linear Discriminant Analysis and Leave One Out Cross Validation); sensitivities 91.6-100% and specificities 97.7-99.9%.



Fig. 1: PE FTIR Spectrometer

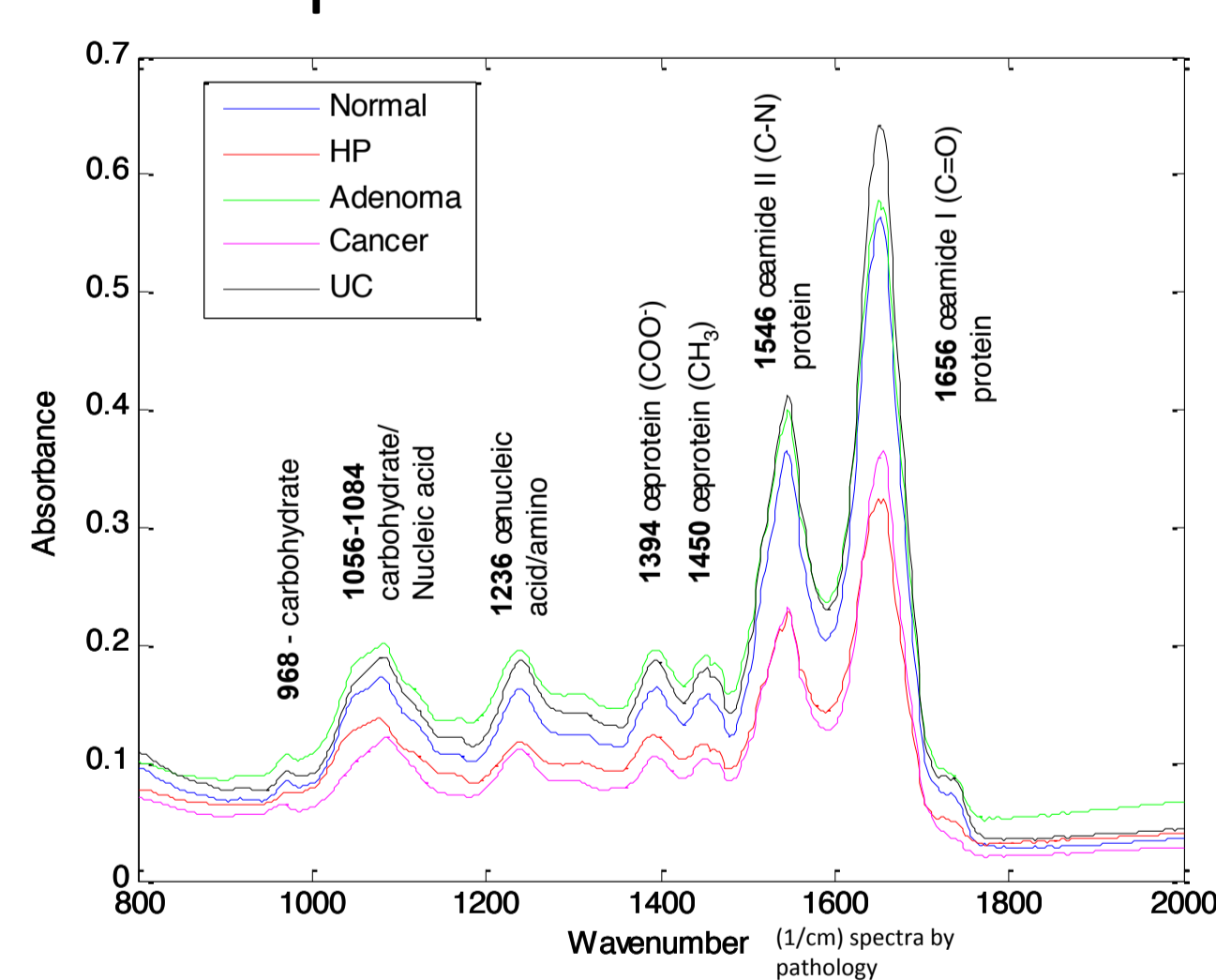


Fig. 2: Mean FTIR

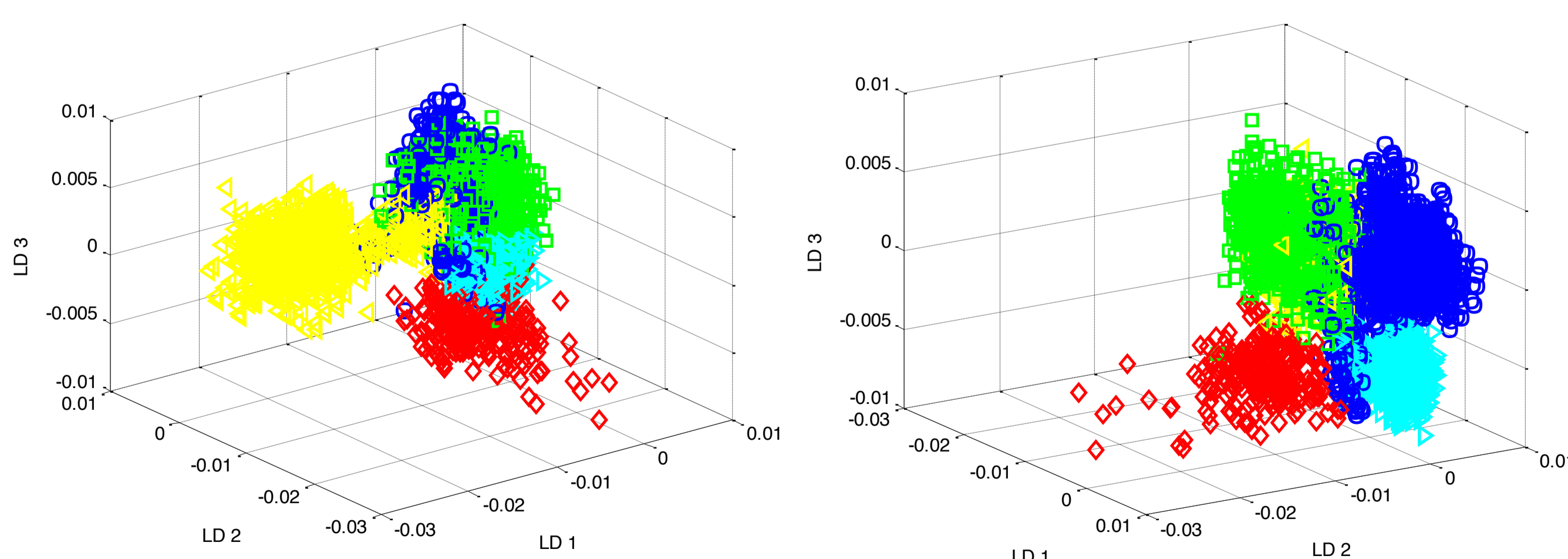


Fig. 3: Linear discriminant score plots showing good visual discrimination between spectra. Normal (blue), hyperplastic polyp (red), adenoma (green), adenocarcinoma (yellow) and ulcerative colitis (cyan).

## High Resolution Imaging of Colorectal disease

### Sample collection & preparation:

- 65 blocks of archive formalin fixed paraffin embedded (FFPE) colorectal tissue was microtomed onto CaF2 slides (10µm thick) for FTIR imaging.
- Contiguous sections were stained with Haematoxylin & Eosin for review by a specialist GI pathologist & identified as normal, dysplasia, polyp cancer, cancer or epithelial misplacement.

### Infrared spectroscopy:

- Spectral maps of samples were measured using Agilent 620 FTIR imaging system in transmission mode with 1.1 micron resolution (figure 4).
- Spectra were selected from areas of epithelium for analysis using 'in house' developed software. Mean spectra for each pathology group are shown in figure.
- Principal Component Analysis with Linear Discriminant Analysis of the spectral peaks was performed to elucidate spectral differences across the dataset.



Fig. 4: Agilent high-res FTIR Spectrometer

## Conclusions

Infrared spectral imaging demonstrates the ability to map tissue sections at high resolution, providing biochemical information that correlates with disease state and suitability for the automated analysis of specimens.

The exact nature of the biochemical change that results in the spectral picture has not been delineated. It is hypothesised that the level of apoptosis changes with dysplasia and, thus, apoptotic breakdown products may themselves have a distinctive autofluorescent or spectral signature that can be used in diagnosis.

Melanosis coli, a benign condition of the colon, is characterised by epithelial cell apoptosis. Using this tissue as a template may, thus, enable the identification of apoptotic breakdown products and determine their presence in colonic and oesophageal tissue.

## Acknowledgements

Funding for this research was provided by CRUK, BDRF, GHNHSFT.

## References

- J. J. Wood, C. Kendall, G. R. Lloyd, N. A. Shepherd, T. A. Cook, and N. Stone (2011). Infrared spectroscopy to estimate the gross biochemistry associated with different colorectal pathologies with different colorectal pathologies. Clinical and Biomedical Spectroscopy and Imaging II
- Griggs R (2015). Thesis, University of Exeter

<sup>1</sup>Department of Surgery, Gloucestershire Hospitals NHS Foundation Trust, UK  
<sup>2</sup>Biophotonics Research Unit, Gloucestershire Hospitals NHS Foundation Trust, UK;  
<sup>3</sup>Department of Pathology, Gloucestershire Hospitals NHS Foundation Trust, UK  
<sup>4</sup>Department of Physics, & Astronomy, University of Exeter, UK



# Developments in infrared spectroscopy of colorectal pathology: Towards an understanding of the biochemical changes of dysplasia

E Upchurch<sup>\*1,2,4</sup>, O Old<sup>1,2,4</sup>, R Griggs<sup>1,2,4</sup>, J Woods<sup>1,2</sup>, G Lloyd<sup>2</sup>, M Isabelle<sup>2</sup>, N Shepherd<sup>3</sup>, T Cook<sup>1</sup>, J Nallala<sup>4</sup>, H Barr, N Stone<sup>4</sup> and C Kendall<sup>2</sup>

\*emma.upchurch.glos.nhs.uk

## Introduction

Colorectal cancer is the 2nd most common cause of cancer death in the UK, accounting for over 16000 deaths in 2012. Each year approximately 41000 cases are diagnosed [1]. When diagnosed at an early stage >90% of patients survive for at least 5 years. This drops to <10% when diagnosed at a late stage. Diagnosing early changes representing disease is, therefore, of paramount importance.

## Development of Colorectal Carcinoma

The majority of colorectal carcinomas develop through a well established pathway of adenoma to carcinoma (Figure 1) [2]. Genetic alternations affecting the regulation of the cell cycle occur as the cells progress along this pathway. Apoptosis, the programmed death of a cell, generally increases as cells move along this pathway and become more abnormal.

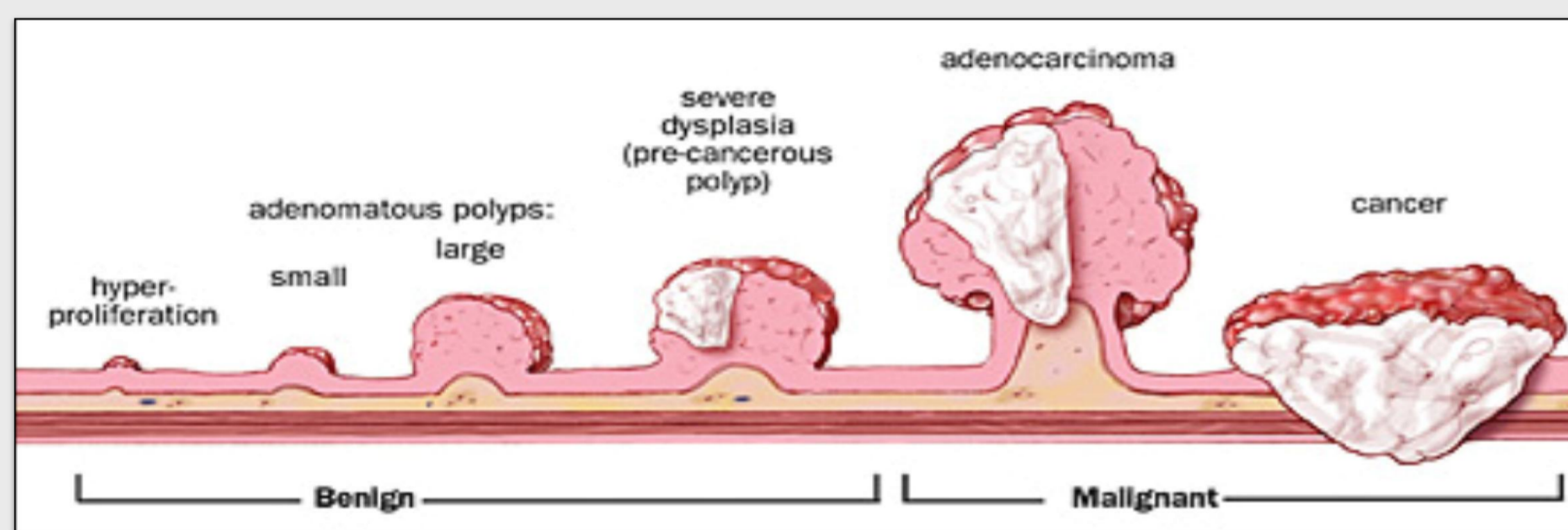


Figure 1: Diagrammatical Representation of the pathway of adenoma - carcinoma

## Classification of Colorectal Pathology

Snap frozen colorectal tissue biopsies were measured using a Perkin Elmer Spotlight 400 Spectrum One infrared imaging system. Spectral maps for each pathology group (normal tissue, hyperproliferative, adenoma, carcinoma and ulcerative colitis) were measured. The mean spectra are shown in Figure 2.

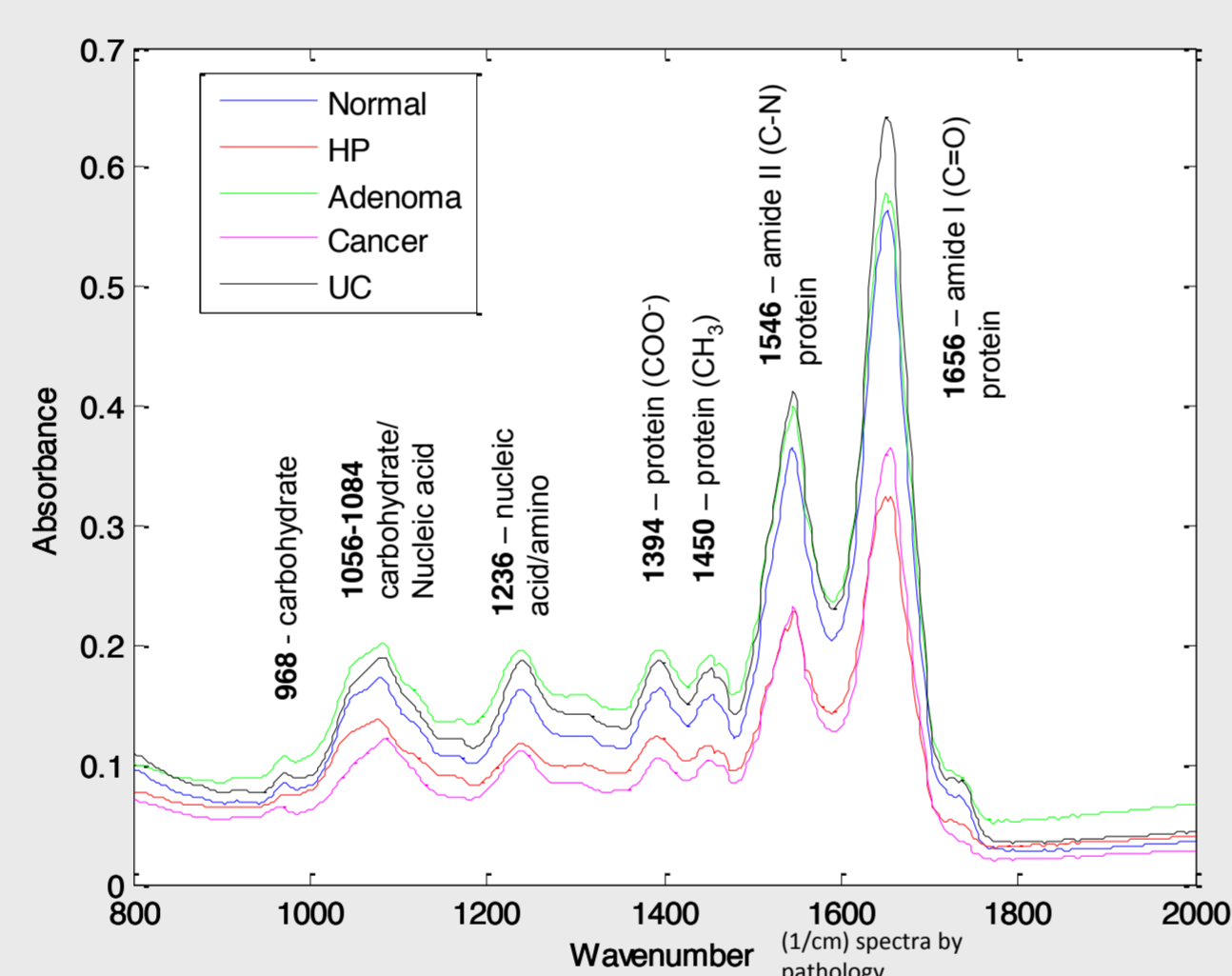


Figure 2: Mean FTIR spectra

Epithelial spectra were classified according to source pathology type using a mathematical model (Principle Components Analysis with Linear Discriminant Analysis and Leave One Out Cross Validation) (Figure 3) with sensitivities of 91.6-100% and specificities of 97.7-99.9%.

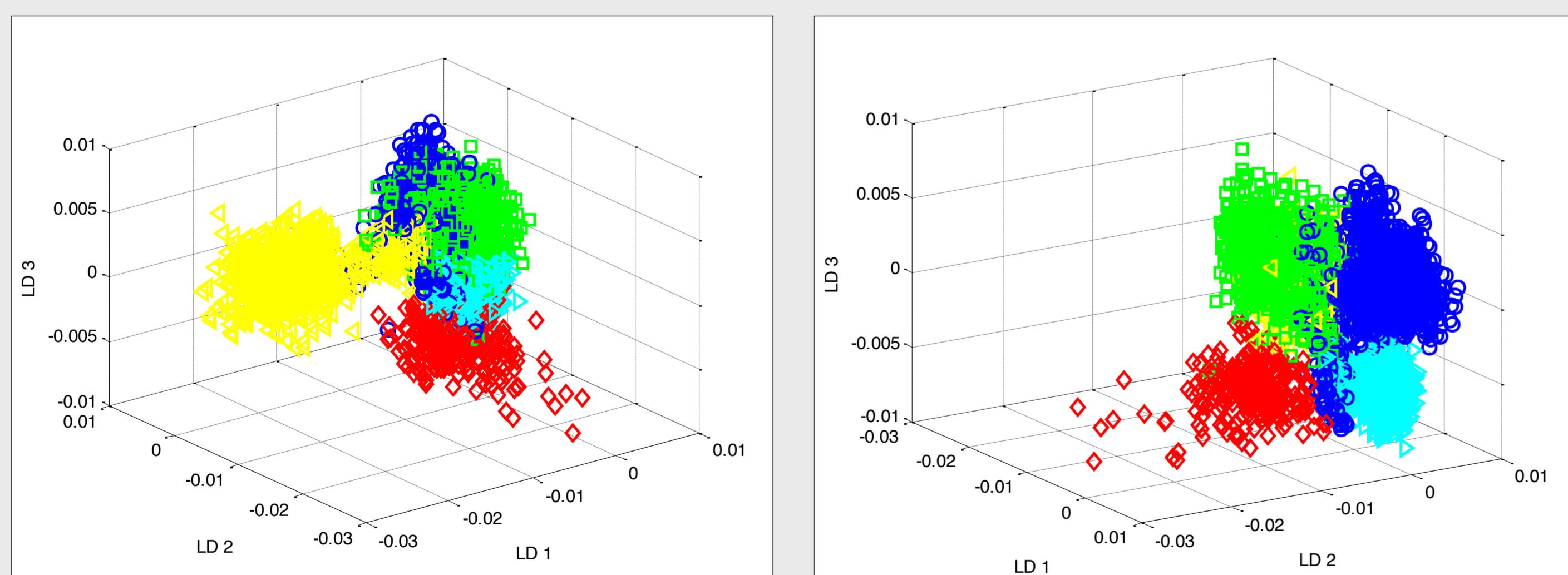


Figure 3: Linear discriminant score plots showing good visual discrimination between spectra. Normal (blue), hyperplastic polyp (red), adenoma (green), adenocarcinoma (yellow) and ulcerative colitis (cyan)

## Acknowledgements

Funding for this research was provided by CRUK, BDRF, GHNHSFT

## References

- [1] CR UK "Cancer Key Facts". Cancer Research UK, 2013
- [2] A, Carey F, Pratt N, Steele R. *BJS*. 2002. 89, 845-860.
- [3] Griggs R (2015). Thesis, University of Exeter
- [4] Ghadially FN et al. 1994. *Histopathology*. 25(3):197-207.
- [5] DaCosta RS et al. 2005. *J Clin Path*. 58(7):766-74.

## High Resolution Imaging

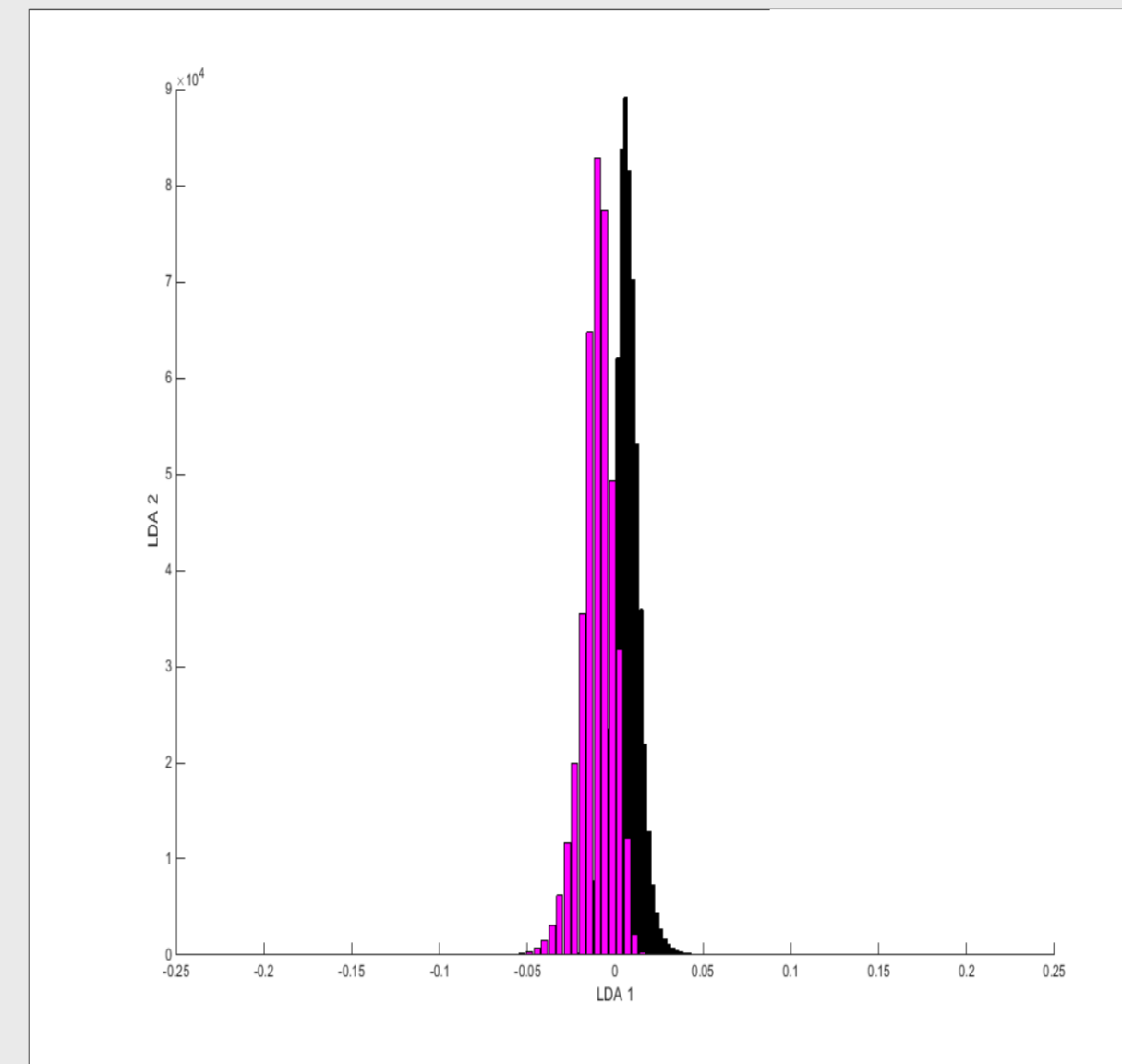


Figure 4: LDA Histogram clustering of Two Group Model. Purple = Epithelial Displacement: Black = Carcinoma

High resolution imaging using the Agilent 620 FTIR imaging system with a pixel resolution of 1.1 microns was able to discriminate between colorectal cancer and colonic epithelial misplacement (Figure 4), a benign pathology of the intestine that mimics invasive carcinoma, causing significant diagnostic difficulties [3]. An average sensitivity of 75% and specificity of 82% was found.

## Can we identify apoptosis?

Infra red imaging has been able to distinguish between different pathology types. High resolution imaging can detect subtle changes in tissues that, visually, pathologists find difficult to differentiate. Could the biochemical changes that occur in dysplasia, i.e.: apoptosis, be detectable with infra red imaging and, thus, enable earlier diagnosis if used clinically?

## Melanosis Coli as a model

Melanosis coli is a benign condition of the colon, characterised by increased apoptosis of the epithelial cells. The apoptotic cell fragments fuse with lysosomes after their phagocytosis by macrophages, resulting in the formation of lipofuscin [4]. Lipofuscin, a breakdown product of apoptosis, causes the classical pigmentation of the colon.



Figure 5: Macroscopic appearance of melanosis coli

All tissues produce autofluorescence when illuminated. Dysplastic epithelial cells were found to be a source of autofluorescence [5]. Lipofuscin may be the source of the autofluorescence seen in dysplastic cells and may represent dysregulated waste disposal.

## Conclusions

Infrared spectral imaging demonstrates the ability to map tissue sections at high resolution, providing biochemical information that correlates with disease state. The exact nature of the biochemical change that results in the spectral picture for each pathology has not been delineated.

As colorectal cancer progresses from adenomatous changes, through dysplasia and finally to adenocarcinoma, and that this progression is characterised by increasing levels of apoptosis, it may be that a portion of the spectral changes are caused by the changes of apoptosis or by the products formed by apoptosis.

Melanosis coli, due to the high volume of lipofuscin, provides an ideal model for characterising and investigating both the pigment and apoptosis. High resolution infra red has been shown to differentiate between tissues that, even to an experienced Histopathologist, are visually unable to be distinguished from each other. It may be that this modality is able to detect differences in the melanosis coli tissue which is due to apoptosis and that, once identified, can be seen in and used to aid differentiation of different colorectal pathologies.

<sup>1</sup> Department of Surgery, Gloucestershire Hospitals NHS Foundation Trust, UK  
<sup>2</sup> Biophotonics Research Unit, Gloucestershire Hospitals NHS Foundation Trust, UK;  
<sup>3</sup> Department of Pathology, Gloucestershire Hospitals NHS Foundation Trust, UK  
<sup>4</sup> Department of Physics, & Astronomy, University of Exeter, UK



## Appendix VI

### Publications

#### Detection of Dysplasia in Barrett's oesophagus: Are there impending optical and spectroscopic solutions?

Upchurch E, Old OJ, Lloyd GR, Isabelle M, Kendall C, Shetty G, Pavlou A, Shepherd N and Barr H. *Gastroenterology, Hepatology and Endoscopy*. 2016. 1(3): 61-67.

#### Principles and Techniques of Vibrational Spectroscopy and Autofluorescence.

Upchurch E, Old OJ, Lloyd GR, Pavlou A, Kendall C, Barr H and Isabelle M. *Recent Advances in Biotechnology*. 2016. Publisher: Avid Science.

#### Image Guided Surgery in GI Cancer.

Upchurch E, Griffiths S, Lloyd GR, Isabelle M, Kendall C and Barr H. *Future Oncology*. 2017.

# Detection of dysplasia in Barrett's oesophagus: Are there impending optical and spectroscopic solutions?

Upchurch E<sup>1\*</sup>, Old OJ<sup>2</sup>, Lloyd GR<sup>1</sup>, Isabelle M<sup>1</sup>, Kendall C<sup>1</sup>, Shetty G<sup>1</sup>, Pavlou A<sup>1</sup>, Shepherd N<sup>3</sup> and Barr H<sup>2</sup>

<sup>1</sup>Biophotonics Unit, Leadon House, Gloucestershire Royal Hospital, Great Western Road, Gloucester, UK

<sup>2</sup>Department of Upper GI Surgery, Gloucestershire Royal Hospital, Great Western Road, Gloucester, UK

<sup>3</sup>Department of Histopathology, Cheltenham General Hospital, Sandford Road, Cheltenham, UK

## Abstract

The incidence of Barrett's oesophagus and oesophageal adenocarcinoma is increasing in Western countries. The outcome for patients with oesophageal cancer is extremely poor with only 15.1% of patients surviving for 5 years. The dismal outcome is largely due to late diagnosis which eliminates many patients from effective treatment.

Oesophageal adenocarcinoma is often preceded by the development of dysplasia in a segment of Barrett's oesophagus. With the current surveillance strategies, it is extremely difficult to not only visualise areas of dysplasia, but also to accurately identify their morphological and architectural changes during histopathological diagnosis. Consensus statements recommend mucosal resection for dysplastic change in the oesophagus, thereby, preventing the development of adenocarcinoma. This strategy requires improved diagnostic tools that can reliably distinguish patients with dysplasia.

Years of research have looked at a variety of different modalities that may aid with the current dilemma of difficulties in diagnosing dysplasia. This review looks at the modalities under development and analyses their advantages and the part they may well play in the future. It also looks at the future avenues that could be explored to aid in the understanding of the disease and to improve the outcomes.

## Introduction

The recent increase in the incidence of Barrett's oesophagus and oesophageal adenocarcinoma, especially in Western countries, has fuelled the sharp rise in the number of studies attempting to understand this disease as well as the development of improved diagnostic modalities that can detect its very early stages and even predict those at greatest risk of disease progression.

Current diagnostic techniques and advancements in surgery with a move to a minimally invasive approach have failed to impact on the mortality rates for oesophageal adenocarcinoma with the 5 year survival floundering at 15.1%, making this the fifth leading cause of cancer-related death in men worldwide [1]. The paramount focus must, therefore, be on the improved detection and diagnosis of the early changes of disease that will facilitate early treatment and will, therefore, revolutionize the mortality statistics.

## Barrett's oesophagus

Barrett's oesophagus, originally described in 1950 [2], is an acquired condition, characterised by the replacement of normal squamous epithelium by columnar epithelium in a process termed metaplasia. It is a premalignant condition that predisposes to the development of oesophageal adenocarcinoma, although the overall risk is small with the conversion rate of oesophageal adenocarcinoma from Barrett's oesophagus being 0.5% per year [3]. It has been established that adenocarcinoma develops through a multi-step morphological pathway, characterised by increasing grades of dysplasia [4], and it is the presence and grade of dysplasia that is currently the only marker that is able to delineate those at a higher risk of progression to adenocarcinoma.

This is, however, not a perfect method. The natural history of high grade dysplasia remains debatable with certain factors correlated with a higher risk of progression, including central obesity, length of Barrett's segment, insulin resistance and serum levels of leptin [5]. The natural course of low grade dysplasia is more hotly contested with some evidence indicating that this can regress, although this may be related to initial inaccurate diagnosis [6]. Persistent low grade dysplasia was, however, associated with disease progression [7].

## Dysplasia

The recognition of dysplasia is extremely complex. The major difficulty is our ability to detect and biopsy the areas with dysplasia. Although metaplasia is apparent macroscopically at endoscopy, areas of dysplasia are not always identifiable. The current protocol is, thus, for random biopsies from each quadrant of the oesophagus at every 1-2 cm interval in a macroscopically columnar lined area, known as the Seattle Protocol. Even if properly adhered to, significant pathology can be missed; 40% of resections undertaken for presumed high grade dysplasia had an occult malignancy detected during histological analysis which had not been identified on the preoperative diagnostic endoscopy [8,9]. Additional studies indicate that 34% of early stage

**Correspondence to:** Emma Upchurch, Clinical Research Fellow, Biophotonics Unit, Leadon House, Gloucestershire Royal Hospital, Gloucester, UK, Tel: +44 300 422 5895, **E-mail:** em\_upchurch@hotmail.com

**Key words:** autofluorescence, Barrett's oesophagus, dysplasia, oesophageal adenocarcinoma, spectroscopy

**Received:** May 02, 2016; **Accepted:** June 07, 2016; **Published:** June 10, 2016

oesophageal cancers (both squamous and adenocarcinoma) had not been recognised in preceding endoscopies [10].

The problem does not end there. Even if areas with dysplasia are randomly selected for biopsy, there can be considerable difficulty in determining the degree of abnormality present. Dysplasia is characterised by multiple morphological changes and it is often the degree of the abnormalities that determines not only if dysplasia is present, but also its grade (Figure 1). The criteria for a diagnosis of low grade dysplasia includes preserved nuclear polarity, nuclear heterogeneity and margination, few mitoses and decreased numbers of transition to adjacent glandular epithelium [11]. Architectural changes should be absent or minimal.

With a complex array of changes, it is hardly surprising that there is a high degree of intra- and inter-observer variability [12-14] in assigning a grade to these patients. The assessment is highly subjective and dependent on experience. It is, however, vitally important as the diagnosis of low grade dysplasia documents a watershed transition in the course of the disease and has significant management implications.

Parallel to the morphological changes seen in dysplasia, genetic alterations occur which alter gene expression and, subsequently, the regulation of the cell cycle. There is evidence, for example, that p16 hypermethylation is an early predictor of progression in Barrett's oesophagus, especially in low grade dysplasia [15]. Extensive evidence shows that p53 overexpression is seen in both cancerous and high grade dysplasia and is, thus, predictive of progression [16]. This could be an excellent predictive tool when its overexpression is detected by immunohistochemistry [17]. Due to the complexity of the control of the cell cycle and the amount of genetic alterations that can occur, it is likely that mutations will vary between patients and there may not be a single trigger that will be able to explain, nor predict, progression, but rather an accumulation of changes that will ultimately push the cell towards carcinoma.

Dysplasia is, nevertheless, despite its problems, the best method that we currently have at our disposal to identify risk of progression to adenocarcinoma and, thus, to identify patients who would benefit from early, minimally invasive endoscopic intervention. Consensus statements generated through a Delphi process [3,18] recommend that endoscopic ablation or resection is undertaken in the presence of established dysplastic degeneration, making the accurate assessment of dysplasia a vital process. This logically leads to improved outcomes as a cohort of patients will be able to avoid the development of oesophageal adenocarcinoma and the major undertaking of an oesophagectomy.



**Figure 1.** Focal area of high grade dysplasia in an endoscopic resection specimen.

## Identifying dysplasia

Endoscopic surveillance and biopsy is at present the mainstay for identifying dysplasia in Barrett's oesophagus. Endoscopic screening for Barrett's oesophagus is, at present, being suggested for men aged 60 years with prolonged (>10 years) reflux symptoms [3] as their risk of progression to dysplasia and adenocarcinoma is greatest. Population based screening is not recommended due to the low rate of conversion of Barrett's oesophagus to adenocarcinoma [19]. Controversy does, however, remain as to the frequency of surveillance endoscopy and which patients require more intensive surveillance and in whom it can be stopped. A large RCT is currently underway to help solve this dilemma [20].

Surveillance has been shown to be beneficial as surveillance leads to diagnosis of oesophageal adenocarcinoma at an earlier stage and, hence, leads to improved survival [21]. The outcomes were better when compared to patients diagnosed outside of a screening programme and dramatically better than those who had already become symptomatic [22].

The main quandary is how to bring forward the diagnosis of dysplasia to allow earlier, and ultimately minimally invasive endoscopic intervention. Even if there is a genetic breakthrough which is able to identify a higher risk cohort, visualisation of the oesophagus with targeted biopsy of abnormal areas alongside a higher degree of assurance in dysplastic staging will still be required. A number of optical techniques have been and are still being investigated for these purposes. They offer the potential of detecting changes very early in the cancerous process, at the microstructural and molecular level, far earlier than the morphological changes that are needed for detection by traditional endoscopy. They offer additional information to differentiate dysplastic from non-dysplastic tissue and high grade from low grade dysplasia.

Optical diagnostic techniques, which are being used and are under development, are high resolution endoscopy, chromoendoscopy, narrow band imaging, optical coherence tomography, autofluorescence, immunophotodiagnostic endoscopy, confocal fluorescence microendoscopy, light scattering spectroscopy, Raman spectroscopy and infrared spectroscopy. No single modality has surged ahead and is able to satisfy all difficulties being faced and it is, thus, increasingly likely that a combination of techniques will be required to enable early disease detection and to reverse the dismal outcomes of oesophageal adenocarcinoma.

## Optical techniques

### High resolution endoscopy (HRE)

Traditional endoscopes are able to generate a 300,000 pixel image. High resolution endoscopes are able to generate images with greater than 1,000,000 pixels. Unsurprisingly, high resolution endoscopes have been shown to have a higher sensitivity than standard white light endoscopy for the detection of Barrett's oesophagus [23, 24], although the majority of evidence focuses on their use by expert endoscopists. The performance of and experience of the endoscopist contributes significantly to the detection of neoplasia, with mean inspection time per cm of Barrett's oesophagus having a significant impact [25]. The improved sensitivity is, by no means, perfect with only 79% of dysplasia detected [23], and with a substantial inter-observer variability identified [23,26]. Consensus guidelines have, nevertheless, recommended its use in expert centres [3] as it does go some way to improving the detection of abnormal areas.

## Chromoendoscopy

High resolution endoscopy has, in some studies, obtained better results when used in conjunction with chromoendoscopy [27] although this is not consistent [26]. Chromoendoscopy describes the exogenous administration of specialised dyes, including Lugol's solution and methylene blue, onto the mucosal surface. They are typically sprayed onto the mucosal surface via a specifically designed catheter at the time of endoscopy. The stains enhance the detection of subtle mucosal irregularities that may otherwise be invisible [28].

Lugol's solution interacts with glycogen within minutes of its application in normal squamous epithelium resulting in a brown / black discoloration. In contrast, it does not stain columnar epithelium and, thus, can be useful in distinguishing squamous from columnar epithelium [28]. It has been shown to be effective in identifying early squamous cell cancer in the oesophagus and has been used for this application by Japanese endoscopists in patients who have previously had a diagnosis of head or neck cancer [29].

Methylene blue stains the intestinal metaplasia that defines Barrett's oesophagus and has an almost 100% correlation with Barrett's epithelium [28]. Despite highlighting areas of Barrett's, the staining does not appear to aid the identification of areas of dysplasia. Acetic acid is another dye which enhances surface topography and has been shown, in some studies, to be superior to white light endoscopy in the localisation of dysplasia in Barrett's oesophagus [30].

Chromoendoscopy seems to be a sensible solution to improve the diagnostic yield of dysplasia, even if it is used as a temporary measure whilst other, better technologies are developed. The practise, however, has not been universally adopted primarily due to difficulties with spray application, time required for spray application and with operator subjectivity meaning that it is still far from ideal.

## Narrow band imaging

Narrow band imaging enhances the resolution of the mucosal surface, aiding visualisation of surface irregularities as well as alterations in the vascular patterns. The mucosa is illuminated with both blue and green light wavelengths. The different wavelengths penetrate the tissue to different degrees resulting in increased resolution. Narrow band blue light displays the superficial capillary networks, due to its increased absorption by haemoglobin [31] and the alterations in vascular pattern that is seen in disease can be identified.

Initial reviews showed high sensitivities for distinguishing gastric mucosa from intestinal metaplasia [32] and subsequent work with further magnification demonstrated a high accuracy in identifying high grade dysplasia [32]. As with the other modalities discussed thus far, however, there is a high level of inter-observer variability in the detection of mucosal irregularities and, although this modality would be easy to integrate into standard endoscopy practises, its use is limited. 14% of endoscopists referring patients to a tertiary centre for further assessment of Barrett's oesophagus had used narrow band imaging [3].

## Optical coherence tomography

Optical coherence tomography (OCT) is an imaging system analogous to ultrasonography in that it uses electromagnetic waves to form images based on the detection of reflected light, rather than reflected sound waves [33]. OCT systems have resolutions of 10-25  $\mu\text{m}$ , which enables the identification of microscopic features, including villi, glands, lymphatic aggregates and blood vessels [28].

Multiple studies have described the *in vivo* use of OCT as a screening tool for Barrett's oesophagus with the ability to distinguish between the appearances of squamous mucosa, gastric cardia, Barrett's oesophagus and adenocarcinoma [38-42]. The sensitivity for the differentiation between high grade dysplasia and adenocarcinoma was, however, only 83% with a specificity of 75% [42], with similar, if not worse results, in a subsequent study [43].

The identification of dysplasia, particularly high grade dysplasia, is the ultimate goal and the results thus far for OCT are, in the majority, not good enough, although a recent review found excellent diagnostic sensitivity and specificity for the detection of Barrett's oesophagus, although not necessarily of dysplasia [44]. This is likely to be linked to the subjective interpretation by the endoscopists, especially as this modality requires interpretation of histopathological changes. Its benefit does, however, lie in the fact that it provides cross-sectional imaging that permits assessment of the depth of invasion and can determine for which patients mucosal resection is a suitable option [34].

The speeds and modes of operation prohibit acquisition of data over large segments of the GI tract [35]. Spectrally encoded confocal endomicroscopy uses a different grating and a wavelength swept laser to image tissues at very high speeds [36]. *In vivo* experiments on anaesthetised living swine suggested that this technology could rapidly (in 2.1 minutes) provide large (5 cm length) contiguous images of the oesophagus [35]. The technology had some technical flaws; however, it is an important step towards the illustrious wide-field scanning that is desperately required.

A novel approach has been the development of a swallowed tethered capsule endomicroscopy device which has been shown to image large portions of the oesophagus with agreement of 94% to manual tissue classification [37]. This form of technology could provide screening data, but patients would need further investigation, likely to be an endoscopy, to obtain tissue or to perform endomucosal resection.

## Autofluorescence

All tissues produce autofluorescence when illuminated by ultraviolet (<400 nm) or short visible light (400-550 nm). The molecules responsible for this are termed fluorophores and the resultant autofluorescent signal is dependent on the concentration and distribution of the fluorophores. Normal, metaplastic and dysplastic tissue will have different autofluorescent spectra as malignant transformation alters the type, concentration and microdistribution of the constituent fluorophores [45].

Tissue autofluorescence can be performed relatively simply with the ability to sample wide areas of the mucosal surface. Different wavelengths penetrate and effectively interrogate the tissue to different depths, resulting in an image which provides clues as to the tissue topography and vasculature [46].

Studies using a variety of systems have had confounding results with some improving detection of dysplasia [47], and others being no better than traditional white light endoscopy [24,48]. A combined video endoscope system with both white light and autofluorescence did improve the detection of new areas of dysplasia [49], but was hampered by the inability to accurately distinguish inflamed tissue with that of dysplasia.

It may be overly hopeful to think that differences in autofluorescence patterns are specific enough to distinguish between low grade dysplasia, high grade dysplasia and adenocarcinoma. Alterations in

autofluorescence would, however, direct the endoscopist to areas of interest which would be further assessed with a different diagnostic modality and/or biopsied. What would be ideal is a marker of dysplasia that has a unique fluorescent signal that would objectively identify the areas of the oesophagus that require further evaluation. No markers have, thus far, been identified; however, it may be that a molecular marker of the processes that are involved in dysplastic formation, such as apoptosis or cellular proliferation, can be found and that they have a unique autofluorescent signal.

Lipofuscin could be a candidate for this role (DaCosta; personal communication). Work looking at the colonic mucosa has shown that dysplastic epithelial cells had increased red autofluorescence intensity when compared to normal and hyperplastic cells and that this increase was due to the presence of large numbers of highly autofluorescent granules which were shown to be lysosomes [50]. Lipofuscin forms due to iron catalysed oxidation and polymerisation of protein and lipid residues [51]. These residues are cell fragments which are the result of apoptosis of epithelial cells.

If lipofuscin is able to be easily detected and enables differentiation between non-dysplastic and dysplastic tissue, and/or between different levels of dysplasia, or indeed if there are alternative markers that can do this, this would increase our ability to perform quick wide field scanning of the entire oesophagus and identify areas requiring magnified investigation.

### Immunophotodiagnostic endoscopy

In a similar approach, studies have looked at combining chromogenic or fluorescent dyes with monoclonal antibodies that are specific for tumour-related antigens. The antibody would bind with the antigen and then emit fluorescence which is detectable and identify abnormal areas of the oesophagus. The clinical application of this has, thus far, had limited success which may be due to the lack of specific markers or the sub-optimal contrast differentiation between tissue types [46].

A glimmer of hope is lectins. Cell surface lectins are altered in the progression from Barrett's oesophagus to adenocarcinoma causing changes in binding patterns which can be identified [53]. This modality is highly attractive and as our understanding of the molecular basis of dysplasia and adenocarcinoma increases, further dysplasia associated markers may well be discovered.

### Confocal fluorescence microendoscopy

Confocal fluorescence microendoscopy is an extension of autofluorescence. It images endogenous and exogenous fluorophores within the cells of the tissue sections [21] and provides a histological image of the tissue [52]. In *ex vivo* samples, dysplastic and non-dysplastic Barrett's oesophagus fluoresced mainly in the green spectrum with the main contribution from the mucosal layer. High grade dysplasia was able to be differentiated from that of non dysplastic Barrett's based on the assessment of the microstructural tissue changes [52]. This suggests that Barrett's oesophagus can be detected by mucosal autofluorescence [31], but the further delineation of dysplastic tissue requires the histological component of this modality which is a subjective measure.

### Spectroscopy

Spectroscopy offers the ability to detect subtle biochemical changes in tissues and, thus, aids the differentiation of various tissue types, including that of dysplastic tissue. There is a substantial volume of

work in the literature that confirms the ability of different forms of spectroscopy to differentiate between pathology states in a wide range of organ systems, including the oesophagus. Despite many years of evidence, however, there has been no move of spectroscopy into routine clinical practise.

**Light scattering spectroscopy:** Light scattering spectroscopy, also known as elastic scattering spectroscopy, provides microstructural information about tissue based on the reflectance of scattered white light. The backscattered light from epithelial nuclei can identify nuclear enlargement and crowding and this can be used to detect dysplasia with sensitivities and specificities of >90% [54]. Subsequent studies have obtained reasonable results and have also been able to differentiate high risk sites from inflammation with sensitivities and specificities of 79% [55].

The main disadvantage of this tool, as with other methods of spectroscopy, is that it is unable to sample a large volume of the oesophagus. Other forms of spectroscopy provide greater information regarding tissue composition and, thus, it seems unlikely that light scattering spectroscopy will become a main stream tool to aid our identification of dysplasia.

**Raman spectroscopy:** Compared to the other spectroscopic techniques under investigation, Raman spectroscopy provides the most detailed information about the molecular composition of tissue. It relies on the inelastic scattering of monochromatic light, where the scattered photon's energy is altered by interaction with the molecular bonds present and results in a change in frequency. This information is extracted and enables the molecular composition of a tissue to be determined (Figure 2) [46].

The ability of Raman spectroscopy to discriminate between different pathology groups in a variety of *ex vivo* tissue groups has been well documented. In the oesophagus, in an analysis of snap-frozen biopsy samples, Raman analysis was able to discriminate between 8 different pathology groups, including subtypes of Barrett's oesophagus [56]. Fibre optic probes for Raman analysis via a needle probe or endoscope can enable tissue access for *in vivo* analysis [57].

From the turn of the century, a number of groups have trialed *in vivo* Raman probes. Work in 2011 demonstrated the identification of cancer in the oesophagus with a sensitivity of 91% and a specificity of 94% and, importantly, with an acquisition time of 0.4-0.5 seconds [58]. Dysplastic change was, however, not differentiated.

Despite rapid spectral acquisition times, a major limitation of Raman probe measurement is that only a small volume of mucosa

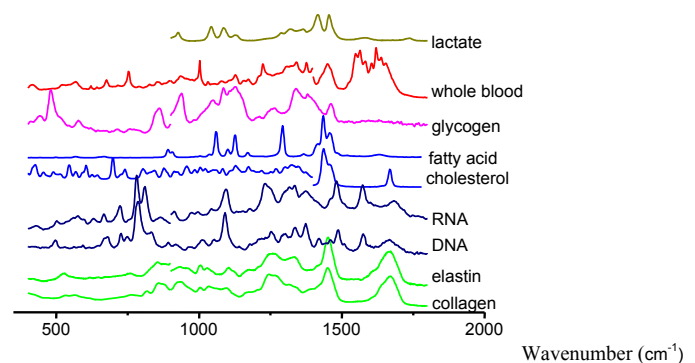


**Figure 2.** Examples of Raman spectra measured from a variety of human molecular constituents. Characteristic Raman peaks are seen for each substance at reproducible positions.

can be interrogated at one time. This prohibits its use as a wide field scanning modality, but would make it an ideal instrument for point measurements to aid *in vivo* diagnosis. Raman probes can, and have been, used in conjunction with other modalities which are able to scan wide areas of the oesophagus to overcome this barrier and this is discussed later. The narrow field imaging of Raman would, however, be well suited to other *in vivo* applications, such as real time targeted therapy during endomucosal resection to establish resection margin clearance [59], although it would need to be able to distinguish areas of dysplasia as well as adenocarcinoma.

Rather than replacing the gold standard of histopathology for diagnosis, Raman spectroscopy could be utilised in the laboratory for the analysis of *ex vivo* samples to aid diagnosis, particularly when there is a lack of consensus regarding the presence and/or grade of dysplasia. Rapid mapping of tissue sections using Raman has the potential to be used as an automated histopathology tool. It has been shown that 2 mm diameter sections can be mapped over a time scale of 30-90 minutes, and that this was sufficient to discriminate pathology [60]. This would provide an additional tool for the pathologist when analysing biopsy samples. Current work is focused on investigating system transferability when using Raman to map oesophageal tissue sections to facilitate this function [61].

**Fourier-transform infra-red spectroscopy:** Infrared spectroscopy exploits the feature that tissue absorbs light at characteristic wavelengths which are determined by the vibrational motions of covalently bonded atoms. FTIR is able to collate a rapid molecular fingerprint of tissue with information regarding different tissue constituents such as DNA and glycogen. The pattern of the spectra generated is sensitive to small changes in multiple tissue constituents and, therefore, is different for the different pathologies [62]. For example, increased DNA and glycoprotein content predicts the presence of dysplasia in Barrett's oesophagus and this is consistent with histopathology [63].

The development of adenocarcinoma follows a well established pattern which begins prior to any morphological changes. Gene mutation is the primary event, followed by changes in the biomolecules of the tissue. FTIR has the potential to detect these changes and potentially identify changes prior to those described as precancerous, *i.e.*: at the earliest stage of dysplastic change. As with Raman, however, this is not currently a method whereby the entire oesophagus can be screened with FTIR to identify these areas. An additional hindrance of IR is the strong influence of water with peaks overlapping with the Amide I band of proteins, affecting the diagnostic ability of this technique [64]. Fibre-optic evanescent wave spectroscopy (FEWS)-FTIR with endoscope compatible fibre-optic silver halide probes has been shown to be feasible, although the development of *in vivo* tissue drying is likely to improve results [65].

The role of FTIR is, therefore, likely to be complimentary to Raman in aiding histopathological diagnosis of biopsied material.

### The way ahead

An ideal diagnostic model to identify dysplasia in the oesophagus would enable real time scanning of a vast area of mucosa, ideally the entire oesophagus. It would be able to accurately identify areas of low grade dysplasia, high grade dysplasia and adenocarcinoma and differentiate these from active inflammation and other pathologies with a high degree of specificity. It would be easy to set up and use and be cost effective. Unfortunately it does not exist.

What then is the solution? A multi-modal approach is needed

to tackle the two predominant problems that face the diagnosis of dysplasia in Barrett's oesophagus.

A wide field detection is required that is able to assess the whole oesophagus and identify areas requiring more specific review. Autofluorescence would be simple and easy to employ and if a marker of dysplasia could be identified then this would make this modality the principal choice. A narrow field modality would then be utilised at the same endoscopy to further delineate these areas. The narrow field modalities, predominantly those of Raman and FTIR, provide additional and complimentary information to that of histopathology. Using all modalities in conjunction will provide the greatest information regarding the disease state of the tissue, increasing the accuracy of diagnosis and providing detailed information regarding the cancerous changes that take place. It will only be with complimentary working with pathology, rather than an attempt to replace them, that we will develop the greatest understanding of the changes that occur in cancerous change in the oesophagus.

Evidence is starting to filter in of the benefit of a multimodal approach. For example, the combination of Raman spectroscopy and optical coherence tomography has been shown to be superior to either modality in isolation at discriminating between colonic adenocarcinoma and normal colon [66]. A dual probe combining fluorescence and Raman spectroscopy was shown to have good correlation with histopathology when used for *ex vivo* melanocytic lesions [67] and a recent study using the same two modalities in the same probe demonstrated the potential of this technology to be used *in vivo* [68]. The combination of autofluorescence and Raman has taken an early lead in the ideal modality combination as the two provide complimentary information.

### Conclusion

There is still a long way to go. Each modality needs to be perfected and translated into clinical care and then the ideal combination needs to be selected. This may, however, not be the same for every patient and the advantages of each may alter depending on the patient. Nevertheless, the incidence of both Barrett's oesophagus and adenocarcinoma are climbing and the requirement for new and improved diagnostic tools is greater than ever.

### References

1. CR UK (2013) Cancer Key Facts. *Cancer Research UK*.
2. BARRETT NR (1950) Chronic peptic ulcer of the oesophagus and 'oesophagitis'. *Br J Surg* 38: 175-182. [[Crossref](#)]
3. Bennett C, Moayyedi P, Corley DA et al. (2015) BOB CAT: a Large-Scale Review and Delphi Consensus for Management of Barrett's Esophagus with No Dysplasia, Indefinite for, or Low-Grade Dysplasia. *Am J Gastroenterol* 110: 662-682. [[Crossref](#)]
4. Fléjou JF (2005) Barrett's oesophagus: from metaplasia to dysplasia and cancer. *Gut* 54 Suppl 1: i6-12. [[Crossref](#)]
5. Duggan C, Onstad L, Hardikar S, Blount PL, Reid BJ, et al. (2013) Association between markers of obesity and progression from Barrett's esophagus to esophageal adenocarcinoma. *Clin Gastroenterol Hepatol* 11: 934-943. [[Crossref](#)]
6. Duits LC, Phoa KN, Curvers WL, Ten Kate FJ, Meijer GA, et al. (2015) Barrett's oesophagus patients with low-grade dysplasia can be accurately risk-stratified after histological review by an expert pathology panel. *Gut* 64: 700-706. [[Crossref](#)]
7. Phoa KN, van Vilsteren FG, Weusten BL, Bisschops R, Schoon EJ, et al. (2014) Radiofrequency ablation vs endoscopic surveillance for patients with Barrett esophagus and low-grade dysplasia: a randomized clinical trial. *JAMA* 311: 1209-1217. [[Crossref](#)]
8. Heitmiller RF, Redmond M, Hamilton SR (1996) Barrett's esophagus with high-grade dysplasia. An indication for prophylactic esophagectomy. *Ann Surg* 224: 66-71. [[Crossref](#)]

9. Falk GW, Rice TW, Goldblum JR, Richter JE. (1999) Jumbo biopsy forceps still misses unsuspected cancer in Barrett's oesophagus with high-grade dysplasia. *Gastrointestinal Endoscopy* 49: 170-176. [[Crossref](#)]
10. Chadwick G, Groene O, Hoare J, Hardwick RH, Riley S, et al. (2014) A population-based, retrospective, cohort study of esophageal cancer missed at endoscopy. *Endoscopy* 46: 553-560. [[Crossref](#)]
11. WHO (2010) Classification of Tumours of the Digestive System, 4th edn ed. IARC Press: Lyon.
12. Lee YC, Cook MB, Bhatia S, Chow WH, El-Omar EM, et al. (2010) Interobserver reliability in the endoscopic diagnosis and grading of Barrett's esophagus: an Asian multinational study. *Endoscopy* 42: 699-704. [[Crossref](#)]
13. Kerkhof M, Van Dekken H, Steyerberg EW, Meijer GA, Mulder AH, et al. (2007) Grading of dysplasia in Barrett's oesophagus: substantial interobserver variation between general and gastrointestinal pathologists. *Histopathology* 50: 920-927. [[Crossref](#)]
14. Gaddam S, Mathur SC, Singh M, Arora J, Wani SB, et al. (2011) Novel probe-based confocal laser endomicroscopy criteria and interobserver agreement for the detection of dysplasia in Barrett's esophagus. *Am J Gastroenterol* 106: 1961-1969. [[Crossref](#)]
15. Wang JS, Guo M, Montgomery EA, Thompson RE, Cosby H, et al. (2009) DNA promoter hypermethylation of p16 and APC predicts neoplastic progression in Barrett's esophagus. *Am J Gastroenterol* 104: 2153-2160. [[Crossref](#)]
16. Hardwick RH, Shepherd NA, Moorghen M, Newcomb PV, Alderson D (1994) Adenocarcinoma arising in Barrett's oesophagus: evidence for the participation of p53 dysfunction in the dysplasia/carcinoma sequence. *Gut* 35: 764-768. [[Crossref](#)]
17. Kastelein F, Biermann K, Steyerberg EW, Verheij J, Kalisvaart M, et al. (2013) Aberrant p53 protein expression is associated with an increased risk of neoplastic progression in patients with Barrett's oesophagus. *Gut* 62: 1676-1683. [[Crossref](#)]
18. Bennett C, Vakili N, Bergman J, Harrison R, Odze R et al. (2012) Consensus Statements for Management of Barrett's Dysplasia and Early-Stage Esophageal Adenocarcinoma, Based on a Delphi Process. *Gastroenterology* 143: 336-346. [[Crossref](#)]
19. Bhat S, Coleman HG, Yousef F, Johnston BT, McManus DT, et al. (2011) Risk of malignant progression in Barrett's esophagus patients: results from a large population-based study. *J Natl Cancer Inst* 103: 1049-1057. [[Crossref](#)]
20. Old O, Moayyedi P, Love S, Roberts C, Hapeshi J, et al. (2015) Barrett's Oesophagus Surveillance versus endoscopy at need Study (BOSS): protocol and analysis plan for a multicentre randomised controlled trial. *J Med Screen* 22: 158-164. [[Crossref](#)]
21. Bhat SK, McManus DT, Coleman HG, Johnston BT, Cardwell CR, et al. (2015) Oesophageal adenocarcinoma and prior diagnosis of Barrett's oesophagus: a population-based study. *Gut* 64: 20-25. [[Crossref](#)]
22. El-Serag HB, Naik AD, Duan Z, Shakhatreh M, Helm A, et al. (2015) Surveillance endoscopy is associated with improved outcomes of oesophageal adenocarcinoma detected in patients with Barrett's oesophagus. *Gut* [[Crossref](#)]
23. Kara MA, Peters FP, Rosmolen WD, Krishnadath KK, ten Kate FJ, et al. (2005) High-resolution endoscopy plus chromoendoscopy or narrow-band imaging in Barrett's esophagus: a prospective randomized crossover study. *Endoscopy* 37: 929-936. [[Crossref](#)]
24. Kara MA, Smits ME, Rosmolen WD, Bultje AC, Ten Kate FJ, et al. (2005) A randomised crossover study comparing light-induced fluorescence endoscopy with standard videoendoscopy for the detection of early neoplasia in Barrett's oesophagus. *Gastrointest Endosc* 61: 671-678. [[Crossref](#)]
25. Gupta N, Gaddam S, Wani SB, Bansal A, Rastogi A, Sharma P (2011) Longer Barrett's inspection time (Bit) is associated with a higher detection rate of high grade dysplasia (HGD) and early esophageal adenocarcinoma (EAC). *Gastroenterology* 1: S198-S199. [[Crossref](#)]
26. Curvers W, Baak L, Kiesslich R, Van Oijen A, Rabenstein T, et al. (2008) Chromoendoscopy and narrow-band imaging compared with high-resolution magnification endoscopy in Barrett's esophagus. *Gastroenterology* 134: 670-679. [[Crossref](#)]
27. Gill RS, Singh R (2012) Endoscopic imaging in Barrett's esophagus: current practice and future applications. *Ann Gastroenterol* 25: 89-95. [[Crossref](#)]
28. DaCosta RS, Wilson BC, Marcon NE (2003) Photodiagnostic techniques for the endoscopic detection of premalignant gastrointestinal lesions. *Digestive Endoscopy* 15: 153-173.
29. Ina H, Shi buya H, Ohashi I, Kitagawa M (1994) The frequency of a concomitant early esophageal cancer in male patients with oral and oropharyngeal cancer: Screening results using Lugol dye endoscopy. *Cancer* 73: 2038-2041. [[Crossref](#)]
30. Longcroft-Wheaton G, Kandaswamy P, Bhandari P (2011) Acetic acid enhanced chromoendoscopy is more cost effective than protocol guided biopsies in a high risk Barrett's population: results from a large prospective series. *Gut* 60: 32-33.
31. Kara MA, Ennahachi M, Fockens P, ten Kate FJ, Bergman JJ (2006) Detection and classification of the mucosal and vascular patterns (mucosal morphology) in Barrett's esophagus by using narrow band imaging. *Gastrointest Endosc* 64: 155-166. [[Crossref](#)]
32. Curvers WL, Van den Broek FJ, Reitsma JB, Dekker E, Bergman JJ (2009) Systematic review of narrow-band imaging for the detection and differentiation of abnormalities in the esophagus and stomach. *Gastrointest Endosc* 69: 307-317. [[Crossref](#)]
33. Filip M, Iordache S, Săftoiu A, Ciurea T (2011) Autofluorescence imaging and magnification endoscopy. *World J Gastroenterol* 17: 9-14. [[Crossref](#)]
34. Lightdale CJ (2013) Optical coherence tomography in Barrett's esophagus. *Gastrointest Endosc Clin N Am* 23: 549-563. [[Crossref](#)]
35. Kang D, Schlachter SC, Carruth RW, Kim M, Wu T, et al. (2014) Comprehensive confocal endomicroscopy of the esophagus in vivo. *Endosc Int Open* 2: E135-140. [[Crossref](#)]
36. Tearney GJ, Webb RH, Bouma BE (1998) Spectrally encoded confocal microscopy. *Opt Lett* 23: 1152-1154. [[Crossref](#)]
37. Ughi GJ, Gora MJ, Swager AF, Soomro A, Grant C, et al. (2016) Automated segmentation and characterisation of esophageal wall in vivo by tethered capsule optical coherence tomography endomicroscopy. *Biomedical Optics Express* 7: 409-419. [[Crossref](#)]
38. Zuccaro G, Gladkova N, Vargo J, Feldchtein F, Zagaynova E, et al. (2001) Optical coherence tomography of the esophagus and proximal stomach in health and disease. *Am J Gastroenterol* 96: 2633-2639. [[Crossref](#)]
39. Poneros JM, Brand S, Bouma BE, Tearney GJ, Compton CC, Nishioka NS (2001) Diagnosis of specialised intestinal metaplasia by optical coherence tomography. *Gastroenterology* 120: 7-12. [[Crossref](#)]
40. Li XD, Boppart SA, Van Dam J, Mashimo H, Mutinga M, et al. (2000) Optical coherence tomography: advanced technology for the endoscopic imaging of Barrett's esophagus. *Endoscopy* 32: 921-930. [[Crossref](#)]
41. Evans JA, Nishioka NS (2005) The use of optical coherence tomography in screening and surveillance of Barrett's esophagus. *Clin Gastroenterol Hepatol* 3: S8-11. [[Crossref](#)]
42. Evans JA, Poneros JM, Bouma BE, Bressner J, Halpern EF, et al. (2006) Optical Coherence Tomography to Identify Intramucosal Carcinoma and High-Grade Dysplasia in Barrett's Esophagus. *Clinical Gastroenterology and Hepatology* 4: 38-43. [[Crossref](#)]
43. Evans JA, Bouma BE, Bressner J, Shishkov M, Lauwers GY, et al. (2007) Identifying Intestinal Metaplasia at the Squamocolumnar Junction by using Optical Coherence Tomography. *Gastrointestinal Endoscopy* 65: 50-56. [[Crossref](#)]
44. Robles LY, Singh S, Fisichella PM (2015) Emerging enhanced imaging technologies of the esophagus: spectroscopy, confocal laser endomicroscopy and optical coherence tomography. *J Surg Research* 195: 502-514. [[Crossref](#)]
45. Kara M, DaCosta RS, Wilson BC, Marcon NE, Bergman J (2004) Autofluorescence-based detection of early neoplasia in patients with Barrett's esophagus. *Dig Dis* 22: 134-141. [[Crossref](#)]
46. DaCosta RS, Wilson BC, Marcon NE (2006) Spectroscopy and fluorescence in esophageal diseases. *Best Pract Res Clin Gastroenterol* 20: 41-57. [[Crossref](#)]
47. Haringsma J, Poley J, Blok P, et al. (2005) Detection of intraepithelial neoplasia in Barrett's esophagus using autofluorescence endoscopy. DDW
48. Egger K, Werner M, Meining A, Ott R, Allescher HD, et al. (2003) Biopsy surveillance is still necessary in patients with Barrett's oesophagus despite new endoscopic imaging techniques. *Gut* 52: 18-23. [[Crossref](#)]
49. Kara MA, Peters FP, Ten Kate FJ, Van Deventer SJ, Fockens P, et al. (2005) Endoscopic video autofluorescence imaging may improve the detection of early neoplasia in patients with Barrett's esophagus. *Gastrointest Endosc* 61: 679-685. [[Crossref](#)]
50. DaCosta RS, Andersson H, Cirocco M, Marcon NE, Wilson BC (2005) Autofluorescence Characterisation of Isolated Whole Crypts and Primary Cultured Human Epithelial Cells from Normal, Hyperplastic, and Adenomatous Colonic Mucosa. *Journal of Clinical Pathology* 58: 766-774. [[Crossref](#)]
51. Ghadially FN, Walley VM (1994) Melanoses of the gastrointestinal tract. *Histopathology* 25: 197-207. [[Crossref](#)]



52. Kara MA, DaCosta RS, Streutker CJ, Marcon NE, Bergman JJ, et al. (2007) Characterization of tissue autofluorescence in Barrett's esophagus by confocal fluorescence microscopy. *Dis Esophagus* 20: 141-150. [[Crossref](#)]
53. Bird-Lieberman EL, Neves AA, Lao-Sirieix P, O'Donovan M, Novelli M, et al. (2012) Molecular imaging using fluorescent lectins permits rapid endoscopic identification of dysplasia in Barrett's esophagus. *Nature Medicine* 18: 315-322. [[Crossref](#)]
54. Wallace MB, Perelman LT, Backman V, Crawford JM, Fitzmaurice M, et al. (2000) Endoscopic detection of dysplasia in patients with Barrett's esophagus using light scattering spectroscopy. *Gastroenterology* 119: 677-682. [[Crossref](#)]
55. Lovat LB, Johnson K, Mackenzie GD, Clark BR, Novelli MR, et al. (2006) Elastic scattering spectroscopy accurately detects high grade dysplasia and cancer in Barrett's esophagus. *Gut* 55: 1078-1083. [[Crossref](#)]
56. Kendall C, Stone N, Shepherd N, Geboes K, Warren B, et al. (2003) Raman spectroscopy, a potential tool for the objective identification and classification of neoplasia in Barrett's oesophagus. *J Pathol* 200: 602-609. [[Crossref](#)]
57. Wong Kee Song LM, Wilson BC (2005) Endoscopic detection of early upper GI cancers. *Best Pract Res Clin Gastroenterol* 19: 833-856. [[Crossref](#)]
58. Bergholt MS, Zheng W, Lin K, Ho KY, Teh M, et al. (2011) In vivo diagnosis of esophageal cancer using image-guided Raman Endoscopy and Biomolecular Modelling. *Technology in Cancer* 10: 103-112. [[Crossref](#)]
59. Almond LM, Hutchings J, Shepherd N, Barr H, Stone N, et al. (2011) Raman spectroscopy: a potential tool for early objective diagnosis of neoplasia in the oesophagus. *J Biophotonics* 4: 685-695. [[Crossref](#)]
60. Hutchings J, Kendall C, Shepherd N, Barr H, Stone N (2010) Evaluation of linear discriminant analysis for automated Raman histological mapping of esophageal high-grade dysplasia. *J Biomed Opt* 15: 066015. [[Crossref](#)]
61. Isabelle M, Dorney J, Lewis A (2016) Multi-centre Raman spectral mapping of oesophageal cancer tissues: a study to assess system transferability. *Faraday Discuss.*
62. Wang TD, Triadafilopoulos G, Crawford JM, Dixon LR, Bhandari T, et al. (2007) Detection of endogenous biomolecules in Barrett's esophagus by Fourier transform infrared spectroscopy. *Proc Natl Acad Sci U S A* 104: 15864-15869. [[Crossref](#)]
63. Bancroft JD, Gamble M (2002) Theory and Practice of Histological Techniques (Churchill-Livingstone, New York). 5th Edition.
64. Zhao R, Quaroni L, Casson AG. (2009) Fourier transform infrared (FTIR) spectromicroscopic characterisation of stem-like cell populations in human esophageal normal and adenocarcinoma cell lines. *Analyst* 135: 53-61. [[Crossref](#)]
65. Mackanos MA, Contag CH (2010) Fiber-optic probes enable cancer detection with FTIR spectroscopy. *Trends Biotechnol* 28: 317-323. [[Crossref](#)]
66. Ashok PV, Praveen BB, Bellini N, Riches A, Dholakia K, Herrington CS. (2013) Multimodal approach using Raman spectroscopy and optical coherence tomography for the discrimination of colonic adenocarcinoma from normal colon. *Biomedical Optics Express* 4: 2179-2186. [[Crossref](#)]
67. Cicchi R, Cosci A, Rossari S, Kapsokalyvas D, Baria E, et al. (2014) Combined fluorescence-Raman spectroscopic setup for the diagnosis of melanocytic lesions. *Journal of Biophotonics* 7: 86-95. [[Crossref](#)]
68. Dochow S, Ma D, Latka I, Bocklitz T, Hartl B, et al. (2015) Combined fiber probe for fluorescence lifetime and Raman spectroscopy. *Anal Bioanal Chem* 407: 8291-8301. [[Crossref](#)]

## Chapter 1

# Principles and Techniques of Vibrational Spectroscopy and Autofluorescence

Upchurch E<sup>1\*</sup>, Old OJ<sup>2</sup>, Lloyd GR<sup>1</sup>, Pavlou A<sup>1</sup>, Kendall C<sup>1</sup>, Barr H<sup>2</sup> and Isabelle M<sup>1</sup>

<sup>1</sup>Biophotonics Unit, Leadon House, Gloucestershire Royal Hospital, UK

<sup>2</sup>Department of Upper GI Surgery, Gloucestershire Royal Hospital, UK

**\*Corresponding Author:** Upchurch E, Biophotonics Unit, Leadon House, Gloucestershire Royal Hospital, Great Western Road, Gloucester, GL1 3NN, UK

First Published **October 22, 2016**

Copyright: © 2016 Upchurch E, et al.

*This article is distributed under the terms of the Creative Commons Attribution 4.0 International License (<http://creativecommons.org/licenses/by/4.0/>), which permits unrestricted use, distribution, and reproduction in any medium, provided you give appropriate credit to the original author(s) and the source.*

## Abstract

The principles and techniques that have long been established in the world of Physics are beginning to merge with the field of clinical medicine. Optical and vibrational spectroscopy techniques provide biochemical and molecular information. This information can be used to differentiate between different types of tissue and, thus, aid diagnosis, augmenting the methods already in routine clinical practise.

This chapter explains the underlying principles of optical and vibrational spectroscopy and the current research into some of the areas where these techniques are facilitating our understanding and management of disease.

## Introduction: Optical and Vibrational Spectroscopy

When light interacts with a material, multiple processes can occur; reflection, transmission, scattering, absorption, fluorescence or vibration. These processes take place when the incidental radiation induces changes in the energy level of the material. The change in energy can be detected and can provide valuable information regarding the underlying material.

Vibrational spectroscopy, alongside autofluorescence, provides information regarding the biochemical composition of a tissue in a non destructive manner by producing spectra based on the interaction of the light with the tissue. Chemometric analysis of the spectrum can char-

acterise and classify the tissue based on the information obtained.

This information is less subjective and additional to that gained by histopathological review and, thus, these techniques are being developed and evaluated for their use in clinical diagnostics, both for ex vivo tissue and biological samples and for in vivo, real time diagnosis.

### Raman Spectroscopy

Molecules are made up of atoms that are held together by chemical bonds. Each chemical bond has a characteristic vibrational energy. When illuminated by electromagnetic radiation, usually from a laser light source, the bonds vibrate as the molecule enters a virtual energy state. A photon, from the light source itself, is absorbed by the material, exciting an electron into a higher virtual energy level (Figure 1). As the electron decays back to a lower energy level, it emits a scattered photon. If the electron decays back to the same starting energy level, this is a form of elastic scattering, also known as Rayleigh scattering (Figure 2).

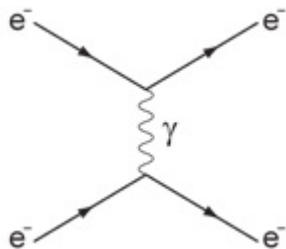


**Figure 1:** Feynman diagram of scattering between two electrons by emission of a virtual photon.

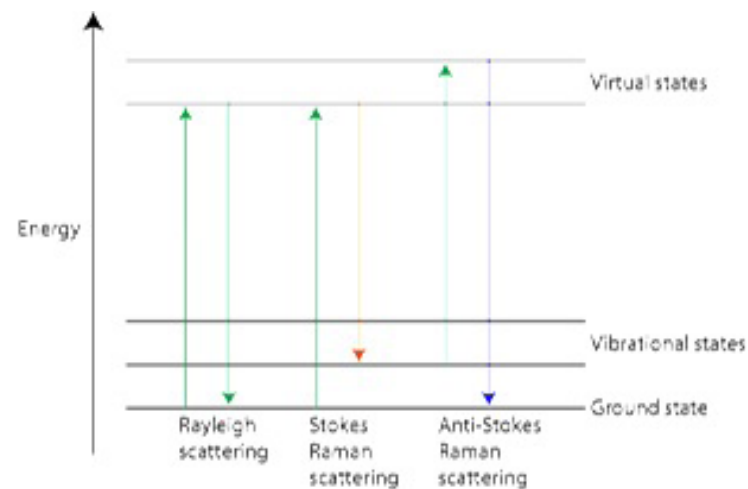


**Figure 2:** Stokes and Anti-Stokes Shift.

When the incident photon interacts with the electric dipole of the molecule, the excited electron can decay back to a different energy level from that of its starting position. This is known as inelastic scattering, and the difference in energy level between the incident (non-scattered) photons and the scattered photons corresponds to the energy of the molecular vibration. This inelastic scattering of light was predicted by Adolf Smekal in 1923 [1], however, it was not observed in practise until 5 years later, where it was named after one of its discoverers, Sir Chandrasekhara Venkata Raman [2].

Two forms of Raman scattering exist, depending on the final energy level of the electron. If the final energy level of the electron is more energetic than the original

state, the inelastically scattered photon will be shifted to a lower frequency. This shift is known as a Stokes shift. If, however, the final vibrational state is less energetic, the photon will be shifted to a higher frequency, known as an anti-Stokes shift (Figure 2).

The detection of the scattered photons, therefore, provides a unique spectrum of Raman peaks based on the bonds present within the sample and is, thus, a molecular fingerprint of the tissue sample (Figure 3). A wealth of information regarding the chemical bonds associated with DNA, RNA, proteins, lipids, other biomolecules and even a single cell can be interpreted. The intensity of the scatter is directly proportional to the concentration of responsible molecules within the specimen and, therefore, also provides a quantitative measure.

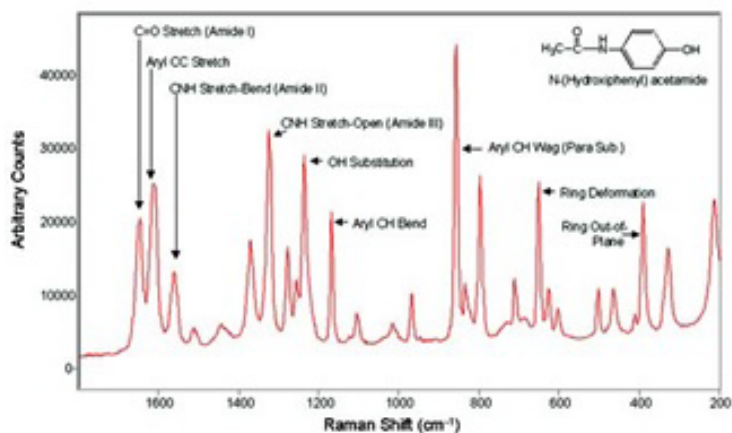


Figure 3: Example of a Raman Spectrum [3].

The use of visible or near infra-red light results in very weak Raman signals from the –OH bond present in water molecules and, hence, water contributes minimally to the resultant spectra [4]. This is a significant advantage as it means that fresh tissue, either ex vivo or in vivo, with no prior preparation is able to be analysed without interference from the water. Raman spectroscopy, nevertheless, faces other difficulties. Only a fraction of the photons are inelastically scattered ( $1/10^6$ - $10^9$ ) resulting in an inherently weak signal [5]. This is further compounded by ambient light which must be removed to reduce unwanted and distracting spectral contributions [5].

Several advanced Raman based techniques have been developed which produce a stronger signal. Resonance Raman and Resonance hyper Raman spectroscopy do this by adjusting the energy of the incoming laser. Coherent anti-Stokes Raman spectroscopy (CARS) employs multiple photons, whereas, surface enhanced Raman spectroscopy (SERS) uses specially prepared metal surfaces to enhance the signal.

An additional disadvantage of Raman is that it is only able to penetrate a few hundred microns into the tissue [6]. Spatially offset Raman spectroscopy (SORS) uses the principle that photons migrate to measure spectra from surface areas at distances from the excitation point. A scaled subtraction of the spectra from spatially offset points enables the production of pure spectra from the individual layers of the sample [7]. The advancement of this and other Raman techniques are overcoming the disad-

vantages, however, as the majority of research is based on the traditional Raman techniques, this chapter will focus on this work.

### Fourier Transform Infrared Spectroscopy (FTIR)

Infrared spectroscopy is one of the most widely used and important analytical methods employed in science. Infrared radiation was initially discovered in 1800 by Sir William Herschel. It was, however, not until the commercially driven IR spectrometers of the 1970s that the technique became so broadly applied.

When a beam of infrared radiation is passed through a tissue sample, each chemical bond within the molecule will vibrate. These vibrations occur in a variety of ways; symmetrical stretching, antisymmetrical stretching, scissoring, rocking, wagging and twisting (Figure 4). When the frequency of the infrared radiation is the same as that of the vibrational frequency of the chemical bond, the dipole moment of the molecule alters, albeit only temporarily. This transition results from the absorption of a photon.

By measuring the transmitted light, the amount of energy absorbed at each frequency (or wavelength) can be determined and an absorbance spectrum is generated. The complexity of this spectrum depends on the complexity of the molecule as the more complex a molecule, the more bonds and, therefore, more peaks the spectra will have (Figure 5).

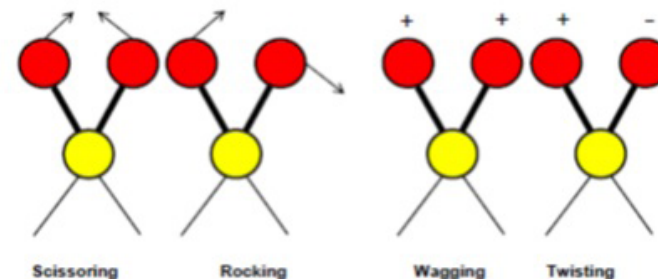


**Figure 4:** Schematic Diagram of some of the vibrations that molecular bonds undergo when excited.

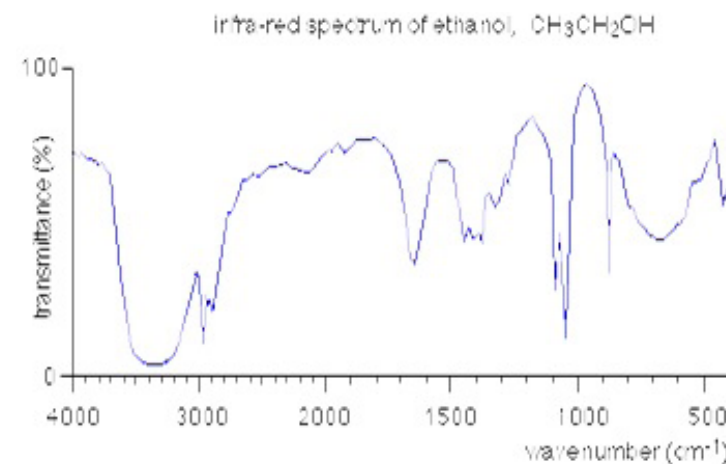


**Figure 5:** Infrared Spectrum of Ethanol ( $\text{CH}_3\text{CH}_2\text{OH}$ ).

Fourier Transform Infrared (FTIR) spectroscopy (Figure 6) uses an interferometer to guide infrared light prior to its transmission through the sample. A moving mirror inside the interferometer alters the distribution of

infrared light, allowing the simultaneous collection of information from multiple frequencies. Not only does this speed up the process, but it also reduces the signal-to-noise ratio. Virtually all modern infrared spectrometers are FTIR.

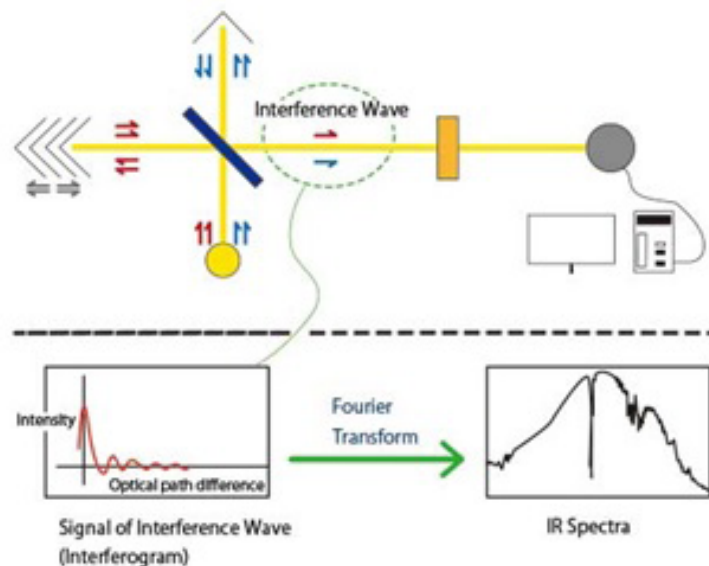


**Figure 6:** Schematic Representation of FTIR Spectroscopy  
(Courtesy: Jasco, UK).

Despite the advantages of both speed of acquisition and the requirement of only a small amount of sample, FTIR has a major limitation. Water is highly absorbent in the mid infrared range ( $4000 - 400\text{cm}^{-1}$ ), the range at which most other vibrations occur. As the majority of bio-

logical tissue has high water content, this affects the ability to gain meaningful data from in vivo measurements.

Although its use with fresh tissue is limited due to the presence of water, FTIR is ideal for use with paraffin-embedded tissue samples as the ability to correct for the absorption of paraffin has been determined and validated [8]. These preparations are routinely used in histopathology for Haematoxylin and Eosin (H&E) staining and immunohistochemistry and, thus, this technique could be used as an adjunct in the laboratory without additional sample preparation.

Infrared spectra can be hampered by distortion from resonant Mie scattering and reflectance [9]. This can be reduced by using Attenuated Total Reflectance (ATR) spectroscopy. In ATR spectroscopy, the sample is placed in contact with a sensing element (IR transmission crystal) which affects the angle of light, producing an evanescent standing wave [10]. An evanescent wave is an oscillating electric or magnetic field which does not propagate as an electromagnetic wave, but instead concentrates its energy in the vicinity of the source. This enables higher spatial resolution as well as the ability to control the sample penetration depth, however, it does require that contact exists between the sample and the probe, introducing the opportunity for contamination.

As with other technologies, there is a drive to produce real time, in vivo measurements. Fibre-optic evanescent wave spectroscopy (FEWS)-FTIR with endoscope com-

patible fibre-optic silver halide probes have been shown to be feasible [11], however, the technology is not, as yet, ready for routine clinical use and further advances are required, particularly in relation to reference data and the selection of suitable tips that enable use with current endoscopes.

### Autofluorescence

All tissues produce autofluorescence when illuminated by ultraviolet (<400nm) or short visible (400-550nm) light. Fluorophores, the constituent biomolecules of the tissue, emit longer wavelengths when illuminated and are, thus, responsible for the resultant fluorescence [12]. The majority of fluorophores are found in the submucosa layer of the tissue, with collagen and elastin producing highly green fluorescent signals. A weaker contribution is produced by the mucosal components of epithelium and lamina propria.

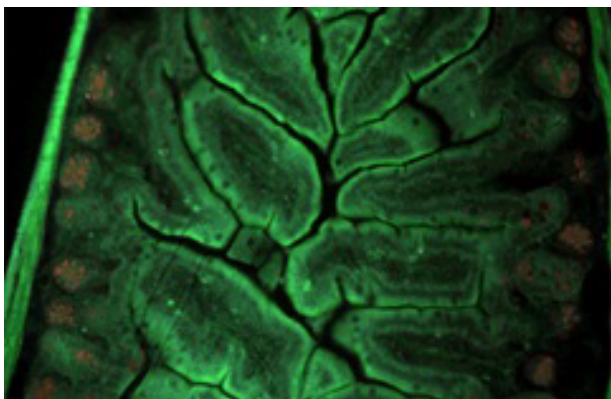


**Figure 7:** Autofluorescent image of the intestine of a mouse.

Different disease processes in tissues will produce different autofluorescent patterns as the type, concentration and microdistribution of the fluorophores will also alter [13, 14]. For example, the ratio of fluorescence intensity of tryptophan to that of NADH changes in cancerous tissue [15].

Tissue autofluorescence has the ability to sample wide areas of mucosal surface in a short space of time. Confocal fluorescence microendoscopy is an extension of this process, imaging endogenous and exogenous fluorophores within the cells of tissue sections [16], providing a detailed histological image of the tissue [17]. This may enable the detection of primary changes in cells which may be the initial change in the disease process.

## Clinical Applications

### Cancer Diagnostics

Cancer is responsible for an enormous burden of disease with 14.1 million cases diagnosed worldwide in 2012, and 8.2 million deaths in the same year [18]. Despite an extraordinary amount of effort and financial outlay, the eradication of, or even the control of advanced disease has failed to materialise [19].

The classical model of the clonal evolution of cancer cells, originally proposed by Nowell in a landmark paper in 1976, suggests that neoplasms arise from a single cell of origin. Tumour progression is the result of acquired genetic variability within the original clone which allows

the sequential selection of more aggressive sublines [20]. Cancer cells follow a Gompertzian model of replication with an early, almost exponential growth rate, followed by a slower growth rate which finally reaches a plateau as tumours grow larger in size. The majority of the growth, as shown in figure 8, occurs when the tumour is clinically undetectable.

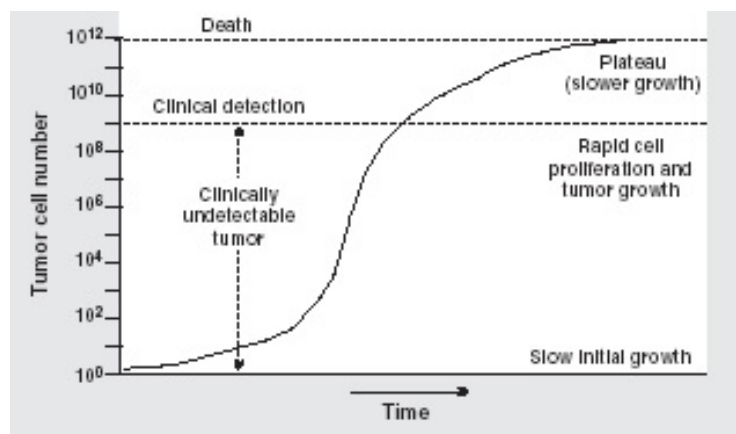


**Figure 8:** Gompertzian Model of Tumour growth.

Although cancer therapy has had its successes, in reality, very few advanced or metastatic malignancies can be eradicated or even effectively controlled. The accumulation of genetic change that occurs over time as the original clone replicates, provides opportunities for at least some of the cancer cells to evade the provided therapy, to survive and to continue to replicate. Early detection and intervention of precancerous changes prior to the advanced stages

of disease would alleviate the need to outwit the cancer cells, and reduce the morbidity and mortality burden of cancer.

Cancer diagnostics utilises a variety of imaging modalities dependent on the presentation of the patient and tumour location. The gold standard for diagnosis is histopathological tissue diagnosis which requires direct access to and biopsy of the tumour or its draining lymph node (if there is spread to the lymphatic system). Histopathologists use morphological and architectural information, often in combination with, immunohistochemical staining, to interpret the sample. In some cases, this is extremely difficult and there can be significant inter-observer variability in the analysis of the appearances. This can delay, or even alter, management decisions. In addition, histopathological diagnosis requires the changes to be morphological visible and, thus, may eliminate the window of opportunity for earlier diagnosis where changes are not macroscopically visible.

Spectroscopic analysis provides information on the biochemical constituents of the tissue and could, therefore, identify changes that predate morphological alterations. Automated classification systems could be developed for use in the laboratory in conjunction with histopathology to enable earlier and less subjective detection of cancerous and precancerous changes. The development of fibre-optic probes, in addition, has paved the way for in vivo measurements with the added benefits of real time diag-



nosis, thus, helping to identify potentially abnormal areas at the time of imaging.

Research has looked at the application of these technologies in a variety of different cancers. This chapter will focus on developments in cancers of the GI tract (oesophagus, stomach and colorectum), and the brain. Work on breast, cervical, lung, bone, prostate, head and neck and skin cancer will not be covered here.

### Oesophageal Carcinoma

The incidence of oesophageal adenocarcinoma is increasing in Western countries with no concurrent improvement in survival figures [18]. Oesophageal adenocarcinoma is often preceded by Barrett's oesophagus which is the metaplastic replacement of normal squamous epithelium by columnar epithelium. The development of dysplasia within Barrett's oesophagus is the best marker for progression to adenocarcinoma and current guidelines [21, 22] indicate that treatment, in the form of endoscopic resection and complete ablation, should occur in the presence of high grade dysplasia.

Dysplasia in Barrett's oesophagus is difficult to identify. Macroscopically it appears identical to non-dysplastic Barrett's oesophagus. The current biopsy protocol, the Seattle regimen, takes four quadrant biopsies every 2 cm and can easily miss areas of dysplasia. Even if an area of dysplasia is selected for biopsy, there exists a significant amount of inter-observer variability, even among specialised GI Histopathologists, in its diagnosis [23-25].

Alternative modalities to aid the identification and classification of dysplasia in Barrett's oesophagus are highly sought after to both prevent and improve the outcomes for those with oesophageal carcinoma.

### Raman Spectroscopy in the Oesophagus

The ability of Raman spectroscopy to discriminate between different pathology groups in the oesophagus has been well documented. In an analysis of snap-frozen biopsy samples, Raman analysis was able to discriminate between 8 different pathology groups, including subtypes of Barrett's oesophagus [26].

The next stage is the development of an in vivo Raman probe and this has been trialled from the turn of the century. Work in 2011 demonstrated that the identification of cancer in the oesophagus could occur with a sensitivity of 91% and a specificity of 94% and, importantly, with an acquisition time of 0.4-0.5 seconds [27]. Dysplastic change was, however, not differentiated in this study. This work followed earlier studies with a variety of probes [28-32] which had different sensitivities for pathology detection and different acquisition times. The development of a variety of probes will, undoubtedly, help to further the advancement in technology and enable the development of a probe which can be used routinely in clinical practise.

Rather than replacing the gold standard of histopathology for diagnosis, Raman spectroscopy could be utilised in the laboratory to aid analysis of the specimens. Rapid mapping of tissue sections using Raman has the

potential to be used as an automated histopathology tool. It has been shown that 2mm diameter sections can be mapped over a time scale of 30-90 minutes, and that this was sufficient to discriminate between pathologies [33]. This would provide an additional tool for the pathologist when analysing and interpreting biopsy samples.

### FTIR in the Oesophagus

The development of adenocarcinoma follows a well established pattern which begins prior to any morphological changes. Gene mutation is the primary event, followed by changes in the biomolecules of the tissue. FTIR has the potential to detect these changes and potentially identify changes prior to those traditionally described as precancerous, i.e.: at the earliest stage of dysplastic change. It has been demonstrated that DNA, protein, glycoprotein and glycogen account for absorption in the 950-1800  $\text{cm}^{-1}$  region and that changes here are able to identify dysplasia in fresh oesophageal samples with a high sensitivity and specificity [34].

A hindrance of IR is the strong influence of water with peaks overlapping with the Amide I band of proteins, affecting the diagnostic ability of this technique [35]. This has slowed the ability to develop in vivo probes, however, fibre-optic evanescent wave spectroscopy (FEWS)-FTIR with endoscope compatible fibre-optic silver halide probes has been shown to be feasible [11].

### Autofluorescence in the Oesophagus

Studies using a variety of autofluorescent systems have had confounding results with some improving the detection of dysplasia [36], and others being no better than traditional white light endoscopy [37]. A combined video endoscope system with both white light and autofluorescence did improve the detection of new areas of dysplasia [38], but was hampered by the inability to accurately distinguish inflamed tissue with that of dysplasia. An obvious advantage is, however, the ability to image a wide field and, thus, examine the entire oesophagus, something that is impossible to do with Raman or FTIR spectroscopy in isolation. Its use could be as a 'red flag' technique to highlight suspicious areas prior to a more detailed vibrational spectroscopy analysis.

### Gastric Carcinoma

Gastric cancer is the 4<sup>th</sup> commonest worldwide cancer, although incidences vary significantly [18]. In the UK, it accounts for only 2% of all new cases of cancer (approximately 7100 new cases / annum), whereas in the Far East, the incidence is as much as 4 times higher [39]. In Japan there are 31.1 new cases / 100000 population, 41.4 in South Korea, 29.9 in China and 34.0 in Mongolia [39].

Survival rates for gastric cancer, akin to its incidence, vary widely with a 15% overall survival in the UK [18]. As with all cancers, in those with early disease, survival can be increased. Survival rates of 90% are seen in specialist centres in Japan in patients with submucosal disease

[40]. Due to the high incidence, Japan introduced a National Screening programme in the 1960's. This combines barium double-contrast radiography with endoscopy in those with detected abnormalities. Despite the exemplary survival rates seen in Japan, it is unclear how much of an impact the screening programme itself has had [41].

With or without screening, the ability to accurately detect precancerous changes in the stomach, in a similar vein to that of detecting dysplasia in Barrett's Oesophagus, is the primary factor in enabling early treatment and, thus, improving the survival rate.

### **Raman Spectroscopy in the Stomach**

Following on from work demonstrating significant differences in Raman spectra between normal and dysplastic gastric tissue, development of an *in vivo* Raman probe has moved this technology closer to clinical application.

The first *in vivo* Raman spectroscopy study of gastric dysplasia and normal tissue was reported by Huang et al in 2010 [42] with a specificity and sensitivity of 96.3% and 94.4% respectively. The first *in vivo* study comparing gastric cancer to normal tissue was published in the same year [43] with equally good results.

The distinction between intestinal and diffuse types of gastric cancer is important as it affects the treatment options for the patient. Differences in the subtypes have been demonstrated in the spectral regions that relate to

proteins, nucleic acids and lipids and have enabled the differentiation based on their spectra with high predictive accuracies [44]. These results were repeated in work from different research groups [45].

The first results from a real time *in vivo* system were published in 2012 [46] (previous *in vivo* work had saved spectra with analysis at a later time) with a total of 2748 spectra from 308 patients analysed with a processing time of 0.5 seconds. Diagnostic accuracies in the 80-90% range were demonstrated for the identification of gastric cancer. Recent work by Wang et al [47] with a real time probe combining both fingerprint (800-1800  $\text{cm}^{-1}$ ) and high wavenumber (2800-3600  $\text{cm}^{-1}$ ) spectra provided diagnostic sensitivities of 96.1%, 81.8% and 88.2% and specificities of 86.7%, 95.3% and 95.6% for normal, dysplastic and cancerous tissue.

The demonstration of real time *in vivo* diagnosis is a vital development that is required if this technology is to be used during endoscopic resection and endoscopic submucosal dissection. Raman spectroscopy could be utilised to ensure all abnormal tissue is resected with adequate margins and subsequently be used to reassess the resection area for recurrence. The results demonstrated in the stomach are a significant step forward, however, there is still a long way to go before this technology becomes a routine adjunct in clinical practise.

### FTIR Spectroscopy in the Stomach

There has been a reduced focus on the use of FTIR in the stomach, presumably due to the leaps made in the real time in vivo measurement that has occurred with Raman spectroscopy. FTIR is also able to differentiate normal from cancerous tissue and can differentiate these tissues from superficial gastritis and atrophic gastritis, although the sensitivity for atrophic gastritis was only 60% in some studies [48].

It has been speculated that the serum of patients with gastric cancer differs from that of healthy controls [49]. In one study, FTIR has shown this difference to be detectable based on serum RNA/DNA ratios. Raman spectroscopy has also demonstrated a difference with increases seen in nucleic acid, collagen, phospholipid and phenylalanine content and decreases in amino acid and saccharide content in patients with cancer [50]. Whether this is repeatable and specific remains to be seen, however, if it is, it could provide a useful screening test using these technologies in an ex vivo manner.

### Autofluorescence in the Stomach

Autofluorescence has been researched in the stomach, as in the rest of the GI tract, with conflicting results. Although highly sensitive (96.4%), this technology had a very low specificity (49.1%) for the detection of early gastric neoplasms [51]. This was primarily due to the abnormal fluorescence of a large proportion of benign lesions.

In addition, inflammatory processes in the stomach, such as gastritis, can produce changes in the fluorescence leading to difficulties in the differentiation of the two pathologies. Despite this, however, autofluorescence has been shown to detect 25% of lesions that are missed by white light endoscopy [52]. The combination of autofluorescence with Raman has been evaluated for the identification of cancer from normal tissue and found to have an accuracy of 92.2% [53]. If utilised, it is likely that autofluorescence will be used in combination, such as this, as opposed to a single modality.

### Colorectal Carcinoma

Colorectal cancer is the third commonest cancer worldwide. It is widely accepted that the adenoma – carcinoma sequence represents the progression by which most, if not all, colorectal cancers arise [54]. If adenomas are detected at endoscopy, this offers an opportunity for early diagnosis and endoscopic resection prior to established cancer arising. There are, however, a number of challenges involved in the identification and classification of polyps.

The miss rates for small (<1cm) adenomas can be in the order of 25-50% [55, 56]. Although the significance of missing small adenomas is unclear, that of missing large adenomas (>10mm) and carcinomas is apparent and occurs in 5.8% and 5.4% of cases respectively [57]. This is partly related to the quality of the colonoscopy, including the preparation of the bowel and the endoscopist's tech-

nique, however, it is felt that some lesions are missed, predominantly in the right colon, because they are flat and relatively subtle [56]. Disappointingly, at present, high definition white light endoscopy has shown only a modest improvement [58] and narrow band imaging conflicting results [59, 60].

In addition to the problems faced in lesion detection, there can be difficulty in assigning pathology. The ability to differentiate between hyperproliferative and dysplastic change in adenomas can be challenging. Determining the nature of the polyp accurately has significant implications for both immediate management and future surveillance. Diminutive polyps (<5mm) rarely harbour advanced disease and if this could be assured in vivo, without biopsy, this would reduce an already overburdened histopathology service and reserve their expertise for other areas. There is currently a debate regarding not sending these polyps for histology with a 'resect and destroy' policy. In all polyps, a very important question after determining its nature, is the resection base; what is left behind in the patient. The detection of precancerous lesions is further complicated in areas of underlying inflammatory bowel disease where the ability to discriminate between pathologies is trickier.

### **Raman spectroscopy in the Colon and Rectum**

Initial studies analysing colorectal tissue were found to have sensitivities of over 90% when differentiating normal mucosa from metaplastic and adenomatous polyps

and from adenocarcinomas [61, 62]. The real push, as with other areas of the GI tract, has been towards the development of an in vivo probe. As with other endoscopic probes, the probe has a number of requirements: it needs to fit through the accessory channel of a colonoscope (typically 2.8-3.2mm diameter), it needs to withstand the manipulation and articulation that the colonoscope needs to go through to reach the caecum and it must be biocompatible and be able to withstand the decontamination and disinfection processes. Alongside perfecting the technology of spectroscopy, these requirements add further intricacies to the development process.

Results from the first in vivo probe, the 'Visionex' probe were published in 2003 [63]. In vivo spectra from 10 adenomas and 9 hyperplastic polyps were obtained with an estimated depth of 500µm with an acquisition time of 5 seconds (which is a reasonable length of time for contact with a peristalsing colonic mucosa to be maintained). The two pathologies were discriminated with a sensitivity of 100% and specificity of 95%.

Recent developments with the use of high wave number Raman has resulted in a reduction in acquisition time without a loss in diagnostic accuracy. Short et al [64] used wavenumbers of 2050-3100 cm<sup>-1</sup> to differentiate between normal tissue and tubular adenoma with a 1 second acquisition time. A simultaneous FP (fingerprint) and HW (high wavenumber) Raman endoscopic technique was shown to be able to characterise mucosa from different

areas of the colon with only a 0.5 second acquisition time [65]. This probe was able to selectively target the epithelial lining which is associated with the early changes of carcinogenesis and would suggest promising results in the ability to differentiate disease pathologies.

As well as *in vivo* analysis of tissues, Raman spectroscopy could be used as an adjunctive tool for histopathologists to use when analysing biopsy specimens. Rapid Raman mapping of snap frozen sections with subsequent chemometric analysis has demonstrated the ability to identify subtle histological features of colonic polyps [66]. This method could ultimately be utilised as an automated sample analysis to add to the information gained from histopathologists, or as a first line measure to identify normal and benign tissue, thus, freeing up pathologists time to focus on uncertain or malignant samples.

### **FTIR Spectroscopy in the Colon and Rectum**

Initial work using FTIR in colorectal cancer was published over 25 years ago when Rigas et al demonstrated a difference in IR spectra between normal and cancerous fresh colonic tissue [67]. This has been repeatedly demonstrated in further studies, including *in vivo* work during surgical resection [68].

The greatest difficulty in diagnosis is, however, distinguishing adenomatous tissue with varying grades of dysplasia as well as inflammatory and hyperproliferative tissue. Studies have proven that these different pathologies

are able to be differentiated based on their IR spectra [69] with increases in the lipid/protein ratio with higher grades of dysplasia. The change in ratio is presumed to be secondary to the higher cell turnover and subsequent change in DNA levels that occur with dysplasia and malignancy. Later experiments included inflammatory diseases in the samples and maintained a high predictive accuracy (sensitivity of 91.6-100% and specificity of 97.7-99.9%) [70].

High resolution IR mapping has been able to detect subtle biochemical changes in tissue and has, thus, been shown to differentiate the benign condition of epithelial misplacement from carcinoma [71]. This differentiation has proved to be problematic to histopathologists based on similar morphological appearances. The ability to be able to distinguish subtle differences may pave the way for the detection of earlier changes in the cancerous pathway.

### **Autofluorescence in the Colon and Rectum**

Diminutive polyps (<5mm) that occur in the colon rarely harbour advanced disease. It has, thus, been suggested that, as opposed to resection and routine histopathological diagnosis, these lesions are diagnosed at the time of colonoscopy based on their macroscopic characteristics [72, 73]. In addition, hyperplastic polyps, which are believed to be without neoplastic potential, could be diagnosed at the time of endoscopy and prevent the additional time, cost and potential side effects that polyp removal would carry.

Autofluorescence could be a simple technique used

in colonoscopy to aid the identification of and differentiation of colonic polyps. The results are, however, conflicting with some showing differentiation with an accuracy greater than that of white light endoscopy, whilst others reporting low specificity [74].

The detection of dysplasia in inflammatory bowel disease is particularly important. The reason for this is twofold. Firstly the incidence of colorectal cancer in this cohort of patients can be as high as 18% after 30 years of disease [75], and secondly the underlying inflammation makes identification of underlying dysplasia problematic with the two often being mistaken. Autofluorescence has been shown to identify additional areas of dysplasia in patients with quiescent Ulcerative Colitis, areas that white light endoscopy had missed [76]. In active disease, however, its role is shakier as autofluorescence has, similarly to other areas of the GI tract, been unable to differentiate active inflammation from dysplasia. It may be that a dual system of modalities is needed in this cohort, with autofluorescence being used to identify active inflammation or dysplasia and vibrational spectroscopy confirming which disease process is taking place.

### Intracranial Tumours

Intracranial tumours encompass a broad range of pathological entities, ranging from benign to high-grade lesions. Multiple cells of origin exist, including mesothelial cells, glial cells, pituitary cells and metastatic de-

posits, resulting in a range of tumours with different natural histories, management decisions and outcomes.

A combination of imaging techniques alongside surgical biopsy or excision is used for accurate diagnosis. The mainstay of treatment, where possible, is surgical excision. The need to accurately delineate the excision border to ensure complete surgical excision whilst preventing unnecessary neurological deficit is unmet with current imaging modalities.

### Raman Spectroscopy in the Cranium

Raman probes, using the high wavenumber spectral region of 2400 – 3800  $\text{cm}^{-1}$ , are able to differentiate and characterise ex-vivo porcine brain tissue [77]. The transition of normal brain tissue to neoplastic tissue is connected to a unique change in the composition and concentration of lipids [78]. Changes in the main protein bands as well as reductions in the phosphate-to-carbohydrate ratio are seen with increasing grade of glioma [79], indicating that different grades of tumour, as well as tissue type are able to be identified.

One of the major difficulties faced in the excision of brain tumours is ensuring that all tumour is removed without compromising normal, functioning tissue. In vivo Raman probes are under investigation [80] to aid the detection of intracerebral tumours by brain surface mapping and also to map the exact edges of the tumour. This technique has been tested with promising results in vivo

in mice to image undetectable tumour margins [80] and, thus, aid complete surgical excision.

### **FTIR Spectroscopy in the Cranium**

Research using FTIR to aid identification and characterisation of brain tumours has furthered the understanding of the changes that occur with this transition and other intracranial disease processes. As well as the changes in the composition of lipids seen with Raman spectroscopy, the secondary structure of fibrillar and non-fibrillar collagens was found to be different in solid and diffuse brain tumours [81]. Ongoing research work is investigating the structure of proteins in Parkinson's Disease [82] and the role of ischaemia in cerebral pathologies [83]. Using FTIR to further the understanding of the changes that occur may enable the development of new and novel treatments for a variety of pathologies.

### **Non-Cancer Diagnostics**

Multiple pathologies, not limited to cancer, lead to chemical and structural changes, resulting in characteristic vibrational spectra. These can be used as a marker of the disease to aid diagnostics as well as the understanding of the disease. Vibrational spectroscopy in prion disease, kidney stones, diabetes and osteoarthritis as well as atherosclerosis is being actively investigated. I will discuss research in atherosclerosis as an example.

### **Atherosclerosis**

Cardiovascular disease is the leading cause of mortality in the Western world causing 31% of all deaths [84]. Atherosclerosis, the process that leads to cardiovascular disease, describes the chronic, often asymptomatic, development of plaques which narrow the lumen of the arteries resulting in a reduction in blood flow. The rupture of these vulnerable atherosclerotic plaques can occur after years of indolent development and accounts for the majority of clinically significant cardiovascular events.

Atherosclerosis is a lipoprotein driven disease culminating in plaque formation via a process of intimal inflammation, necrosis, fibrosis and calcification. The plaque consists of three distinct components; the atheroma (meaning 'lump of gruel'), composed mainly of macrophages; cholesterol crystals; and calcium. The exact composition of the plaque is directly related to its stability and, hence, the likelihood of rupture. Being able to determine which plaques are unstable will aid the identification of patients who will benefit from aggressive treatment and, thus, improve the outcomes from cardiovascular disease.

### **Raman Spectroscopy in Atherosclerosis**

Spectroscopic techniques are able to study the distinct chemical changes that occur during atherosclerosis and provide vital data regarding the composition of the plaque that cannot be detected with current imaging technologies. Current technologies are able to detect plaques and stenotic lesions but, at present, no technique has been able to identify which are vulnerable plaques.



Following on from work on ex vivo samples, recent developments in Raman optical fibre probe technology has allowed for the first real time in vivo characterisation of atherosclerotic plaques. The probe was utilised during carotid endarterectomy and femoral artery bypass surgery and demonstrated the potential to identify vulnerable plaques with a sensitivity and specificity of 79 and 85% [85]. These results were similar to those obtained using fluorescence spectroscopy in an in vivo rabbit model [86].

### IR Spectroscopy in Atherosclerosis

The plaque most likely to rupture is the thin-capped fibroatheroma with high inflammatory and lipid content. Near infra-red spectroscopy has been shown to identify the histological features of plaque vulnerability in human aortic plaques obtained at autopsy. A 90% sensitivity and specificity for the identification of lipid rich plaques as well as the presence of inflammatory cells was detected by this method [87].

An intravascular near infra-red spectroscopy system for the detection of lipid core coronary plaques demonstrated in the SPECTACL Study [88] the feasibility of the invasive detection of coronary lipid core proteins, although the initial results had an unacceptably high rate of failure to gain adequate interpretation. If these limitations can be overcome, this technology, either in isolation or with other vibrational modalities, could be used to aid the decision making in which plaques require intensive and

immediate management. In addition, understanding why plaques are vulnerable may improve our ability to stabilise, or even prevent their occurrence.

### Biofluids

Biofluids, such as blood and urine, are advantageous for diagnostic tests as they are non-invasive and allow multiple sampling when compared to the often small tissue volumes obtained from biopsies. Unfortunately, however, biomolecules of interest are not always present in a sufficient concentration to allow measurement. Drop coated deposition Raman spectroscopy (DCDRS) pre-concentrates the proteins to enable subsequent analysis [89], thus, overcoming this potential drawback.

### Malaria

Although malaria has virtually disappeared from Europe and the USA, it remains a major problem in tropical countries where it causes 300-500 million cases and 2-3 million deaths per year. It is said to have caused 'the greatest harm to the greatest number' of all infectious diseases (Sir Frank Macfarlane Burnet).

Malaria is transmitted to humans by the Anopheles mosquito where the organisms are injected into the human bloodstream, invading both liver and red blood cells, resulting in their structural and morphological alteration which impairs their circulation. Malaria is diagnosed in the laboratory by microscopic examination of a Giemsa-stained smear of peripheral blood. Early diagnosis is im-

portant for enabling effective treatment, whilst avoiding the unnecessary and expensive use of anti-malarials when not required.

The study of red blood cells by Raman spectroscopy has been extensively undertaken. More recently, the analysis of plasma as an alternative to blood smears has been evaluated. Raman spectroscopy was able to monitor the changes in plasma that occur during Plasmodium infection in mice. On the first day after infection, changes in the Raman bands that correspond to haemoglobin and hemozoin were seen, whereas, changes in the membranes of erythrocytes that are detected by blood films are detectable at around day 4 [90].

The ability to identify and diagnose malaria in asymptomatic carriers and in patients with low parasitaemia would appear to be advantageous. FTIR microscopy using a Focal Plane Array (FPA) imaging detector is able to diagnose malaria parasites at a single cell level using a standard glass microscope slide [91]. It seems highly improbable that vibrational spectroscopy will find a place in the diagnosis of malaria in the clinics and rural hospitals of developing countries where the disease is endemic. The technology and the understanding of the disease may, nevertheless, aid and advance the development of additional treatments and the illustrious malaria vaccination.

## The Inflammatory Response

A large number of medical conditions, including but not restricted to infectious disease, cause inflammation. Monitoring of the C-reactive protein (CRP) in blood samples is used as a sensitive, but non-specific biomarker of inflammation. CRP is an acute phase protein of hepatic origin. Its role in inflammation is to activate the complement system. This enhances the ability of both antibodies and phagocytic cells to clear microbes and damaged cells.

In some cases, it is difficult to differentiate between infectious and non-infectious causes of inflammation. This differentiation can have a significant impact on the management of the patient. Procalcitonin (PCT), the peptide precursor of the hormone calcitonin, rises in response to a proinflammatory stimulus of bacterial origin. It does not rise significantly with viral or non-infectious inflammation and, thus, can be used to aid in the identification of bacterial infections. It can, however, take over 24 hours for a definitive result.

Raman spectroscopy has, in small studies, been shown to differentiate inflammation due to infectious to that of non-infectious causes with an accuracy of 80% [92]. If shown to be repeatable in large scale studies, this modality could be used as an adjunct in the laboratory in selected cases to aid patient management, particularly with regard to the accurate and appropriate administration of antibiotics.

## Summary

The field of clinical medicine needs to utilise the principles and technologies that exist in other areas of science to further the understanding of disease processes, to facilitate earlier diagnosis and, thus, to improve the management and outcome of patients. This chapter exemplifies how the world of Physics is helping to provide answers to questions which are currently unanswered in medicine and has shown the broad areas that have been and are continuing to be investigated.

## References

- Smekal A. Zur Quantentheorie der Dispersion. *Naturwissenschaften*. 1923; 11: 873–875.
- Raman CV. A new radiation. *Indian J. Phys.* 1928; 2: 387–398.
- Eckenrode B, Bartick E, Harvey S et al. Raman spectrum of acetaminophen acquired Tylenol-brand tablet placed on the sampling stage of a Chromex Sentinel portable Raman system. 2001.
- Kong K, Kendall C, Stone N, Notingher I. Raman spectroscopy for medical diagnostics--From in-vitro biofluid assays to in-vivo cancer detection. *Adv Drug Deliv Rev.* 2015; 89: 121-134.
- Kendall C, Isabelle M, Bazant-Hegemark F, Hutchings J, Orr L, et al. Vibrational spectroscopy: a clinical tool for cancer diagnostics. *Analyst.* 2009; 134: 1029-1045.
- Matousek P, Stone N. Emerging concepts in deep Raman spectroscopy of biological tissue. *Analyst.* 2009; 134: 1058-1066.
- Matousek P. In: R Salzer, H Siesler, editors. *Infrared and Raman Spectroscopic Imaging*. Weinheim: Wiley-VCH. 2009; 405-426.
- Nallala J, Gobinet C, Diebold MD, Untereiner V, Bouch O, et al. Infrared spectral imaging as a novel approach for histopathological recognition in colon cancer diagnosis. *J Biomed Opt.* 2012; 17: 116013.
- Bassan P. University of Manchester: Thesis: Light scattering during infrared spectroscopic measurements of biomedical samples. 2011.
- Barth A. Infrared spectroscopy of proteins. *Biochim Biophys Acta.* 2007; 1767: 1073-1101.
- Mackanos MA, Contag CH. Fiber-optic probes enable cancer detection with FTIR spectroscopy. *Trends Biotechnol.* 2010; 28: 317-323.
- Haringsma J, Tytgat GN. Fluorescence and autofluorescence. *Baillieres Best Pract Res Clin Gastroenterol.* 1999; 13: 1-10.
- DaCosta RS, Andersson H, Cirocco M, Marcon

- NE, Wilson BC, et al. Autofluorescence characterisation of isolated whole crypts and primary cultured human epithelial cells from normal, hyperplastic, and adenomatous colonic mucosa. *J Clin Pathol.* 2005; 58: 766-774.
14. Zonios GI, Cothren RM, Arendt JT, Wu J, Van Dam J, et al. Morphological model of human colon tissue fluorescence. *IEEE Trans Biomed Eng.* 1996; 43: 113-122.
  15. Pradhan A, Pal P, Durocher G, Villeneuve L, Balassy A, et al. Steady state and time-resolved fluorescence properties of metastatic and non-metastatic malignant cells from different species. *J Photochem Photobiol.* 1995; 31: 101-112.
  16. Bhat SK, McManus DT, Coleman HG, Johnston BT, Cardwell CR, et al. Oesophageal adenocarcinoma and prior diagnosis of Barrett's oesophagus: a population-based study. *Gut.* 2015; 64: 20-25.
  17. Kara MA, DaCosta RS, Streutker CJ, Marcon NE, Bergman JJ, et al. Characterization of tissue autofluorescence in Barrett's esophagus by confocal fluorescence microscopy. *Dis Esophagus.* 2007; 20: 141-150.
  18. CR UK. Cancer Key Facts. Cancer Research UK. 2013.
  19. Jemal A, Siegel R, Ward E, Hao Y, Xu J, et al. Cancer statistics, 2008. *CA Cancer J Clin.* 2008; 58: 71-96.
  20. Nowell PC. The clonal evolution of tumor cell populations. *Science.* 1976; 194: 23-28.
  21. Bennett C, Moayyedi P, Corley DA, DeCaestecker J, Falck-Ytter Y, et al. BOB CAT: a Large-Scale Review and Delphi Consensus for Management of Barrett's Esophagus with No Dysplasia, Indefinite for, or Low-Grade Dysplasia. *Am J Gastroenterol.* 2015; 110: 662-682.
  22. Bennett C, Vakil N, Bergman J, Harrison R, Odze R, et al. Consensus statements for management of Barrett's dysplasia and early-stage esophageal adenocarcinoma, based on a Delphi process. *Gastroenterology.* 2012; 143: 336-346.
  23. Lee YC, Cook MB, Bhatia S, Chow WH, El-Omar EM, et al. Interobserver reliability in the endoscopic diagnosis and grading of Barrett's esophagus: an Asian multinational study. *Endoscopy.* 2010; 42: 699-704.
  24. Kerkhof M, van Dekken H, Steyerberg EW, Meijer GA, Mulder AH, et al. Grading of dysplasia in Barrett's oesophagus: substantial interobserver variation between general and gastrointestinal pathologists. *Histopathology.* 2007; 50: 920-927.
  25. Gaddam S, Mathur SC, Singh M, Arora J, Wani SB,

- et al. Novel probe-based confocal laser endomicroscopy criteria and interobserver agreement for the detection of dysplasia in Barrett's esophagus. *Am J Gastroenterol.* 2011; 106: 1961-1969.
26. Kendall C, Stone N, Shepherd N, Geboes K, Warren B, et al. Raman spectroscopy, a potential tool for the objective identification and classification of neoplasia in Barrett's oesophagus. *J Pathol.* 2003; 200: 602-609.
27. Bergholt MS, Zheng W, Lin K, Ho KY, Teh M, et al. Characterising variability in in-vivo Raman spectra of different anatomical locations in the upper gastrointestinal tract toward cancer detection. *J Biomed Opt.* 2011; 16: 037003.
28. Almond LM, Hutchings J, Kendall C, Day JC, Stevens OA, et al. Assessment of a custom-built Raman spectroscopic probe for diagnosis of early oesophageal neoplasia. *J Biomed Opt.* 2012; 17: 081421-081421.
29. Almond LM, Hutchings J, Lloyd G, Barr H, Shepherd N. Endoscopic Raman spectroscopy enables objective diagnosis of dysplasia in Barrett's esophagus. *Gastrointest Endosc.* 2014; 79: 37-45.
30. Shim MG, Song LM, Marcon NE, Wilson BC. In vivo near-infrared Raman spectroscopy: demonstration of feasibility during clinical gastrointestinal endoscopy. *Photochem Photobiol.* 2000; 72: 146-150.
31. Wong Kee Song L, Molckovsky A, Wang K et al. In: Vo-Dinh T, Grundfest W, Benaron D, Cohn G, editors. *Proceedings of SPIE.* 2005; 140-146.
32. Wong Kee Song LM, Wilson BC. Endoscopic detection of early upper GI cancers. *Best Pract Res Clin Gastroenterol.* 2005; 19: 833-856.
33. Hutchings J, Kendall C, Shepherd N, Barr H, Stone N, et al. Evaluation of linear discriminant analysis for automated Raman histological mapping of esophageal high-grade dysplasia. *J Biomed Opt.* 2010; 15: 066015.
34. Wang TD, Triadafilopoulos G, Crawford JM, Dixon LR, Bhandari T, et al. Detection of endogenous biomolecules in Barrett's esophagus by Fourier transform infrared spectroscopy. *Proc Natl Acad Sci U S A.* 2007; 104: 15864-15869.
35. Zhao R, Quaroni L, Casson AG. Fourier transform infrared (FTIR) spectromicroscopic characterisation of stem-like cell populations in human esophageal normal and adenocarcinoma cell lines. *Analyst.* 2009; 135: 53-61.
36. Haringsma J, Poley J, Blok P et al. Detection of intraepithelial neoplasia in Barrett's esophagus using autofluorescence endoscopy. *DDW (abstract #3550).* 2005.
37. Kara MA, Smits ME, Rosmolen WD, Bultje AC, Ten Kate FJ, et al. A randomized crossover study comparing light-induced fluorescence endoscopy

- with standard videoendoscopy for the detection of early neoplasia in Barrett's esophagus. *Gastrointest Endosc.* 2005; 61: 671-678.
38. Kara MA, Peters FP, Ten Kate FJ, Van Deventer SJ, Fockens P, et al. Endoscopic video autofluorescence imaging may improve the detection of early neoplasia in patients with Barrett's esophagus. *Gastrointest Endosc.* 2005; 61: 679-685.
  39. Jemal A, Center M, DeSantis C, Ward E. Global patterns of cancer incidence and mortality rates and trends. *American Association of Cancer Research.* 2010; 19: 1893-1907.
  40. Raimes A. *Oesophagogastric Surgery. A Companion to Specialist Surgical Practice*, 4th edn. Aunders: Elsevier. 2009.
  41. Leung WK, Wu MS, Kakugawa Y, Kim JJ, Yeoh KG, et al. Screening for gastric cancer in Asia: current evidence and practice. *Lancet Oncol.* 2008; 9: 279-287.
  42. Huang Z, Bergholt MS, Zheng W, Lin K, Ho KY, et al. In vivo early diagnosis of gastric dysplasia using narrow-band image-guided Raman endoscopy. *J Biomed Opt.* 2010; 15: 037017.
  43. Huang Z, Teh SK, Zheng W, Lin K, Ho KY, et al. In vivo detection of epithelial neoplasia in the stomach using image-guided Raman endoscopy. *Biosens Bioelectron.* 2010; 26: 383-389.
  44. Teh SK, Zheng W, Ho KY, Teh M, Yeoh KG, et al. Near-infrared Raman spectroscopy for early diagnosis and typing of adenocarcinoma in the stomach. *Br J Surg.* 2010; 97: 550-557.
  45. Kawabata T, Kikuchi H, Okazaki S, Yamamoto M, Hiramatsu Y, et al. Near-infrared multichannel Raman spectroscopy with a 1064 nm excitation wavelength for ex vivo diagnosis of gastric cancer. *J Surg Res.* 2011; 169: e137-143.
  46. Duraipandian S, Sylvest Bergholt M, Zheng W, Yu Ho K, Teh M, et al. Real time Raman spectroscopy for in vivo, online gastric cancer diagnosis during clinical endoscopic examination. *J Biomed Opt.* 2012; 17: 081418.
  47. Wang J, Lin K, Zheng W, Ho KY, Teh M, et al. Fiber-optic Raman spectroscopy for in vivo diagnosis of gastric dysplasia. *Faraday Discuss.* 2016; 187: 377-392.
  48. Li QB, Sun XJ, Xu YZ, Yang LM, Zhang YF, et al. Diagnosis of gastric inflammation and malignancy in endoscopic biopsies based on Fourier transform infrared spectroscopy. *Clin Chem.* 2005; 51: 346-350.
  49. Daping Sheng, Yican Wu, Xin Wang, Dake Huang, Xianliang Chen, et al. Comparison of serum from gastric cancer patients and from healthy persons using FTIR spectroscopy. *Spectrochimica Acta Part A: Molecular and Biomolecular Spectroscopy.* 2013; 116: 365-369.

50. Feng S, Pan J, Wu Y, Lin D, Chen Y, et al. Study on gastric cancer blood plasma based on surface-enhanced Raman spectroscopy combined with multivariate analysis. *Sci China: Life Sci.* 2011; 54: 828-834.
51. Ohkawa A, Miwa H, Namihisa A, Kobayashi O, Nakaniwa N, et al. Diagnostic performance of light-induced fluorescence endoscopy for gastric neoplasms. *Endoscopy.* 2004; 36: 515-521.
52. Kato M, Kaise M, Yonezawa J, Yoshida Y, Tajiri H, et al. Autofluorescence endoscopy versus conventional white light endoscopy for the detection of superficial gastric neoplasia: a prospective comparative study. *Endoscopy.* 2007; 39: 937-941.
53. Bergholt MS, Zheng W, Lin K, Ho KY, Teh M, et al. Combining near-infrared-excited autofluorescence and Raman spectroscopy improves in vivo diagnosis of gastric cancer. *Biosensors and Bioelectronics.* 2011; 26: 4101-4110.
54. Leslie A, Carey FA, Pratt NR, Steele RJ. The colorectal adenoma-carcinoma sequence. *Br J Surg.* 2002; 89: 845-860.
55. van Rijn JC, Reitsma JB, Stoker J, Bossuyt PM, van Deventer SJ, et al. Polyp miss rate determined by tandem colonoscopy: a systematic review. *Am J Gastroenterol.* 2006; 101: 343-350.
56. Leufkens AM, van Oijen MG, Vleggaar FP, Siersema PD. Factors influencing the miss rate of polyps in a back-to-back colonoscopy study. *Endoscopy.* 2012; 44: 470-475.
57. Ahn SB, Han DS, Bae JH, Byun TJ, Kim JP, et al. The Miss Rate for Colorectal Adenoma Determined by Quality-Adjusted, Back-to-Back Colonoscopies. *Gut Liver.* 2012; 6: 64-70.
58. Subramanian V, Mannath J, Hawkey CJ, Ragunath K. High definition colonoscopy vs. standard video endoscopy for the detection of colonic polyps: a meta-analysis. *Endoscopy.* 2011; 43: 499-505.
59. Nagorni A, Bjelakovic G, Petrovic B. Narrow band imaging versus conventional white light colonoscopy for the detection of colorectal polyps. *Cochrane Database Syst Rev.* 2012; 1: CD008361.
60. Dinesen L, Chua TJ, Kaffes AJ. Meta-analysis of narrow-band imaging versus conventional colonoscopy for adenoma detection. *Gastrointest Endosc.* 2012; 75: 604-611.
61. Shim M, Wilson B, Marple E, Wach M. Study of fiber-optic probes for in vivo medical Raman spectroscopy. *Appl Spectrosc.* 1999; 53: 619-627.
62. Smith J, Kendall C, Sammon A, Christie-Brown J, Stone N, et al. Raman spectral mapping in the assessment of axillary lymph nodes in breast cancer. *Technol Cancer Res Treat.* 2003; 2: 327-332.
63. Molckovsky A, Song LM, Shim MG, Marcon NE, Wilson BC, et al. Diagnostic potential of near-infrared Raman spectroscopy in the colon: differ-

- entiating adenomatous from hyperplastic polyps. *Gastrointest Endosc.* 2003; 57: 396-402.
64. Short MA, Tai IT, Owen D, Zeng H. Using high frequency Raman spectra for colonic neoplasia detection. *Opt Express.* 2013; 21: 5025-5034.
65. Mads SB, Kan L, Jianfeng W, Wei Z, Hongzhi X, et al. Simultaneous fingerprint and high wave-number fiber-optic Raman spectroscopy enhances real-time in vivo diagnosis of adenomatous polyps during colonoscopy. *Journal of Biophotonics.* 2016; 9: 333-342.
66. Hutchings J, Kendall C, Shepherd N, Barr H, Stone N, et al. Evaluation of linear discriminant analysis for automated Raman histological mapping of esophageal high-grade dysplasia. *J Biomed Opt.* 2010; 15: 066015.
67. Rigas B, Morgello S, Goldman IS, Wong PT. Human colorectal cancers display abnormal Fourier-transform infrared spectra. *Proc Natl Acad Sci U S A.* 1990; 87: 8140-8144.
68. Li QB, Xu Z, Zhang NW, Zhang L, Wang F, et al. In vivo and in situ detection of colorectal cancer using Fourier transform infrared spectroscopy. *World J Gastroenterol.* 2005; 11: 327-330.
69. Zwielly A, Mordechai S, Sinielnikov I, Salman A, Bogomolny E, et al. Advanced statistical techniques applied to comprehensive FTIR spectra on human colonic tissues. *Med Phys.* 2010; 37: 1047-1055.
70. Wood JJ, Kendall C, Hutchings J, Lloyd GR, Stone N, et al. Evaluation of a confocal Raman probe for pathological diagnosis during colonoscopy. *Colorectal Dis.* 2014; 16: 732-738.
71. Griggs R. High Resolution Infrared Spectroscopic Analysis of Human Colorectal Pathology. Thesis for the Degree of MReS, University of Exeter. 2015.
72. Ignjatovic A, East JE, Suzuki N, Vance M, Guenther T, et al. Optical diagnosis of small colorectal polyps at routine colonoscopy (Detect InSpect Characterise Resect and Discard; DISCARD trial): a prospective cohort study. *Lancet Oncol.* 2009; 10: 1171-1178.
73. East JE, Saunders BP. Narrow band imaging at colonoscopy: seeing through a glass darkly or the light of a new dawn? *Expert Rev Gastroenterol Hepatol.* 2008; 2: 1-4.
74. Ignjatovic A, East JE, Guenther T, Hoare J, Morris J, et al. What is the most reliable imaging modality for small colonic polyp characterization? Study of white-light, autofluorescence, and narrow-band imaging. *Endoscopy.* 2011; 43: 94-99.
75. Eaden JA, Abrams KR, Mayberry JF. The risk of colorectal cancer in ulcerative colitis: a meta-analysis. *Gut.* 2001; 48: 526-535.
76. van den Broek FJ, Fockens P, van Eeden S, Reits-



- ma JB, Hardwick JC, et al. Endoscopic tri-modal imaging for surveillance in ulcerative colitis: randomised comparison of high-resolution endoscopy and autofluorescence imaging for neoplasia detection; and evaluation of narrow-band imaging for classification of lesions. *Gut*. 2008; 57: 1083-1089.
77. Koljenović S, Schut TC, Wolthuis R, Vincent AJ, Hendriks-Hagevi G, et al. Raman spectroscopic characterization of porcine brain tissue using a single fiber-optic probe. *Anal Chem*. 2007; 79: 557-564.
78. Krafft C, Neudert L, Simat T, Salzer R. New infrared Raman spectra of human brain lipids. *Spectrochimica Acta Part A: Molecule and Biomolecular Spectroscopy*. 2009; 61: 1529-1535.
79. Gajjar K, Heppenstall LD, Pang W, Ashton KM, Trevisan J, et al. Diagnostic segregation of human brain tumours using Fourier-transform infrared and/or Raman spectroscopy coupled with discriminant analysis. *Anal Methods*. 2012; 5: 89-102.
80. Kirsch M, Schackert G, Salzer R, Krafft C. Raman spectroscopic imaging for in vivo detection of cerebral brain metastases. *Anal Bioanal Chem*. 2010; 398: 1707-1713.
81. Noreen R, Chien CC, Delugin M, Yao S, Pineau R, et al. Detection of collagens in brain tumors based on FTIR imaging and chemometrics. *Anal Bioanal Chem*. 2011; 401: 845-852.
82. Araki K, Yagi N, Ikemoto Y, Yagi H. Synchrotron FTIR micro-spectroscopy for structural analysis of Lewy bodies in the brain of Parkinson's disease patients. *Sci Rep*. 2015; 5: 17625.
83. Hackett MJ, Britz CJ, Paterson PG, Nichol H, Pickering IJ, et al. In situ biospectroscopic investigation of rapid ischemic and postmortem induced biochemical alterations in the rat brain. *ACS Chem Neurosci*. 2015; 6: 226-238.
84. Walter H, Sadeque-Iqbal F, Ulysse R, Castillo D, Fitzpatrick A, et al. The effectiveness of school-based family asthma educational programs on the quality of life and number of asthma exacerbations of children aged five to 18 years diagnosed with asthma: a systematic review protocol. *JBI Database System Rev Implement Rep*. 2015; 13: 69-81.
85. Motz JT, Fitzmaurice M, Miller A, Gandhi SJ, Haka AS, et al. In vivo Raman spectral pathology of human atherosclerosis and vulnerable plaque. *J Biomed Opt*. 2006; 11: 021003.
86. Marcu L, Fang Q, Jo JA, Papaioannou T, Dorafshar A, et al. In vivo detection of macrophages in a rabbit atherosclerotic model by time-resolved laser induced fluorescence spectroscopy. *Atherosclerosis*. 2005; 181: 295-303.
87. Moreno PR, Lodder RA, Purushothaman KR,

- Charash WE, O'Connor WN, et al. Detection of Lipid Pool, Thin Fibrous Cap, and Inflammatory Cells in Human Aortic Atherosclerotic Plaques by Near-Infrared Spectroscopy. *Circulation*. 2002; 105: 923-927.
88. Waxman S, Dixon SR, L'Allier P, Moses JW, Petersen JL, et al. In Vivo Validation of a Catheter-Based Near-Infrared Spectroscopy System for Detection of Lipid Core Coronary Plaques: Initial Results of the SPECTACL Study. *J Am Coll Cardiol Img*. 2009; 2: 858-868.
89. Filik J, Stone N. Drop coating deposition Raman spectroscopy of protein mixtures. *Analyst*. 2007; 132: 544-550.
90. Hobro AJ, Konishi A, Coban C, Smith NI. Raman spectroscopic analysis of malaria disease progression via blood and plasma samples. *Analyst*. 2013; 138: 3927-3933.
91. Perez-Guaita D, Andrew D, Heraud P, Beeson J, Anderson D, et al. High resolution FTIR imaging provides automated discrimination and detection of single malaria parasite infected erythrocytes on glass. *Faraday Discuss*. 2016; 187: 341-352.
92. Neugebauer U, Trenkmann S, Bocklitz T, Schmerler D, Kiehntopf M, et al. Fast differentiation of SIRS and sepsis from blood plasma of ICU patients using Raman spectroscopy. *J Biophotonics*. 2014; 7: 232-240.

## Bibliography

- Abrams J, Fields S, Lightdale C and Neugut A. 2008. "Racial and Ethnic Disparities in the Prevalence of Barrett's Esophagus Among Patients Who Undergo Upper Endoscopy." *Clinical Gastroenterology and Hepatology*. 6(1):30-34.
- Agarwal A, Polineni R *et al.* 2012. "Role of epigenetic alterations in the pathogenesis of Barrett's esophagus and esophageal adenocarcinoma." *International Journal of Clinical and Experimental Pathology*. 5(5):382-396.
- Akasaka Y and Ishii T. 2007. "Histopathology and molecular pathology of intestinal metaplasia." *Current Diagnostic Pathology*. 13(4):331-339.
- Alderson D and Wijnhoven B. 2016. "Interventions for Barrett's oesophagus and early cancer." *British Journal of Surgery*. 103(5):475-6.
- Almond L, Hodson J *et al.* 2014. "Meta-analysis of endoscopic therapy for low-grade dysplasia in Barrett's oesophagus." *BJS*. 101(10):1187-95.
- Anaparthi R, Gaddam S *et al.* 2013. "Association between length of barrett's esophagus and risk of high-grade dysplasia or adenocarcinoma in patients without dysplasia." *Clinical Gastroenterology and Hepatology*. 11(11):1430-6.
- Ansari B, Coates P, Greenstein B and Hall P. 1993. "In situ end-labelling detects DNA strand breaks in apoptosis and other physiological and pathological states." *J Pathol*. 170:1-8.
- Aotake T, Lu C *et al.* 1999. "Changes of Angiogenesis and Tumor Cell Apoptosis during Colorectal Carcinogenesis." *Clinical Cancer Research*. 5:135-142.
- Baak P, Kate J *et al.* 2002. "Routine morphometrical analysis can improve reproducibility of dysplasia grade in Barrett's oesophagus surveillance biopsies." *J Clin Pathol*. 55:910-916.
- Badizadegan K, Backman V *et al.* 2004. "Spectroscopic diagnosis and imaging of invisible pre-cancer." *Faraday Discuss*. 126:265-279.
- Bailey T, Biddlestone L *et al.* 1998. "Altered Cadherin and Catenin Complexes in the Barrett's Esophagus-Dysplasia-Adenocarcinoma Sequence Correlation with Disease Progression and Dedifferentiation." *American Journal of Pathology*. 152(1): 135-144.
- Baker M, Trevisan I *et al.* 2014. "Using Fourier transform IR spectroscopy to analyze biological materials." *Nature Protocols*. 9(8):1771-1791.
- Barbour A, Jones M *et al.* 2010. "Risk Stratification for Early Esophageal Adenocarcinoma: Analysis of Lymphatic Spread and Prognostic Factors." *Ann Surg Oncol*. 17:2494-2502.

- Bedi A, Pasricha P *et al.* 1995. "Inhibition of Apoptosis during Development of Colorectal Cancer." *Cancer Research*. 55:1811-1816.
- Bennett C, Moayyedi P *et al.* 2015. "BOB CAT: A Large-Scale Review and Delphi Consensus for Management of Barrett's Esophagus With No Dysplasia, Indefinite for, or Low-Grade Dysplasia." *Am J Gastroenterol*. 110(5):662-82.
- Bergholt M, Zheng W *et al.* 2011. "In Vivo Diagnosis of Esophageal Cancer Using Image-Guided Raman Endoscopy and Biomolecular Modeling." *Technology in Cancer Research and Treatment*. 10(2):103-112.
- Bergholt M, Zheng W *et al.* 2014. "Fiberoptic Confocal Raman Spectroscopy for Real-Time In Vivo Diagnosis of Dysplasia in Barrett's Esophagus." *Gastroenterology*. 146(1):27-32.
- Bronner M, Reed C and Furth E. 1995. "The bcl-2 proto-oncogene and the gastrointestinal epithelial tumor progression model." *Am J Pathol*. 146(1):20-6.
- Brown L, Devesa S and Ho W. 2008. "Incidence of adenocarcinoma of the esophagus among white Americans by sex, stage, and age." *Journal of the National Cancer Institute*. 100:1184-1187.
- Bhat S, Coleman H *et al.* 2011. "Risk of malignant progression in Barrett's Esophagus patients: Results from a large population-based study." *Journal of the National Cancer*. 103:1049-1057.
- Brien O, Keane M *et al.* 1992. "Precursors of colorectal carcinoma. Biopsy and biologic markers." *Cancer*. 70(5):1317-1327.
- Brodie C, Crotty P and Gaffney E. 2004. "Morphologically distinct patterns of apoptosis correlate with size and high-grade dysplasia in colonic adenomas." *Histopathology*. 44:240-246.
- Brunk U and Terman A. 2002. "Lipofuscin: mechanisms of age-related accumulation and influence on cell function." *Free Radical Biology and Medicine*. 33(5):611-619.
- Burggraaf J, Kamerling I *et al.* 2015. "Detection of colorectal polyps in humans using an intravenously administered fluorescent peptide targeted against c-Met." *Nature Medicine*. 21:955-961.
- Buskens C, Westerterp M *et al.* 2004. "Prediction of appropriateness of local endoscopic treatment for high-grade dysplasia and early adenocarcinoma by EUS and histopathologic features." *Gastrointest Endosc*. 60(5):703-10.
- Byers R, Marsh P *et al.* 1997. "Melanosis coli is associated with an increase in colonic epithelial apoptosis and not with laxative use." *Histopathology*. 30(2):160-164.
- Carey L, Pratt N and Steele R. 2002. "The colorectal adenoma-carcinoma sequence." *BJS*. 89:845-860.

Carr N. 2000. "M30 expression demonstrates apoptotic cells, correlates with in situ end-labeling, and is associated with Ki-67 expression in large intestinal neoplasms." *Arch Pathol Lab Med.* 124:1768-1772.

Chak A, Lee T *et al.* 2002. "Familial aggregation of Barrett's oesophagus, oesophageal adenocarcinoma, and oesophagogastric junctional adenocarcinoma in Caucasian adults." *Gut.* 51:323-328.

Chang E, Morris C *et al.* 2007. "The Effect of Antireflux Surgery on Esophageal Carcinogenesis in Patients With Barrett Esophagus: A Systematic Review." *Ann Surg.* 246:11-21.

Chatelain D and Fléjou J. 2003. "High-grade dysplasia and superficial adenocarcinoma in Barrett's esophagus: histological mapping and expression of p53, p21 and Bcl-2 oncoproteins." *Virchows Arch.* 442(1):18-24.

Chen Y, Dai J *et al.* 2014. "Raman spectroscopy analysis of the biochemical characteristics of molecules associated with the malignant transformation of gastric mucosa." *PLOS One.* 9(4):1-11.

Cleta A and Bottiroli C. 2014. "Autofluorescence spectroscopy and imaging: A tool for biomedical research and diagnosis." *European Journal of Histochemistry.* 58:320-337.

Coda S, Thompson A *et al.* 2014. "Fluorescence lifetime spectroscopy of tissue autofluorescence in normal and diseased colon measured ex vivo using a fiber-optic probe." *Biomedical Optics.* 5(2):515-538.

Coleman H, Bhat S *et al.* 2011. "Increasing incidence of Barrett's oesophagus: A population-based study." *European Journal of Epidemiology.* 26:739-745.

Conlon K and McMahon R. 2002. "Minimally invasive surgery in the diagnosis and treatment of upper gastrointestinal tract malignancy." *Annals of Surgical Oncology.* 9(8):725-737.

Connelly M, Keku T *et al.* 2002. "Nonsteroidal anti-inflammatory drugs, apoptosis, and colorectal adenomas." *Gastroenterology.* 123(6):1770-1777.

Conti C, Ferraris P *et al.* 2008. "FT-IR microimaging spectroscopy: A comparison between healthy and neoplastic human colon tissues." *Journal of Molecular Structure.* 881:46-51.

Cook M, Wild C and Forman D. 2005. "A systematic review and meta-analysis of the sex ratio for Barrett's esophagus, erosive reflux disease, and nonerosive reflux disease." *American Journal of Epidemiology.* 162(11):1050-1061.

Cooper G, Yuan Z *et al.* 2002. "Association of prediagnosis endoscopy with stage and survival in adenocarcinoma of the esophagus and gastric cardia." *Cancer.* 95(1):32-38.

- Cooper G, Kou T and Chak A. 2009. "Receipt of previous diagnoses and endoscopy and outcome from esophageal adenocarcinoma: a population-based study with temporal trends." *Am J Gastroenterol.* 104(6):1356-62.
- Corley D, Kubo A *et al.* 1994. "Race, ethnicity, sex and temporal differences in Barrett's oesophagus diagnosis: a large community-based study." *Gut.* 58(2):182-188.
- Corley D, Levin T *et al.* 2002. "Surveillance and Survival in Barrett's Adenocarcinomas: A Population-Based Study." *Gastroenterology.* 122:633-40.
- Correa P. 1992. "Human Gastric Carcinogenesis: A Multistep and Multifactorial Process." *Cancer Research.* 52:6735-6740.
- Croce A and Bottiroli G. 2014. "Autofluorescence spectroscopy and imaging: A tool for biomedical research and diagnosis." *European Journal of Histochemistry.* 58(2461):320-337.
- Crosnier D, Stamataki D and Lewis J. 2006. "Organizing cell renewal in the intestine: stem cells, signals and combinatorial control." *Nature Reviews: Genetics.* 7:349-359.
- DaCosta R, Wilson B and Marcon N. 2002. "New optical technologies for earlier endoscopic diagnosis of premalignant gastrointestinal lesions." *Journal of gastroenterology and hepatology.* 17:s85-104.
- DaCosta R, Andersson H and Wilson B. 2003. "Molecular fluorescence excitation-emission matrices relevant to tissue spectroscopy." *Photochemistry and Photobiology.* 78(4):384-392.
- DaCosta R, Wilson B *et al.* 2003. "Photodiagnostic Techniques for the Endoscopic Detection of Premalignant Gastrointestinal Lesions." *Digestive Endoscopy.* 15:153-173.
- DaCosta R, Wilson B *et al.* 2004. "Autofluorescence-Based Detection of Early Neoplasia in Patients with Barrett's Esophagus." *Digestive Diseases.* 22:134-141.
- DaCosta R, Andersson M *et al.* 2005. "Autofluorescence characterisation of isolated whole crypts and primary cultured human epithelial cells from normal, hyperplastic, and adenomatous colonic mucosa." *J Clin Pathol.* 58:766-774.
- DaCosta R, Wilson B *et al.* 2005. "Spectroscopy and fluorescence in esophageal diseases." *Clinical Gastroenterology.* 20(1):41-57.
- DaCosta R, Wilson B and Marcon N. 2009. "Optical techniques for the endoscopic detection of dysplastic colonic lesions." *Curr Opin Gastroenterol.* 21:70-79.
- Dar M, Goldbulm J *et al.* 2003. "Can extent of high grade dysplasia in Barrett's oesophagus predict the presence of adenocarcinoma at Oesophagectomy?" *Gut.* 52:486-89.

De Jonge P, Van Blankenstein M *et al.* 2014. "Barrett's oesophagus: epidemiology, cancer risk and implications for management." *Gut*. 63:191-202.

Desai T, Krishnan K *et al.* 2012. "The incidence of oesophageal adenocarcinoma in non-dysplastic Barrett's oesophagus: a meta-analysis." *Gut*. 61:970-976.

Devesa S, Blot W *et al.* 1998. "Changing Patterns in the Incidence of Esophageal and Gastric Carcinoma in the United States." *Cancer*. 83:2049-53.

Di Pietro M, Boerwinkel D *et al.* 2014. "The combination of autofluorescence endoscopy and molecular biomarkers is a novel diagnostic tool for dysplasia in Barrett's oesophagus." *Gut*. 64(1):49-56.

Diem M, Gerwert K, Wood B *et al.* 2016. "Advanced Vibrational Spectroscopy for Biomedical Applications: General Discussion." *Faraday Discussions*. 187:155-186.

Duits L, Nadine Phoa K *et al.* 2014. "Barrett's oesophagus patients with low-grade dysplasia can be accurately risk-stratified after histological review by an expert pathology panel." *Gut*. 64:700-706.

Dvorak K, Payne C *et al.* "Bile acids in combination with low pH induce oxidative stress and oxidative DNA damage: relevance to the pathogenesis of Barrett's oesophagus." *Gut*. 56:763-771.

Edelstein Z, Bronner M *et al.* 2009. "Risk factors for Barrett's esophagus among patients with gastroesophageal reflux disease: A community clinic-based case-control study." *Am J Gastroenterol*. 104(4):834-842.

El-Serag H, Aguirre T *et al.* 2004. "Proton pump inhibitors are associated with reduced incidence of dysplasia in Barrett's esophagus." *Am J Gastroenterol*. 99(10):1877-83.

Eriksson N, Kärkkäinen P and Arkkila P. 2008. "Prevalence and distribution of gastric intestinal metaplasia and its subtypes." *Digestive and Liver Disease*. 40:355-360.

Eskelinen E and Saftig P. 2008. "Autophagy: A lysosomal degradation pathway with a central role in health and disease." *Molecular Cell Research*. 1793:664-673.

Espino A, Cirocco M *et al.* 2014. "Advanced imaging technologies for the detection of dysplasia and early cancer in Barrett's esophagus." *Clinical endoscopy*. 47(1):47-54.

Falk G, Rice T *et al.* 1999. "Jumbo biopsy forceps protocol still misses unsuspected cancer in Barrett's esophagus with high-grade dysplasia." *Gastrointest Endoscopy*. 49:170-6.

- Falk G. 2015. "Barrett's oesophagus: Frequency and prediction of dysplasia and cancer." *Best Pract Res Clin Gastroenterol.* 29(1):125-38.
- Fléjou J, Sagan C *et al.* 1994. "Reproducibility of histological criteria of dysplasia in Barrett mucosa." *Gastroenterol Clin Biol.* 18:31-34.
- Fléjou JF. 2004. "Barrett's oesophagus: from metaplasia to dysplasia and cancer." *Gut.* 54:6-12.
- Fitzgerald R, di Pietro M *et al.* 2014. "British Society of Gastroenterology guidelines on the diagnosis and management of Barrett's oesophagus." *Gut.* 63(1):7-42.
- Freeman, J. 2008. "Melanosis in the small and large intestine." *J Gastroenterol.* 14(27):4296-4299.
- Garcea G, Sharma R *et al.* 2003. "Molecular biomarkers of colorectal carcinogenesis and their role in surveillance and early intervention." *European Journal of Cancer.* 39:1041-1052.
- Gazi E, Dwyer J, Lockyer NP *et al.* 2005. "Fixation protocols for subcellular imaging by synchrotron-based Fourier transform infrared microspectroscopy." *Biopolymers.* 77:18-30.
- Georgakopoulou E, Tsimaratou K *et al.* 2013. "Specific lipofuscin staining as a novel biomarker to detect replicative and stress-induced senescence. A method applicable in cryo-preserved and archival tissues." *Aging.* 5(1):37-50.
- Georgakoudi I, Jacobson B *et al.* 2001. "Fluorescence, Reflectance, and Light-Scattering Spectroscopy for Evaluating Dysplasia in Patients With Barrett's Esophagus." *Gastroenterology.* 120:1620-1629.
- Georgakoudi I, Jacobson B *et al.* 2002. "NAD(P)H and collagen as in vivo quantitative fluorescent biomarkers of epithelial precancerous changes." *Cancer Research.* 62:682-687.
- Ghadially F and Walley V. "Melanoses of the GI Tract." *Histopathology.* 25:197-207.
- Gindea C, Birla R *et al.* 2014. "Surveillance in Barrett Esophagus." *Journal of Medicine and Life.* 7(3):61-67.
- Glick D, Barth S and Macleod K. 2010. "Autophagy: cellular and molecular mechanisms." *J Pathol.* 221(1):3-12.
- Goldbulm J. 2003. "Barrett's Esophagus and Barrett's-Related Dysplasia." *Pathology.* 16(4):316-324.
- Goodarzi M, Correa A *et al.* 2009. "Anti-phosphorylated histone H3 expression in Barrett's esophagus, low-grade dysplasia, high-grade dysplasia, and adenocarcinoma." *Modern Pathology.* 22:1612-21.



- Gown A and Willingham M. 2002. "Improved Detection of Apoptotic Cells in Archival Paraffin Sections: Immunohistochemistry Using Antibodies to Cleaved Caspase 3." *The Journal of Histochemistry & Cytochemistry*. 50(4):449-454.
- Gozuacik D and Kimchi A. 2004. "Autophagy as a cell death and tumor suppressor mechanism." *Oncogene*. 23:2891-2906.
- Grasl-Kraupp B, Ruttkay-Nedecky B *et al.* 1995. "In situ detection of fragmented DNA (tunel assay) fails to discriminate among apoptosis, necrosis, and autolytic cell death: A cautionary note." *Hepatology*. 21:1465-1468.
- Green A, Tawil A *et al.* 2011. "Surgery versus radical endotherapies for early cancer and high grade dysplasia in Barrett's oesophagus." *Cochrane Database Of Systematic Reviews*.
- Gregson E and Fitzgerald R. 2015. "Biomarkers for Dysplastic Barrett's: Ready for Prime Time?" *World J Surg*. 39:568-77.
- Hall P, Coates P *et al.* 1994. "Regulation of cell number in the mammalian gastrointestinal tract: the importance of apoptosis." *Journal of Cell Science*. 107:3569-3577.
- Hardwick R, Shepherd N *et al.* 1994. "Adenocarcinoma arising in Barrett's oesophagus: evidence for the participation of p53 dysfunction in the dysplasia/carcinoma sequence." *Gut*. 35(6):764-768.
- Haringsma J and Tytgat G. 1999. "Fluorescence and autofluorescence." *Baillière's Clinical Gastroenterology*. 13(1):1-10.
- Hawkins N, Lees J *et al.* 1997. "Pathological and Genetic Correlates of Apoptosis in the Progression of Colorectal Neoplasia." *Tumor Biology*. 18(3):146-56.
- Hector S and Prehn J. 2009. "Apoptosis signaling proteins as prognostic biomarkers in colorectal cancer: A review." *Reviews on Cancer*. 1795:117-129.
- Heitmiller R, Redmond M and Hamilton S. 1996. "Barrett's Esophagus with High-Grade Dysplasia. An Indication for Prophylactic Esophagectomy." *Annals of Surgery*. 224:66-71.
- Jankowski J, Singh R *et al.* 2007. "Barrett's Esophagus: Diagnosis, Screening, Surveillance, and Controversies." *Gut and Liver*. 1(2):93-100.
- Herrero A, Pouw R *et al.* 2010. "Risk of lymph node metastasis associated with deeper invasion by early adenocarcinoma of the esophagus and cardia: study based on endoscopic resection specimens." *Endoscopy*. 42(12):1030-6.
- Holubec H, Payne C *et al.* 2005. "Assessment of Apoptosis by Immunohistochemical Markers Compared to Cellular Morphology in Ex Vivo-stressed Colonic Mucosa." *J Histochem Cytochem*. 53(2):229-235.

- Hormi-Carver K, Zhang X *et al.* 2009. "Unlike esophageal squamous cells, barrett's epithelial cells resist apoptosis by activating the nuclear factor-kB pathway." *Cancer Res.* 69(2):672-677.
- Inadomi J, Sampliner R *et al.* 2005. "Screening and Surveillance for Barrett Esophagus in High-Risk Groups: A Cost–Utility Analysis Background: Once-in-a-lifetime screening for Barrett esophagus." *Ann Intern Med.* 138:176-186.
- Inadomi J. 2009. "Surveillance in Barrett's esophagus: A failed premise." *Keio J Med.* 58(1):12-18.
- Jagadesham V and Kelty C. 2014. "Low grade dysplasia in Barrett's esophagus: Should we worry?" *World J Gastrointest Pathophysiol.* 5(2):91-99.
- Jankowski J, Wright N *et al.* 1999. "Molecular Evolution of the Metaplasia-Dysplasia- Adenocarcinoma Sequence in the Esophagus." *The American Journal of Pathology.* 154(4):965-973.
- Jenkins G, Doak S *et al.* 2002. "Genetic pathways involved in the progression of Barrett's metaplasia to adenocarcinoma." *BJS.* 89:824-837.
- Jeung J, Coran J *et al.* 2012. "Hepatocyte paraffin 1 antigen as a biomarker for early diagnosis of Barrett esophagus." *American Journal of Clinical Pathology.* 137(1):111-120.
- Jiang M and Milner J. 2001. "Bcl-2 constitutively suppresses p53-dependent apoptosis in colorectal cancer cells." *Genes and Development.* 17:832-837.
- Kallaway C, Almond L *et al.* 2013. "Advances in the clinical application of Raman spectroscopy for cancer diagnostics." *Photodiagnosis and Photodynamic Therapy.* 10:207-219.
- Kara M, DaCosta R *et al.* 2007. "Characterization of tissue autofluorescence in Barrett's esophagus by confocal fluorescence microscopy." *Diseases of the Esophagus.* 20:141-150.
- Kastelein F, Biermann K *et al.* 2013. "Aberrant p53 protein expression is associated with an increased risk of neoplastic progression in patients with Barrett's oesophagus." *Gut.* 62(12):1676-83.
- Katada N, Hinder R *et al.* 1997. "Apoptosis Is Inhibited Early in the Dysplasia-Carcinoma Sequence of Barrett Esophagus." *Arch Surg.* 132:728-33.
- Katz M and Robison G. 2002. "What is lipofuscin? Defining characteristics and differentiation from other autofluorescent lysosomal storage bodies." *Archives of Gerontology and Geriatrics.* 34:169-184.
- Kaye P, Haider S *et al.* 2009. "Barrett's dysplasia and the Vienna classification: Reproducibility, prediction of progression and impact of consensus reporting and p53 immunohistochemistry." *Histopathology.* 54:699-712.

Kendall C, Stone N et al. 2003. "Raman Spectroscopy, a potential tool for the objective Identification of classification of neoplasia in Barrett's oesophagus." *The Journal of Pathology*. 200(5):602-9.

Kendall C, Smith J, Crow P and Barr H. 2004. "Raman spectroscopy for identification of epithelial cancers." *Faraday Discuss*. 126:141-157.

Kendall C, Isabelle M et al. 2009. "Vibrational spectroscopy: a clinical tool for cancer diagnostics." *Analyst*. 134:1029-1045.

Kerkhof M, Van Dekken H et al. 2007. "Grading of dysplasia in Barrett's oesophagus: Substantial interobserver variation between general and gastrointestinal pathologists." *Histopathology*. 50:920-927.

Kerr J, Winterford C and Harmon B. 1994. "Apoptosis Its Significance in Cancer and Cancer Therapy." *Cancer*. 73:2013-2026.

Khemthongcharoen N, Jolivot R et al. 2014. "Advances in imaging probes and optical microendoscopic imaging techniques for early in vivo cancer assessment." *Advanced Drug Delivery Reviews*. 74:53-74.

Koike M. 1996. "Significance of spontaneous apoptosis during colorectal tumorigenesis." *Journal of Surgical Oncology*. 62:97-108.

Kong K, Kendall C et al. 2015. "Raman spectroscopy for medical diagnostics — From in-vitro biofluid assays to in-vivo cancer detection." *Advanced Drug Delivery Reviews*. 89:121-134.

Koornstra J, de Jong S et al. 2003. "Changes in apoptosis during the development of colorectal cancer: A systematic review of the literature." *Critical Reviews in Oncology and Hematology*. 45(1):37-53.

Koornstra J, Rijcken F et al. 2004. "Assessment of apoptosis by M30 immunoreactivity and the correlation with morphological criteria in normal colorectal mucosa, adenomas and carcinomas." *Histopathology*. 44:9-17.

Koppert L, Wijnhoven B et al. 2005. "The Molecular Biology of Esophageal Adenocarcinoma." *J Surg Oncol*. 92:169-190.

Koskela E, Kulju T and Collan Y. 1989. "Melanosis coli - Prevalence, distribution, and histologic features in 200 consecutive autopsies at Kuopio University Central Hospital." *Diseases of the Colon and Rectum*. 32:235-239.

Krishnamoorthi R and Iyer P. 2015. "Molecular biomarkers added to image-enhanced endoscopic imaging: Will they further improve diagnostic accuracy?" *Clinical Gastroenterology*. 29:561-573.

Kurz T, Terman A and Ulf T. 2007. "Autophagy, ageing and apoptosis: The role of oxidative stress and lysosomal iron." *Brunk Archives of Biochemistry and Biophysics*. 462:220-230.

- Lam-Himlin D, Daniels J *et al.* 2006. "The hippo pathway in human upper gastrointestinal dysplasia and carcinoma: A novel oncogenic pathway." *International Journal of Gastrointestinal Cancer.* 37:103-109.
- Lau C, Sćeapanović O *et al.* 2015. "Re-evaluation of model-based light-scattering spectroscopy for tissue spectroscopy." *Journal of biomedical optics.* 14(2):024031.
- Leedham SJ, Preston SL, McDonald SA *et al.* 2008. "Individual crypt heterogeneity and the origin of metaplastic glandular epithelium in human Barrett's oesophagus." *Gut.* 57(8):1041-8.
- Lestina L. 2001. "An unusual case of melanosis coli." *Gastrointestinal Endoscopy.* 54(1):119-121.
- Levine D, Haggitt P *et al.* 1993. "An endoscopic biopsy protocol can differentiate high-grade dysplasia from early adenocarcinoma in Barrett's esophagus." *Gastroenterology.* 105(1):40-50.
- Levine B and Kroemer G. 2008. "Autophagy in the Pathogenesis of Disease." *Cell.* 132(1):27-42.
- Lewis A, Gaifulina R, Isabelle M *et al.* 2017. "Mirrored stainless steel substrate provides improved signal for Raman spectroscopy of tissue and cells." *J Raman Spectrosc.* 48:119-125.
- Li B and Xie S. 2005. "Autofluorescence excitation-emission matrices for diagnosis of colonic cancer." *World J Gastroenterol.* 11(25):3931-3934.
- Liu L, Hofstetter W *et al.* 2005. "Significance of the Depth of Tumor Invasion and Lymph Node Metastasis in Superficially Invasive (T1) Esophageal Adenocarcinoma." *Am J Surg Pathol.* 29:1079-1085.
- Luo X, Zhang B *et al.* 2012. "Autofluorescence spectroscopy for evaluating dysplasia in colorectal tissues." *Z Med Phys.* 22:40-47.
- Mantsch H, Choo-Smith L and Shaw R. 2002. "Vibrational spectroscopy and medicine: An alliance in the making." *Vibrational Spectroscopy.* 30(1):31-41.
- Masuda N, Ohnishi T, Kawamoto S *et al.* 1999. "Analysis of chemical modification of RNA from formalin-fixed samples and optimization of molecular biology applications for such samples." *Nucleic Acids Res.* 27:4436-43.
- Matsumoto T, Nakamura S *et al.* 2010. "Autofluorescence imaging colonoscopy for the detection of dysplastic lesions in ulcerative colitis: a pilot study." *Colorectal Disease.* 12:e291-e297.
- Mayne G, Bright T *et al.* 2012. "Ablation of Barrett's oesophagus: Towards improved outcomes for oesophageal cancer?" *ANZ Journal of Surgery.* 82(9):592-8.

Maziak D, Do M *et al.* 2007. "Fourier-transform infrared spectroscopic study of characteristic molecular structure in cancer cells of esophagus: An exploratory study." *Cancer Detection and Prevention*. 31:244-253.

Meade A, Clarke C, Draua F *et al.* 2010. "Studies of Chemical Fixation Effects in Human Cell Lines Using Raman Microscopy." *Analytical and Bioanalytical Chemistry*. 396(5):1781-91.

Meining A, Morgner S *et al.* 2001. "Atrophy-metaplasia-dysplasia-carcinoma sequence in the stomach: A reality or merely an hypothesis?" *Best Practice and Research in Clinical Gastroenterology*. 15(6):983-998.

Miranda-Lorenzo I, Dorado J *et al.* 2014. "Intracellular autofluorescence: a biomarker for epithelial cancer stem cells." *Nature Methods*. 11:1161-73.

Moss S, Liu T *et al.* 1996. "Inward growth of colonic adenomatous polyps." *Gastroenterology*. 111:1425-1432.

Murk JL, Posthuma G, Koster AJ *et al.* 2003. "Influence of aldehyde fixation on the morphology of endosomes and lysosomes: quantitative analysis and electron tomography." *Journal of Microscopy*. 212:81-90.

Nadine Phoa K, van Vilstern F *et al.* 2014. "Radiofrequency Ablation vs Endoscopic Surveillance for Patients With Barrett Esophagus and Low-Grade Dysplasia. A Randomized Clinical Trial." *JAMA*. 311(12):1209-1217.

Nallala J, Piot O *et al.* 2013. "Infrared Imaging as a Cancer Diagnostic Tool: Introducing a New Concept of Spectral Barcodes for Identifying Molecular Changes in Colon Tumors." *Cytometry Part A*. 83A:294-300.

Niepsuj K, Niepsuj G *et al.* 2003. "Autofluorescence endoscopy for detection of high-grade dysplasia in short-segment Barrett's esophagus." *Gastrointestinal Endoscopy*. 58(5):715-719.

Ó Faoláin E, Hunter M *et al.* 2005. "Raman Spectroscopic Evaluation of Efficacy of Current Paraffin Wax Section Dewaxing Agents." *J Histochem Cytochem*. 53(1):121-9.

Ofman J, Lewin K *et al.* 2000. "The economic impact of the diagnosis of dysplasia in Barrett's esophagus." *American Journal of Gastroenterology*. 95(10):2946-2952.

Old O, Fullwood L *et al.* 2014. "Vibrational spectroscopy for cancer diagnostics." *Anal Methods*. 6:3901-3917.

Partik A, Kahl-Rainer P *et al.* 1998. "Apoptosis in human colorectal tumours: ultrastructure and quantitative studies on tissue localization and association with bak expression." *Virchows Arch*. 432(5):415-26.

Pech O, Vieth M *et al.* 2007. "Conclusions from the histological diagnosis of low-grade intraepithelial neoplasia in Barrett's oesophagus." *Scandinavian Journal of Gastroenterology*. 426:682-688.

Pech O, Behrens A *et al.* 2008. "Long-term results and risk factor analysis for recurrence after curative endoscopic therapy in 349 patients with high-grade intraepithelial neoplasia and mucosal adenocarcinoma in Barrett's oesophagus." *Gut*. 57:1200-1206.

Peters J, Clark G *et al.* 1994. "Outcome of adenocarcinoma arising in Barrett's esophagus in endoscopically surveyed and nonsurveyed patients." *J Thorac Cardiovasc Surg*. 108(5):813-21.

Piva A, Silva J *et al.* 2011. "Overview of the use of theory to understand infrared and Raman spectra and images of biomolecules: Colorectal cancer as an example." *Theoretical Chemistry Accounts*. 130:1261-1273.

Piva J, Silva J *et al.* 2015. "Biochemical imaging of normal, adenoma, and colorectal adenocarcinoma tissues by fourier transform infrared spectroscopy (FTIR) and morphological correlation by histopathological analysis: Preliminary results." *Res Biomed Eng*. 31(1).

Plentz R, Wiemann S *et al.* 2003. "Telomere shortening of epithelial cells characterises the adenoma-carcinoma transition of human colorectal cancer." *Gut*. 52:1304-1307.

Prasad G, Bansal A *et al.* 2010. "Predictors of progression in Barrett's esophagus: current knowledge and future directions." *Am J Gastroenterol*. 105(7):1490-1502.

Quaroni L and Casson A. 2009. "Characterization of Barrett esophagus and esophageal adenocarcinoma by Fourier-transform infrared microscopy." *Analyst*. 134:1240-1246.

Reid B, Haggitt R *et al.* 1988. "Observer variation in the diagnosis of dysplasia in Barrett's esophagus." *Human Pathology*. 19(2):166-178.

Reid B, Levine D *et al.* 2000. "Predictors of progression to cancer in Barrett's esophagus: Baseline histology and flow cytometry identify low- and high-risk patient subsets." *American Journal of Gastroenterology*. 95(7):1669-1676.

Regitnig P and Denk H. 2000. "Lack of Pseudomelanosis coli in colonic adenomas suggests different pathways of apoptotic bodies in normal and neoplastic colonic mucosa." *Virchows Arch*. 436(6):588-94.

Renehan A, Booth C and Potten C. 2001. "What is apoptosis, and why is it important?" *BMJ*. 322:1536-1538.

Rice T, Mendelin J *et al.* 2006. "Barrett's esophagus: Pathologic considerations and implications for treatment." *Seminars in Thoracic and Cardiovascular Surgery*. 17(4):292-300.

Riegler M and Schoppmann F. 2014. "Selected commentary to "Radiofrequency ablation vs endoscopic surveillance for patients with Barrett

- esophagus and low-grade dysplasia. A randomized clinical trial" *Acta Chirurgica Austriaca*. 46:3.
- Rigas B and Wong T. 1992. "Human Colon Adenocarcinoma Cell Lines Display Infra-red Spectroscopic Features of Malignant Colon Tissues." *Cancer Research*. 52:84-44.
- Rigas B, Morgellot, Goldman I and Wong P. 1990. "Human colorectal cancers display abnormal Fourier-transform infrared spectra (colon cancer/infrared spectroscopy/high-pressure spectroscopy/tumor markers)." *Medical Sciences*. 87:8140-8144.
- Ronkainen J, Aro P *et al*. 2005. "Prevalence of Barrett's esophagus in the general population: An endoscopic study." *Gastroenterology*. 129(6):1825-31.
- Seehafer S and Pearce D. 2006. "You say lipofuscin, we say ceroid: Defining autofluorescent storage material." *Neurobiology of Aging*. 27:576-588.
- Sepesi B, Watson T *et al*. 2010. "Are endoscopic therapies appropriate for superficial submucosal esophageal adenocarcinoma? An analysis of esophagectomy specimens." *J Am Coll Surg*. 210(4):418-27.
- Shaheen N, Crosby M *et al*. 2000. "Is There Publication Bias in the Reporting of Cancer Risk in Barrett's Esophagus?" *Gastroenterology*. 119:333-338.
- Sharma P, Weston A *et al*. 2003. "Magnification chromoendoscopy for the detection of intestinal metaplasia and dysplasia in Barrett's oesophagus." *Gut*. 52:24-27.
- Sharma P, McQuaid K *et al*. 2004. "A critical review of the diagnosis and management of Barrett's esophagus: The AGA Chicago Workshop." *Gastroenterology*. 127:310-330.
- Shetty C, Kendall C *et al*. 2006. "Raman spectroscopy: elucidation of biochemical changes in carcinogenesis of oesophagus." *British Journal of Cancer*. 94:1460-1464.
- Sikkema M, De Jonge P *et al*. 2010. "Risk of Esophageal Adenocarcinoma and Mortality in Patients With Barrett's Esophagus: A Systematic Review and Meta-analysis." *Clinical Gastroenterology and Hepatology*. 8:235-244.
- Song LM, Banerjee S *et al*. 2011. "Report on Emerging Technology: Autofluorescence Imaging." *Gastrointestinal Endoscopy*. 73(4):647-650.
- Srinivasan M, Sedmak D and Jewell S. 2002. "Effect of fixatives and tissue processing on the content and integrity of nucleic acids." *American Journal of Pathology*. 161:1961-71.
- Strater J, Koretz K, Gunthert R and Moller P. 1995. "In situ detection of enterocytic apoptosis in normal colonic mucosa and in familial adenomatous polyposis." *Gut*. 37:819-825.

- Sui G, Zhou S *et al.* 2006. "Mitochondrial DNA mutations in preneoplastic lesions of the gastrointestinal tract: a biomarker for the early detection of cancer." *Molecular Cancer*. 13(5):73-82.
- Sujendran V, Sica G, Warren B and Maynard N. 2005. "Oesophagectomy remains the gold standard for treatment of high-grade dysplasia in Barrett's oesophagus." *European Journal of Cardiothoracic Surgery*. 28:763-766.
- Takubo K, Aida J *et al.* 2009. "Cardiac rather than intestinal-type background in endoscopic resection specimens of minute Barrett adenocarcinoma." *Human Pathology*. 40:65-74.
- Takayama T, Katsuki S *et al.* 1998. "Aberrant crypt foci of the colon as precursors of adenoma and cancer." *The New England Journal of Medicine*. 339(18):1277-1284.
- Talari A, Movasaghi Z, Rehman S and Rehman I. 2014. "Raman Spectroscopy of Biological Tissues." *Applied Spectroscopy Reviews*. 50(1):46-111.
- Terman A and Brunk U. 2001. "Lipofuscin." *The International Journal of Biochemistry & Cell Biology*. 36(8):1400-1404.
- Terman A and Brunk U. 2004. "Aging as a catabolic malfunction." *The International Journal of Biochemistry & Cell Biology*. 36:2365-2375.
- Thomas T, Abrahms K *et al.* 2007. "Meta analysis: Cancer risk in Barrett's oesophagus." *Alimentary Pharmacology and Therapeutics*. 26:1465-1477.
- Thompson B. 2012. "Barrett's esophagus: A review of diagnostic criteria, clinical surveillance practices and new developments." *J Gastrointest Oncol*. 3(3):232-242.
- Thurberg B, Duray P and Odze R. 1999. "Polypoid dysplasia in Barrett's esophagus: a clinicopathologic, immunohistochemical, and molecular study of five cases." *Hum Pathol*. 30(7):745-52.
- Timmer M, Sun G *et al.* 2013. "Predictive biomarkers for Barrett's esophagus: so near and yet so far." *Dis Esophagus*. 26(6):574-581.
- Upchurch E, Old O *et al.* 2016. "Detection of dysplasia in Barrett's oesophagus: Are there impending optical and spectroscopic solutions?" *Gastroenterol Hepatol Endosc*. 1(3):61-67.
- Varghese S, Lao-Sirieix P and Fitzgerald R. 2012. "Identification and clinical implementation of biomarkers for Barrett's esophagus." *Gastroenterology*. 142(3):435-441.
- Van der Wath R, Gerdiner B, Burgess A and Smith D. 2013. "Cell Organisation in the Colonic Crypt: A Theoretical Comparison of the Pedigree and Niche Concepts." *PLoS ONE*. 8(9):1-15.



- Van Grieken N, Meijer G *et al.* 2003. "Increased apoptosis in gastric mucosa adjacent to intestinal metaplasia." *J Clin Pathol.* 56:358-362.
- Van Sandick J, Van Lanschot J *et al.* 1998. "Impact of endoscopic biopsy surveillance of Barrett's oesophagus on pathological stage and clinical outcome of Barrett's carcinoma." *Gut.* 43:216-222.
- Vieth M, Ell C *et al.* 2008. "Histological analysis of endoscopic resection specimens from 326 patients with Barrett's esophagus and early neoplasia." *Endoscopy.* 36(9):776-81.
- Wagnieres G, Star W and Wilson B. 1998. "In Vivo Fluorescence Spectroscopy and Imaging for Oncological Applications." *Photochemistry and Photobiology.* 68(5):603-632.
- Walker N, Bennett R and Axelson R. 1988. "A consequence of anthraquinone-induced apoptosis of colonic epithelial cells." *Am J Pathol.* 131(3):465-76.
- Wang K, Sampliner R and the Practice Parameters Committee of the American College of Gastroenterologists. 2008. "Updated guidelines 2008 for the diagnosis, surveillance and therapy of Barrett's esophagus." *Am J Gastroenterol.* 103(3):788-97.
- Wani S, Falk G *et al.* 2011. "Patients With Nondysplastic Barrett's Esophagus Have Low Risks for Developing Dysplasia or Esophageal Adenocarcinoma." *Clinical Gastroenterology and Hepatology.* 9:220-227.
- Watson A. 1995. "Necrosis and apoptosis in the gastrointestinal tract." *Gut.* 37(2):165-7.
- Watson A. 2004. "Apoptosis and Colorectal Cancer." *Gut.* 53:1701-9.
- Watson A, Heading R and Shepherd N. 2005. British Society of Gastroenterology Guidelines for the diagnosis and management of Barrett's columnar-lined oesophagus." *BSG Guidelines in Gastroenterology.* 1-39.
- Weissleder R and Pittet M. 2008. "Imaging in the era of molecular oncology." *Nature.* 452(7187):580-589.
- West N, Courtney E *et al.* 2009. "Apoptosis in the Colonic Crypt, Colorectal Adenomata, and Manipulation by Chemoprevention." *Cancer Epidemiol Biomarkers Prev.* 18(6):1680-7.
- Westererp M, Koppert L *et al.* 2005. "Outcome of surgical treatment for early adenocarcinoma of the esophagus or gastro-esophageal junction." *Virchows Arch.* 446:497-504.
- Weston A, Sharma P *et al.* 2000. "Long-term follow-up of Barrett's high-grade dysplasia." *Am J Gastroenterol.* 95(8):1888-93.

- Weston A, Banerjee S *et al.* 2001. "p53 protein overexpression in low grade dysplasia (LGD) in Barrett's esophagus: immunohistochemical marker predictive of progression." *Am J Gastroenterol.* 96(5):1355-62.
- Whiteman D, Appleyard M *et al.* 2015. "Australian clinical practice guidelines for the diagnosis and management of Barrett's esophagus and early esophageal adenocarcinoma." *Journal of Gastroenterology and Hepatology.* 30:804-820.
- Whitson M and Falk G. 2015. "Predictors of Progression to High-Grade Dysplasia or Adenocarcinoma in Barrett's Esophagus." *Gastroenterol Clin North Am.* 44(2):299-315.
- Whittles C, Biddlestone L *et al.* 1999. "Apoptotic and proliferative activity in the neoplastic progression of Barrett's oesophagus: A comparative study." *J Pathol.* 187(5):535-40.
- Wijnhoven B, Tilanus H and Dinjens W. 2001. "Molecular Biology of Barrett's Adenocarcinoma." *Annals of Surgery.* 233(3):322-337.
- Wong W, Wright N *et al.* 1999. "Leader Cell proliferation in gastrointestinal mucosa." *J Clin Pathol.* 52:321-333.
- Wu MY, Liang YR, Wu XY and Zhuang CX. 2001. "Relationship between Egr-1 gene expression and apoptosis in esophageal carcinoma and precancerous lesions." *World Journal of Gastroenterology.* 8(6):971-975.
- Yantiss R and Odze R. 2008. "Neoplastic precursor lesions of the upper gastrointestinal tract." *Diagnostic Histopathology.* 14(9):437-452.
- Yousef F, Cardwell C *et al.* 2008. "The incidence of esophageal cancer and high-grade dysplasia in Barrett's esophagus: A systematic review and meta-analysis." *American Journal of Epidemiology.* 186(3):237-249.
- Zagari R, Fuccio L *et al.* 2007. "Gastro-oesophageal reflux symptoms, oesophagitis and Barrett's oesophagus in the general population: the Loiano–Monghidoro study." *Gut.* 57:1354-1359.